

Forward production of charged pions with incident π^\pm on nuclear targets measured at the CERN PS.

HARP Collaboration

October 25, 2018

Abstract

Measurements of the double-differential π^\pm production cross-section in the range of momentum $0.5 \text{ GeV}/c \leq p \leq 8.0 \text{ GeV}/c$ and angle $0.025 \text{ rad} \leq \theta \leq 0.25 \text{ rad}$ in interactions of charged pions on beryllium, carbon, aluminium, copper, tin, tantalum and lead are presented. These data represent the first experimental campaign to systematically measure forward pion hadroproduction.

The data were taken with the large acceptance HARP detector in the T9 beam line of the CERN PS. Incident particles, impinging on a 5% nuclear interaction length target, were identified by an elaborate system of beam detectors. The tracking and identification of the produced particles was performed using the forward spectrometer of the HARP detector. Results are obtained for the double-differential cross-sections $d^2\sigma/dpd\Omega$ mainly at four incident pion beam momenta ($3 \text{ GeV}/c$, $5 \text{ GeV}/c$, $8 \text{ GeV}/c$ and $12 \text{ GeV}/c$). The measurements are compared with the GEANT4 and MARS Monte Carlo simulation.

M. Apollonio^x, A. Artamonov^{f,4}, A. Bagulya^m, G. Barr^p, A. Blondel^g, F. Bobisut^{q,19}, M. Bogomilov^w,
M. Bonesini^{l,*}, C. Booth^u, S. Borghi^{g,12}, S. Bunyatov^d, J. Burguet–Castell^z, M.G. Catanesi^a,
A. Cervera–Villanueva^z, P. Chimenti^x, L. Coney^{15,18}, E. Di Capua^e, U. Dore^s, J. Dumarchez^r, R. Edgecock^b,
M. Ellis^{b,1}, F. Ferri^t, U. Gastaldiⁱ, S. Giani^f, G. Giannini^x, D. Gibin^{q,19}, S. Gilardoni^f, P. Gorbunov^{f,4},
C. Gößling^c, J.J. Gómez–Cadenas^z, A. Grant^f, J.S. Graulich^{k,16}, G. Grégoire^k, V. Grichineⁿ, A. Grossheim^{f,6},
A. Guglielmi^q, L. Howlett^t, A. Ivanchenko^{f,7}, V. Ivanchenko^{f,8}, A. Kayis–Topaksu^{f,9}, M. Kirsanov^m,
D. Kolev^w, A. Krasnoperov^d, J. Martín–Albo^z, C. Meurer^h, M. Mezzetto^q, G. B. Mills^{17,20}, M.C. Morone^{g,13},
P. Novella^z, D. Orestano^{t,20}, V. Palladino^o, J. Panman^f, I. Papadopoulos^f, F. Pastore^{t,20}, S. Piperov^w,
N. Polukhinaⁿ, B. Popov^{d,2}, G. Prior^{g,14}, E. Radicioni^a, D. Schmitz^{15,18}, R. Schroeter^g, G. Skoro^u, M. Sorel^z,
E. Tcherniaev^f, P. Temnikov^y, V. Tereschenko^d, A. Tonazzo^{t,20}, L. Tortora^t, R. Tsenov^w, I. Tsukerman^{f,4},
G. Vidal–Sitjes^{e,3}, C. Wiebusch^{f,10}, P. Zucchelli^{f,5,11}

(HARP collaboration)

-
- (a) Sezione INFN, Bari, Italy
 - (b) Rutherford Appleton Laboratory, Chilton, Didcot, UK
 - (c) Institut für Physik, Universität Dortmund, Germany
 - (d) Joint Institute for Nuclear Research, JINR Dubna, Russia
 - (e) Università degli Studi e Sezione INFN, Ferrara, Italy
 - (f) CERN, Geneva, Switzerland
 - (g) Section de Physique, Université de Genève, Switzerland
 - (h) Institut für Physik, Forschungszentrum Karlsruhe, Germany
 - (i) Laboratori Nazionali di Legnaro dell’ INFN, Legnaro, Italy
 - (k) Institut de Physique Nucléaire, UCL, Louvain-la-Neuve, Belgium
 - (l) Sezione INFN Milano Bicocca, Milano, Italy
 - (m) Institute for Nuclear Research, Moscow, Russia
 - (n) P. N. Lebedev Institute of Physics (FIAN), Russian Academy of Sciences, Moscow, Russia
 - (o) Università “Federico II” e Sezione INFN, Napoli, Italy
 - (p) Nuclear and Astrophysics Laboratory, University of Oxford, UK
 - (q) Sezione INFN, Padova, Italy
 - (r) LPNHE, Universités de Paris VI et VII, Paris, France
 - (s) Università “La Sapienza” e Sezione INFN Roma I, Roma, Italy
 - (t) Sezione INFN Roma III, Roma, Italy
 - (u) Dept. of Physics, University of Sheffield, UK
 - (w) Faculty of Physics, St. Kliment Ohridski University, Sofia, Bulgaria
 - (y) Institute for Nuclear Research and Nuclear Energy, Academy of Sciences, Sofia, Bulgaria
 - (x) Università degli Studi e Sezione INFN, Trieste, Italy
 - (z) Instituto de Física Corpuscular, IFIC, CSIC and Universidad de Valencia, Spain

* Corresponding author.

E-mail address: maurizio.bonesini@mib.infn.it.

¹Now at FNAL, Batavia, Illinois, USA.

²Also supported by LPNHE, Paris, France.

³Now at Imperial College, University of London, UK.

⁴ITEP, Moscow, Russian Federation.

⁵Now at SpinX Technologies, Geneva, Switzerland.

⁶Now at TRIUMF, Vancouver, Canada.

⁷On leave of absence from Novosibirsk University, Russia.

⁸On leave of absence from Ecoanalitica, Moscow State University, Moscow, Russia.

⁹Now at Çukurova University, Adana, Turkey.

¹⁰Now at III Phys. Inst. B, RWTH Aachen, Aachen, Germany.

¹¹On leave of absence from INFN, Sezione di Ferrara, Italy.

¹²Now at CERN, Geneva, Switzerland.

¹³Now at University of Rome Tor Vergata, Italy.

¹⁴Now at Lawrence Berkeley National Laboratory, Berkeley, California, USA.

¹⁵MiniBooNE Collaboration.

¹⁶Now at Section de Physique, Université de Genève, Switzerland, Switzerland.

¹⁷Los Alamos National Laboratory, Los Alamos, USA

¹⁸Columbia University, New York, USA

¹⁹also at Università di Padova, Padova, Italy

²⁰also at Università di Roma III, Roma, Italy

1 Introduction

The HARP experiment [1] at the CERN PS was designed to measure hadron yields from a large range of nuclear targets and for incident particle momenta from 1.5 GeV/ c to 15 GeV/ c . With incident protons, this corresponds to a momentum region of great interest for neutrino beams and far from the coverage by earlier dedicated hadroproduction experiments [2, 3, 4]. Measurements with incident charged pions are relevant for the calculation of cosmic-ray muon and neutrino fluxes using extended air shower simulations. These data are also important to simulate re-interactions in particle detectors and neutrino beam production targets. At present such calculations rely on models with large uncertainties given the lack of experimental data in this energy region.

Covering an extended range of solid targets in the same experiment, it is also possible to perform systematic comparison of hadron production models with measurements at different incoming beam momenta over a large range of target atomic number A .

This paper presents our final measurements of the double-differential cross-section, $d^2\sigma/dpd\Omega$ for π^\pm forward production by incident charged pions of 3 GeV/ c , 5 GeV/ c , 8 GeV/ c and 12 GeV/ c momentum impinging on a thin beryllium, carbon, aluminium, copper, tin, tantalum or lead target of 5% nuclear interaction length (λ_I). In addition, high statistics data at 8.9 GeV/ c (12.9 GeV/ c) on a thin beryllium (aluminium) target are presented.

Some HARP results on pion production in the forward region with incident protons have already been published in papers [5, 6, 7, 8].

Pion production data at low momenta and in the forward region from incident pions are extremely scarce [9]. HARP is the first experiment to provide a high statistics data set, taken with many different targets, full particle identification and large-acceptance detector. The collected statistics, for the different nuclear targets, are reported in Table 1.

Other data with an incident pion beam, up to higher momenta, has been collected by the Fermilab E970-MIPP experiment [10] and more data at other momenta would be available with its proposed upgrade [11].

The paper is organized as follows. In subsection 1.1 we briefly describe the HARP detector, while section 2 is devoted to the main features of the analysis procedure. Section 3 presents results. It is followed by a summary presented in section 4.

1.1 Experimental apparatus

The HARP experiment makes use of a large-acceptance spectrometer consisting of a forward and large-angle detection system. The HARP detector is shown in Fig. 1. A detailed description of the experimental apparatus can be found in Ref. [12]. The forward spectrometer – based on five modules of large area drift chambers (NDC1-5) [13] and a dipole magnet complemented by a set of detectors for particle identification (PID): a time-of-flight wall (TOFW) [14], a large Cherenkov detector (CHE) and an electromagnetic calorimeter (ECAL) – covers polar angles up to 250 mrad. The muon contamination of the beam is measured with a muon identifier consisting of thick iron absorbers and scintillation counters. The large-angle spectrometer – based on a Time Projection Chamber (TPC) and Resistive Plate Chambers (RPCs) located inside a solenoidal magnet – has a large acceptance in momentum and angular range for the pions relevant to the production of the muons in a neutrino factory. For the analysis described here only the forward spectrometer and the beam instrumentation are used.

The HARP experiment, located in the T9 beam of the CERN PS, took data in 2001 and 2002. The momentum definition of the T9 beam is known with a precision of the order of 1% [15].

The target is placed inside the inner field cage (IFC) of the TPC, in an assembly that can be moved in and out of the solenoid magnet. The targets used for the measurements reported here have a cylindrical shape with a nominal diameter of about 30 mm. Their thickness is equivalent to about 5% λ_I .

A set of four multi-wire proportional chambers (MWPCs) measures the position and direction of the incoming beam particles with an accuracy of ≈ 1 mm in position and ≈ 0.2 mrad in angle per projection. A beam time-of-flight system (BTOF) measures the time difference of particles over a 21.4 m path-length. It is made of two identical scintillation hodoscopes, TOFA and TOFB (originally built for the NA52 experiment [16]), which, together with a small target-defining trigger counter, TDS (also used for the trigger), provide particle identification at low momenta. This provides separation of pions, kaons and protons up to 5 GeV/c and determines the initial time at the interaction vertex (t_0). The timing resolution of the combined BTOF system is about 70 ps. A system of two N₂-filled Cherenkov detectors (BCA and BCB) is used to tag electrons at low energies and pions at higher energies. The electron and pion tagging efficiency is found to be close to 100%. At the beam energy used for this analysis the Cherenkov counters select all particles lighter than protons, while the BTOF is used to reject ions. A set of trigger detectors completes the beam instrumentation.

The selection of beam pions is performed as described in [12]. At 3 GeV/c BCB gas pressure is set to tag e^\pm (BCA is evacuated to reduce multiple scattering of the beam) while the TOFs are capable of resolving pions from protons. At 5 GeV/c pions are separated from protons by using joint information from the TOFs and one of the Cherenkovs (usually BCB), while the gas pressure in the other Cherenkov (BCA) is set to tag e^\pm . At higher momenta the e^\pm contamination drops below 1% and the TOF system becomes unable to separate pions from protons efficiently: the beam Cherenkov detectors are used for π -p separation. At the highest beam energy the gas pressure in one of the Cherenkov detectors has been set to distinguish protons from kaons. This allows us to estimate the kaon component to be negligible in the pion beam selection at all momenta.

Table 1: Total number of events and tracks used in the various nuclear 5% λ_I target data sets and the number of incident pions on target as calculated from the pre-scaled incident beam triggers. Numbers are for incident π^+ (in parenthesis for incident π^-) in units of 10^3 events.

Data set (GeV/c)		3	5	8	8.9	12	12.9
Total DAQ events	(Be)	1113 (2233)	1296 (1798)	1935 (1585)	5868	1207 (1227)	
	(C)	1345 (1831)	2628 (1279)	1846 (1399)		1062 (646)	
	(Al)	1159 (1523)	1789 (920)	1707 (1059)		619 (741)	4713
	(Cu)	624 (3325)	2079 (1805)	2089 (1615)		745 (591)	
	(Sn)	1637 (1972)	2828 (1625)	2404(1408)		1803(937)	
	(Ta)	1783 (994)	2084(1435)	1965(1505)		866(961)	
	(Pb)	1911 (1282)	2111(2074)	2266 (1496)		487(1706)	
Accepted beam pions with forward interaction	(Be)	246 (731)	384 (914)	341 (826)	1278	76 (693)	
	(C)	257 (299)	754 (530)	358 (772)		41 (352)	
	(Al)	213(486)	523 (308)	335 (611)		27 (435)	332
	(Cu)	168 (1185)	611 (850)	397 (966)		33 (347)	
	(Sn)	467 (778)	819 (732)	481 (804)		79 (584)	
	(Ta)	561 (426)	600 (671)	388 (893)		37 (536)	
	(Pb)	611 (473)	594 (997)	444 (896)		20 (839)	
Final state π^- selected with PID	(Be)	.9 (24.9)	3.5 (32.1)	6.3 (31.0)	26.7	2.0 (27.5)	
	(C)	.7 (9.1)	5.9 (15.0)	5.9 (24.2)		1.0 (13.7)	
	(Al)	.5 (10.3)	4.0 (6.8)	5.6 (13.4)		.7 (13.4)	9.8
	(Cu)	.3 (18.9)	4.3 (19.0)	6.0 (25.1)		.9 (12.9)	
	(Sn)	.7 (9.1)	4.8 (14.4)	6.9 (16.3)		1.9k (19.4)	
	(Ta)	.6 (3.7)	3.1 (11.5)	4.9 (16.2)		.9k (16.6)	
	(Pb)	.6 (3.4)	3.0 (16.0)	5.2 (16.3)		.5k (25.5)	
Final state π^+ selected with PID	(Be)	8.9 (1.3)	14 (4.8)	13.8 (10.6)	50.0	3.4 (13.1)	
	(C)	8.0 (.5)	23.8 (2.5)	13.3 (8.0)		1.7 (6.7)	
	(Al)	5.2 (.5)	15 (1.3)	12.1 (5.6)		1.2 (7.0)	15.1
	(Cu)	2.8 (1.6)	14.8 (3.5)	12.2 (9.6)		1.4 (6.6)	
	(Sn)	5.9 (.6)	16.8 (2.8)	13.3 (6.1)		3.1 (10.2)	
	(Ta)	5.3 (.2)	10.8 (2.2)	9.4 (6.0)		1.4 (8.7)	
	(Pb)	5.0 (.2)	9.8 (2.9)	10.3 (6.1)		.7 (13.1)	

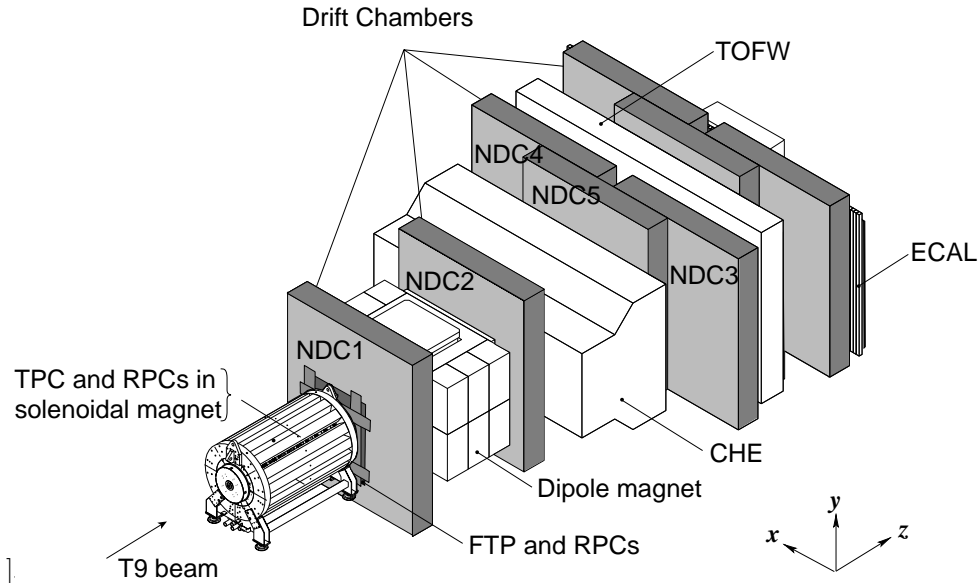


Figure 1: Schematic layout of the HARP detector. The convention for the coordinate system is shown in the lower-right corner.

A downstream trigger in the forward scintillator trigger plane (FTP) was required to record the event, accepting only tracks with a trajectory outside the central hole (60 mm) which allows beam particles to pass. The trigger counter covers the spectrometer acceptance fully and has a high efficiency ($>99.8\%$).

The length of the accelerator spill was 400 ms with a typical intensity of 15 000 beam particles per spill. The average number of events recorded by the data acquisition ranged from 300 to 350 per spill.

The absolute normalization of the number of incident pions was performed using ‘incident-particle’ triggers. These are triggers where the same selection on the beam particle was applied but no selection on the interaction was performed. The rate of this trigger was down-scaled by a factor 64.

2 Data Analysis

2.1 Event and particle selection

A detailed description of the experimental techniques used for data analysis in the HARP forward spectrometer can be found in Ref. [5, 17]. Further details of the improved analysis techniques can be found in [6, 7]. For the current analysis we have used identical reconstruction and PID algorithms, while at the final stage of the analysis the unfolding technique introduced as UFO in [5] has been applied. This technique has already been described in details in Ref. [19].

At the first stage of the analysis a beam pion is selected using the beam time of flight system (TOF-A, TOF-B) and the Cherenkov counters (BCA, BCB) as described in section 1.1. We always require time measurements in TOF-A, TOF-B and/or TDS to be present which are needed for calculating the arrival time of the beam pion at the target.

Secondary track selection criteria, described in [7], are optimized to ensure the quality of momentum reconstruction and a clean time-of-flight measurement while maintaining a high reconstruction efficiency.

The background induced by interactions of beam particles in the materials outside the target is measured by taking data without a target in the target holder (“empty target data”). These data are subject to the same event and track selection criteria as the standard data sets.

To take into account this background the number of particles of the observed type (π^+ , π^-) in the “empty target data” are subtracted bin-by-bin (momentum and angular bins) from the number of particles of the same type. The uncertainty induced by this method is discussed in section 2.3 and labeled “empty target subtraction”. The event statistics is summarized in Table 1.

The negative beam consists of e^- and π^- (with a dominant fraction of π^-), while the positive beam is dominated by protons at high momenta and by π^+ at low momenta ¹. The kaon background is estimated to be <0.5% and is neglected in the analysis, while the muon contamination (tagged by the muon identifier) is around 3% and is subtracted.

The small fraction of pions in the positively charged beam explains the significantly different statistics of the data-sets with incident π^- and π^+ . The relatively small fraction of accepted final state pions compared to the accepted beam pions is due to the stringent quality cuts applied in the analysis. The major loss is due to the small acceptance of the dipole magnet in the vertical plane, and the fact that only focused particles are accepted for analyses. The latter requirement reduces the statistics by a factor two but improves the quality of reconstruction and reduces the background [6].

2.2 Cross-section calculation

The cross-section is calculated as follows

$$\frac{d^2\sigma^\alpha}{dpd\Omega}(p_i, \theta_j) = \frac{A}{N_A\rho t} \cdot \frac{1}{N_{\text{pot}}} \cdot \frac{1}{\Delta p_i \Delta \Omega_j} \cdot \sum_{p'_i, \theta'_j, \alpha'} \mathcal{M}_{p_i \theta_j \alpha p'_i \theta'_j \alpha'}^{\text{cor}} \cdot N^{\alpha'}(p'_i, \theta'_j), \quad (1)$$

where

- $\frac{d^2\sigma^\alpha}{dpd\Omega}(p_i, \theta_j)$ is the cross-section in mb/(GeV/c sr) for the particle type α (p, π^+ or π^-) for each true momentum and angle bin (p_i, θ_j) covered in this analysis;
- $N^{\alpha'}(p'_i, \theta'_j)$ is the number of particles of type α' in bins of reconstructed momentum p'_i and angle θ'_j in the raw data;
- $\mathcal{M}_{p\theta\alpha p'\theta'\alpha'}^{\text{cor}}$ is the correction matrix which accounts for efficiency and resolution of the detector;
- $\frac{A}{N_A\rho t}$, $\frac{1}{N_{\text{pot}}}$ and $\frac{1}{\Delta p_i \Delta \Omega_j}$ are normalization factors, namely:
 - $\frac{N_A\rho t}{A}$ is the number of target nuclei per unit area ²;
 - N_{pot} is the number of incident beam particles on target (particles on target);
 - Δp_i and $\Delta \Omega_j$ are the bin sizes in momentum and solid angle, respectively ³.

We do not make a correction for the attenuation of the incoming beam in the target, so that strictly speaking the cross-sections are valid for $\lambda_I = 5\%$ targets.

The calculation of the correction matrix $\mathcal{M}_{p_i \theta_j \alpha p'_i \theta'_j \alpha'}^{\text{cor}}$ is a rather difficult task. Various techniques are described in the literature to obtain this matrix. As discussed in Ref. [5] for the p-Al analysis of HARP data at 12.9 GeV/c, two complementary analyses have been performed to cross-check internal consistency and possible biases in the respective procedures. A comparison of both analyses shows that the results are consistent within the overall systematic error [5].

In the first method – called “Atlantic” in [5] – the correction matrix $\mathcal{M}_{p_i \theta_j \alpha p'_i \theta'_j \alpha'}^{\text{cor}}$ is decomposed into distinct independent contributions, which are computed mostly using the data themselves. The second

¹the proton fraction in the incoming beam goes from 35% at 3 GeV/c to about 92% at 12 GeV/c

² A - atomic mass, N_A - Avogadro number, ρ - target density and t - target thickness

³ $\Delta p_i = p_i^{\text{max}} - p_i^{\text{min}}$, $\Delta \Omega_j = 2\pi(\cos(\theta_j^{\text{min}}) - \cos(\theta_j^{\text{max}}))$

method – called “UFO” in [5] – is the unfolding method introduced by D’Agostini [18]⁴. This method has been used in the recent HARP publications [8, 19, 20, 21, 22] and it is also applied in the analysis described here (see [7] for additional information).

The Monte Carlo simulation of the HARP setup is based on the GEANT4 package [23, 24]. The detector materials are accurately described in this simulation as well as the relevant features of the detector response and the digitization process. All relevant physics processes are considered, including multiple scattering, energy loss, absorption and re-interactions. The simulation is independent of the beam momentum and particle type because it only generates for each event exactly one secondary particle of a specific particle type inside the target material and propagates it through the complete detector. A small difference (at the few percent level) is observed between the efficiency calculated for events simulated with the single-particle Monte Carlo and with a simulation using a multi-particle hadron-production model. A similar difference is seen between the single-particle Monte Carlo and the efficiencies measured directly from the data. The single-particle Monte Carlo predicts an efficiency more in agreement with the efficiency measured with the data. A momentum-dependent correction factor determined using the efficiency measured with the data is applied to take this into account. The track reconstruction algorithms used in this analysis and the simulation are identical to the ones used for the π^+ production in p-Be collisions [6]. A detailed description of the corrections and their magnitude can be found there.

The reconstruction efficiency (inside the geometrical acceptance) is larger than 95% above 1.5 GeV/ c and drops to 80% at 0.5 GeV/ c . The requirement of a match with a TOFW hit has an efficiency between 90% and 95% above 1.0 GeV/ c and is responsible for the drop in efficiency towards lower momenta. The electron veto rejects about 1% of the pions and protons below 3 GeV/ c with a remaining electron background of less than 0.5%. Below Cherenkov threshold the TOFW separates pions and protons with negligible background and an efficiency of $\approx 98\%$ for pions. Above Cherenkov threshold the efficiency for pions is greater than 99% with only 1.5% of the protons mis-identified as a pion. The kaon background in the pion spectra is smaller than 1%.

The absorption and decay of particles is simulated by the Monte Carlo. The generated single particle can re-interact and produce background particles by hadronic or electromagnetic processes, thus giving rise to tracks in the forward spectrometer (“tertiaries”). In such cases also the additional measurements are entered into the migration matrix thereby taking into account the combined effect of the generated particle and any secondaries it creates. The absorption correction is on average 20%, approximately independent of momentum. Uncertainties in the absorption of secondaries in the dipole spectrometer material are taken into account by a variation of 10% of this effect in the simulation. The effect of pion decay is treated in the same way as the absorption and is 20% at 500 MeV/ c and negligible at 3 GeV/ c .

The uncertainty in the production of background due to tertiary particles is larger. The average correction is $\approx 10\%$ and up to 20% at 1 GeV/ c . The correction includes re-interactions in the detector material as well as a small component coming from re-interactions in the target. The validity of the generators used in the simulation was checked by an analysis of HARP data with incoming protons and charged pions on aluminium and carbon targets at lower momenta (3 GeV/ c and 5 GeV/ c). A 30% variation of the secondary production was applied. The average empty-target subtraction amounts to $\approx 20\%$.

Owing to the redundancy of the tracking system downstream of the target the reconstruction efficiency is very robust under the usual variations of the detector performance during the long data taking periods. Since the momentum is reconstructed without making use of the upstream drift chamber module (which is more sensitive in its performance to the beam intensity) the reconstruction efficiency is uniquely determined by the downstream system. No variation of the overall efficiency has been observed. The performance of the TOFW and CHE system have been monitored to be constant for the data taking periods used in this analysis. The calibration of the detectors was performed on a day-by-day basis.

⁴ The unfolding method tries to put in correspondence the vector of measured observables (such as particle momentum, polar angle and particle type) x_{meas} with the vector of true values x_{true} using a migration matrix: $x_{meas} = M_{migr} \times x_{true}$. The goal of the method is to compute a transformation (correction matrix) to obtain the expected values for x_{true} from the measured ones. The most simple and obvious solution, based on simple matrix inversion M_{migr}^{-1} , is usually unstable and is dominated by large variances and strong negative correlations between neighbouring bins. In the method of D’Agostini, the correction matrix M^{UFO} tries to connect the measurement space (effects) with the space of the true values (causes) using an iterative Bayesian approach, based on Monte Carlo simulations to estimate the probability for a given effect to be produced by a certain cause.

2.3 Error estimation

Different types of sources induce systematic errors for the analysis described here: track yield corrections ($\sim 5\%$), particle identification ($\sim 0.1\%$), momentum and angular reconstruction ($\sim 0.5\%$)⁵. The dominant error is due to track yield correction, in particular due to the subtraction of tertiary particles, with smaller contributions from particle absorption, empty target subtraction and reconstruction efficiency. The strategy to calculate these systematic errors and the different methods used for their evaluation are described in [7] where the numerical values are tabulated. An additional source of error is due to misidentified secondary kaons, which are not considered in the particle identification method used for this analysis and are subtracted on the basis of a Monte Carlo simulation, as in [7]. No explicit correction is made for pions coming from decays of other particles created in the target, as they give a very small contribution according to the selection criteria applied in the analysis.

Examples of experimental uncertainties are shown in Figure 2 for Be target with incident π^- for π^\pm production at two incident beam momenta (5 and 8 GeV/c). They are very similar for the other beam momenta and targets. Going from lighter (Be, C) to heavier targets (Ta, Pb) the corrections for π^0 conversion and absorption/tertiaries increase slightly.

The overall normalization has an uncertainty of $\sim 2\%$ and is mainly due to the uncertainty in the efficiency that beam pions counted in the normalization actually hit the target, with smaller components from the target density and the beam particle counting procedure. On average the total integrated systematic error is around 5 – 6%, with a differential bin-to-bin systematic error of the order of 10 – 11%, to be compared with a statistical integrated (bin-to-bin differential) error of $\sim 2-3\%$ ($\sim 10-13\%$). Systematic and statistical errors are roughly of the same order.

3 Results

The measured double-differential cross-sections for the production of π^+ and π^- in the laboratory system as a function of the momentum and the polar angle for each incident beam momentum are shown in Figures 3 to 9 for targets from Be to Pb. The error bars shown are the square-roots of the diagonal elements in the covariance matrix, where statistical and systematic uncertainties are combined in quadrature. The correlation of the statistical errors (introduced by the unfolding procedure) are typically smaller than 20% for adjacent momentum bins and even smaller for adjacent angular bins. The correlations of the systematic errors are larger, typically 80% for adjacent bins. The overall scale error ($< 2\%$) is not shown. The results of this analysis are also tabulated in Appendix A. We have not included the scale errors in the tables to make it possible to calculate e.g. integrated particle ratios taking the scale errors into account only when applicable, i.e. when different beams are compared.

The dependence of the averaged pion yields on the atomic number A is shown from Fig. 10 to Fig. 13. The pion yields, averaged over two angular regions ($0.05 \text{ rad} \leq \theta < 0.15 \text{ rad}$ and $0.15 \text{ rad} \leq \theta < 0.25 \text{ rad}$) and four momentum regions ($0.5 \text{ GeV}/c \leq p < 1.5 \text{ GeV}/c$, $1.5 \text{ GeV}/c \leq p < 2.5 \text{ GeV}/c$, $2.5 \text{ GeV}/c \leq p < 3.5 \text{ GeV}/c$ and $3.5 \text{ GeV}/c \leq p < 4.5 \text{ GeV}/c$), are shown for four different beam momenta. One observes a smooth behaviour of the averaged yields. The most striking feature is the difference between same-sign and opposite-sign pion production compared to the beam particle. Here one observes a stronger beam energy dependence for opposite-sign production. The A -dependence is similar for π^- and π^+ production if one compares opposite-sign and same-sign production, although one observes that especially at lower beam momenta the opposite-sign pion production saturates earlier towards higher A .

In the following we will show only some comparisons of the HARP data with publicly available Monte Carlo simulations: GEANT4 [23] (version 9.1p02) and MARS [25], not previously tuned to our data-sets, by using different models. The comparison will be shown for a limited set of plots and only for the Be (Figures 14 to 18) and Ta (Figures 19 to 23) targets, as examples of a light and a heavy target.

At intermediate energies (up to 5–10 GeV), GEANT4 uses two types of intra-nuclear cascade models: the

⁵ The quoted error in parenthesis refers to fractional error of the integrated cross-section in the kinematic range covered by the HARP experiment

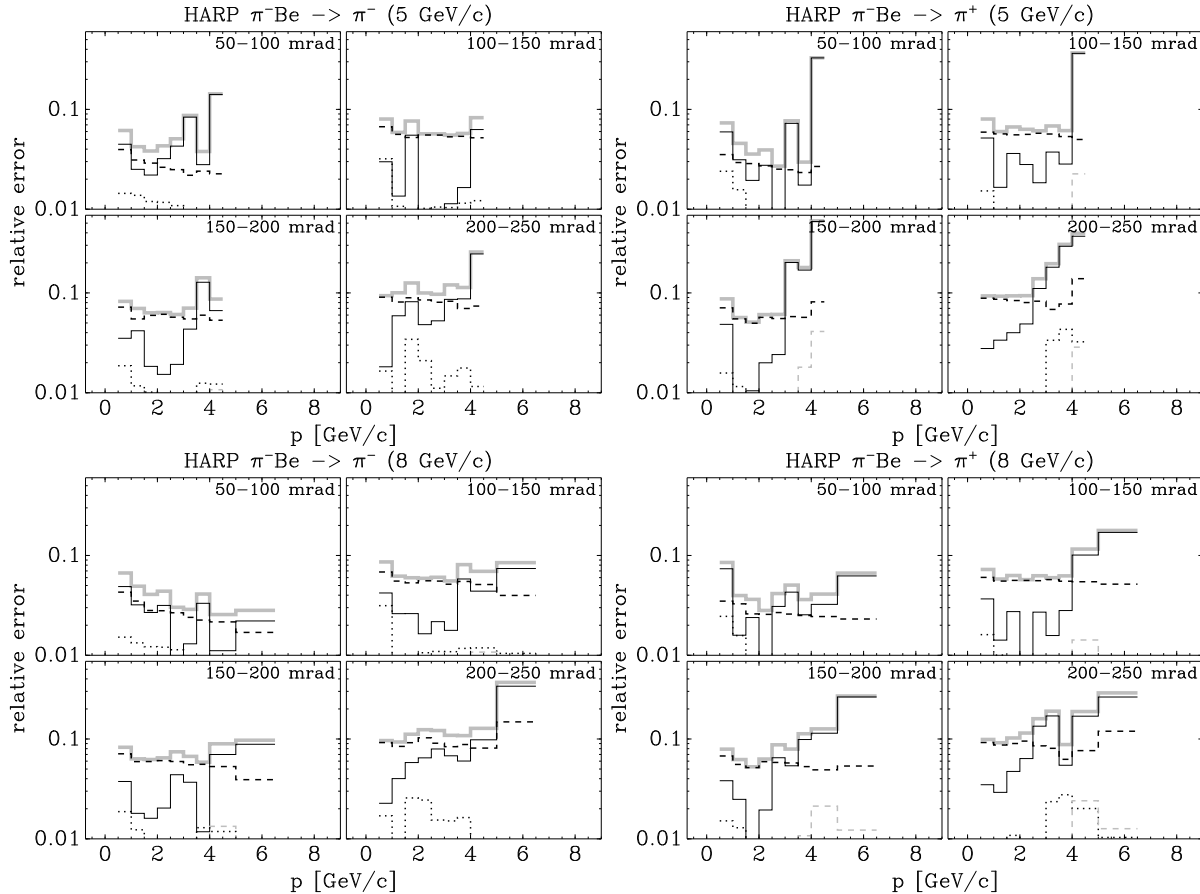


Figure 2: Systematic errors as a function of momentum of the outgoing pions for the particular case of 5 and 8 GeV/c π^- interacting on a beryllium target. Plots in the upper left panel are for incident 5 GeV/c π^- producing π^- , plots in the upper right panel are for 5 GeV/c π^- producing π^+ , plots in the lower left panels are for 8 GeV/c π^- producing π^- and plots in the lower right panel are for 8 GeV/c π^- producing π^+ . Total systematic error (grey solid line) are displayed together with the main components: black short-dashed line for absorption+tertiaries interactions, black dotted line for track efficiency and target pointing efficiency, black dot-dashed line for π^0 subtraction, black solid line for momentum scale+resolution and angle scale, grey short-dashed line for PID.

Bertini model [27, 28] (valid up to ~ 10 GeV) and the binary model [29] (with a validity range up to ~ 3 GeV). Both models treat the target nucleus in detail, taking into account density variations and tracking in the nuclear field. The binary model is based on hadron collisions with nucleons, giving resonances that decay according to their quantum numbers. The Bertini model is based on the cascade code reported in [30] and hadron collisions are assumed to proceed according to free-space partial cross-sections and final-state distributions measured for the incident particle types.

At higher energies, instead, two parton string models, the quark-gluon string (QGS) model [27, 31] and the Fritiof (FTP) model [31] are used, in addition to a High Energy Parametrized model (HEP) derived from the high energy part of the GHEISHA code used inside GEANT3 [32].

The parametrized models of GEANT4 (HEP and LEP) are intended to be fast, but conserve energy and momentum on average and not event by event.

A realistic GEANT4 simulation is built by combining models and physics processes into what is called a “physics list”. In high energy calorimetry the two most commonly used are the QGSP physics list, based on the QGS model, the pre-compound nucleus model and some of the Low Energy Parametrized (LEP)

model ⁶ and the LHEP physics list [26] based on the parametrized LEP model and HEP models.

Currently is also popular the QGSP-BERT physics list in which the Bertini model is used at 3 and 5 GeV/c and the QGSP model at 8 and 12 GeV/c.

⁶ Also this model, at low energy, has its root in the Gheisha code inside GEANT3.

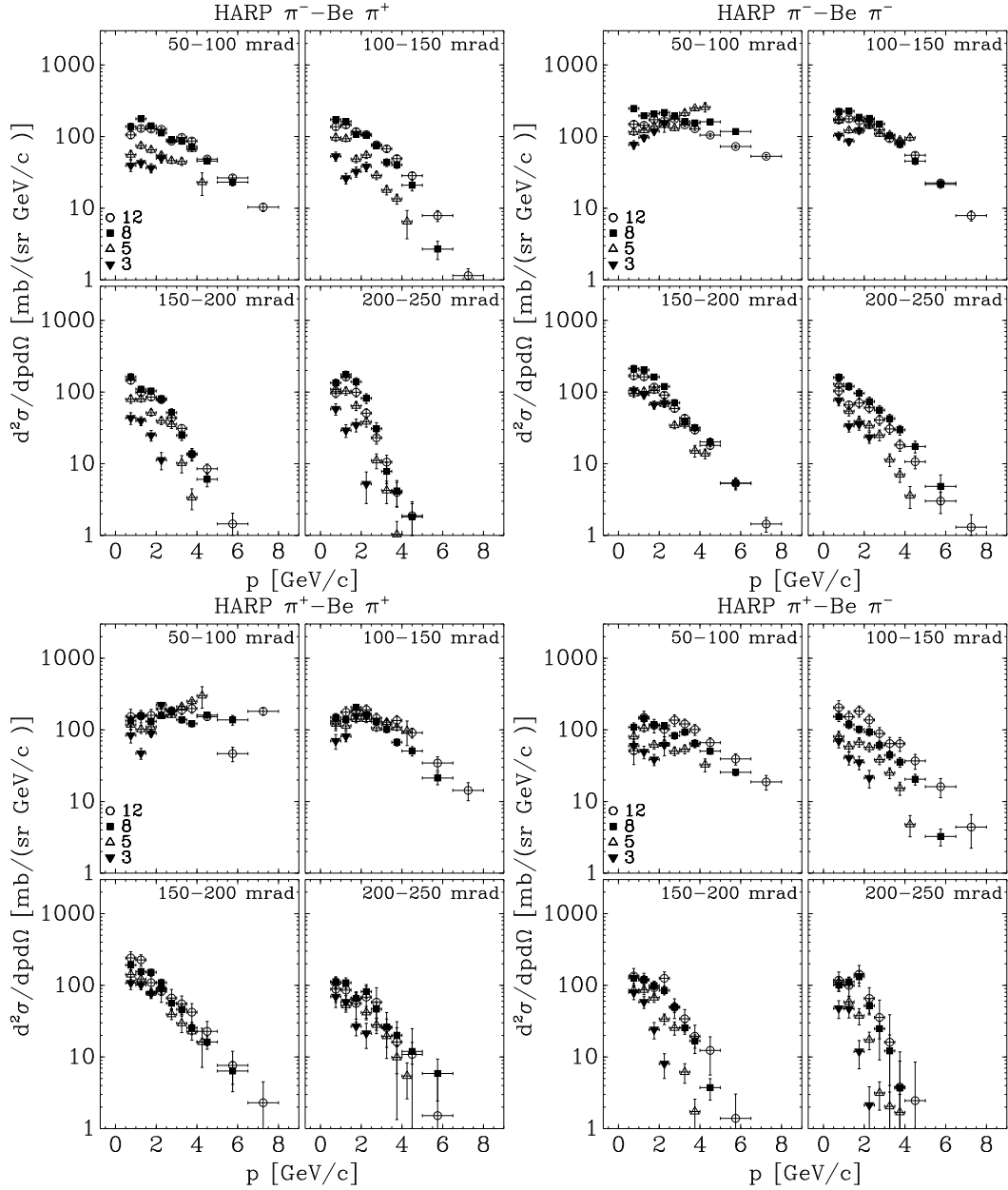


Figure 3: π^- -Be (top) and π^+ -Be (bottom) differential cross-sections for different incoming beam momenta (from 3 to 12 GeV/c). Left panels show the π^+ production, while right panels show the π^- production. In the top right corner of each plot the covered angular range is shown in mrad.

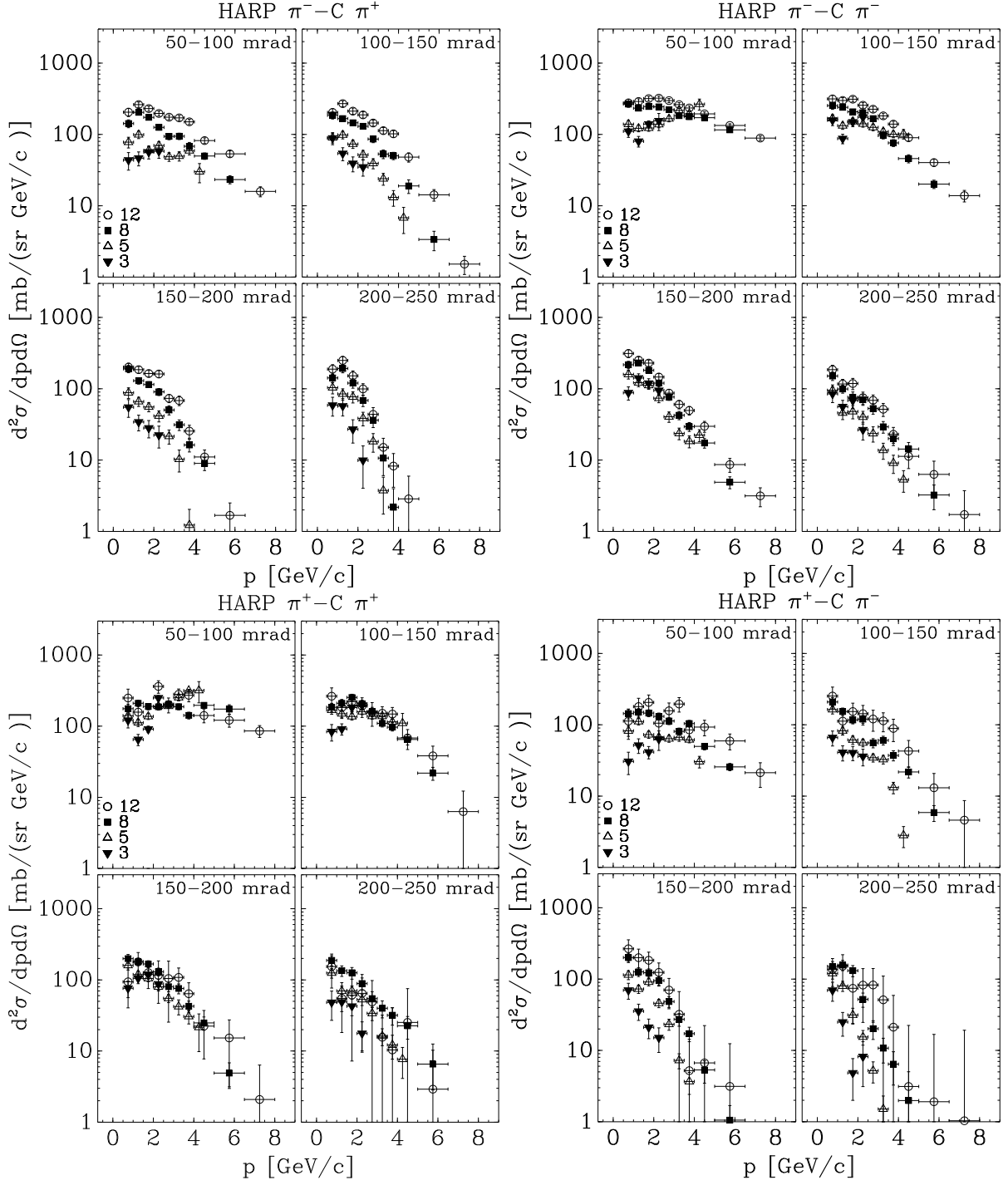


Figure 4: π^- -C (top) and π^+ -C (bottom) differential cross-sections for different incoming beam momenta (from 3 to 12 GeV/c). Left panels show the π^+ production, while right panels show the π^- production. In the top right corner of each plot the covered angular range is shown in mrad.

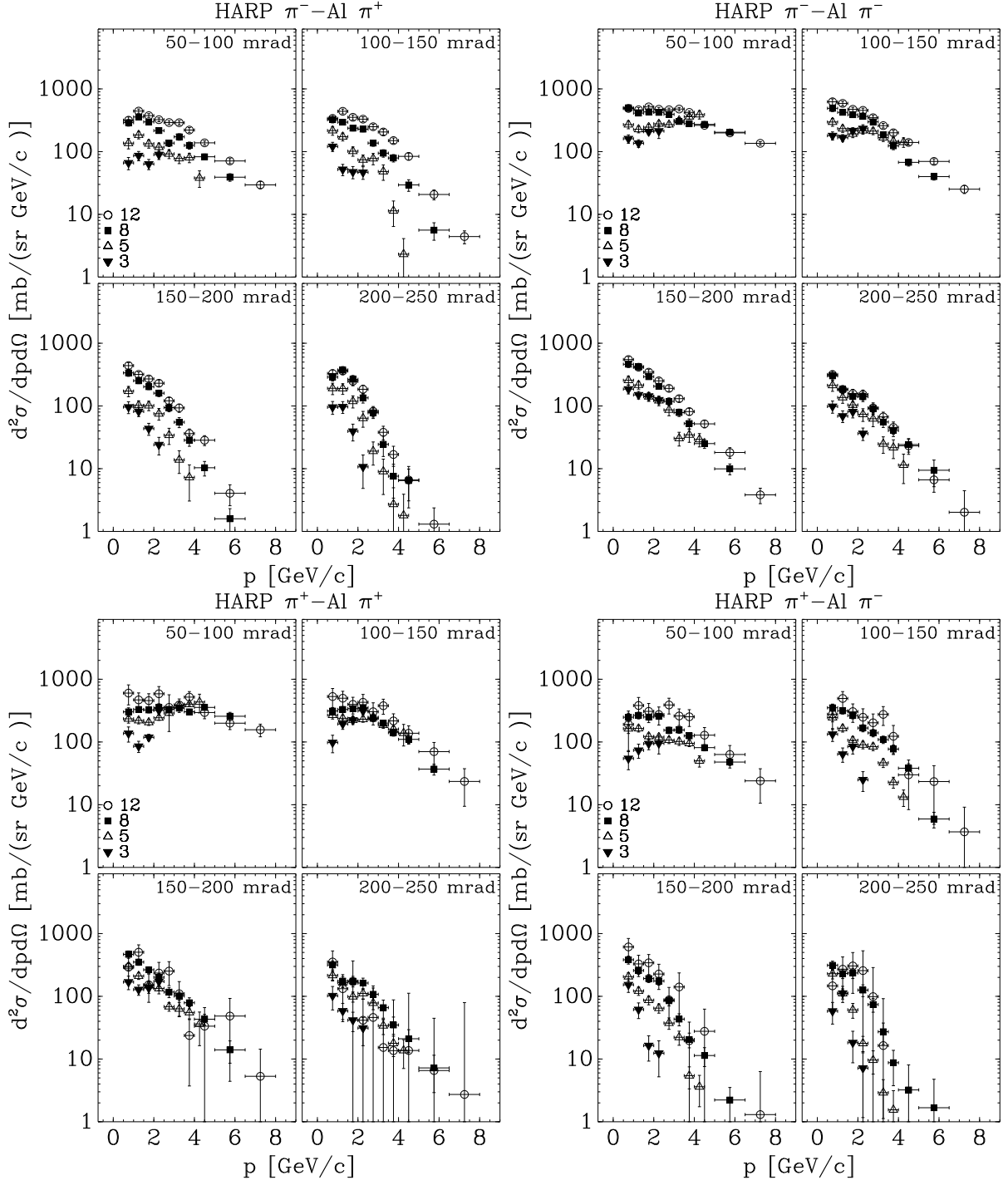


Figure 5: π^- -Al (top) and π^+ -Al (bottom) differential cross-sections for different incoming beam momenta (from 3 to 12 GeV/c). Left panels show the π^+ production, while right panels show the π^- production. In the top right corner of each plot the covered angular range is shown in mrad.

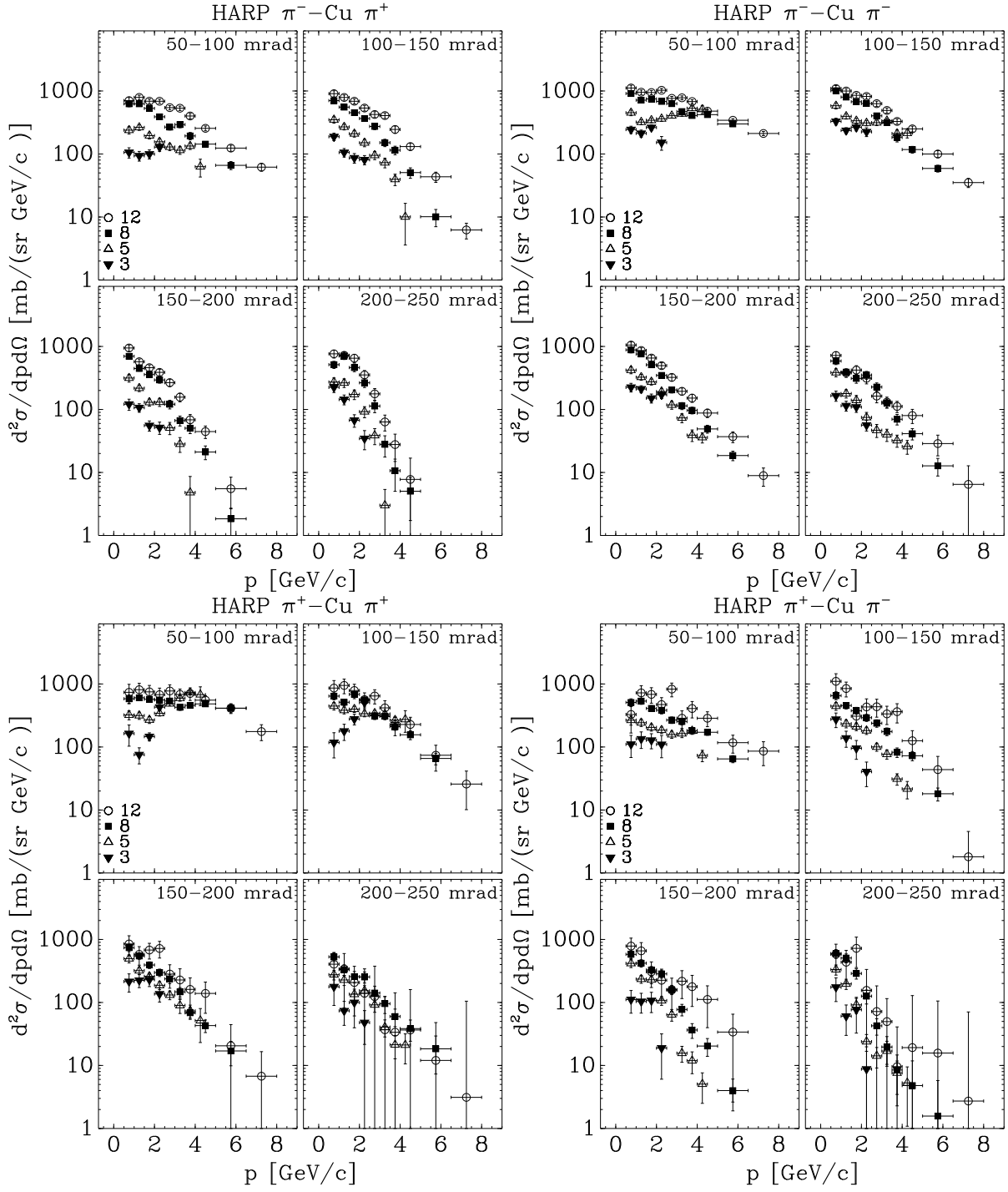


Figure 6: π^- -Cu (top) and π^+ -Cu (bottom) differential cross-sections for different incoming beam momenta (from 3 to 12 GeV/c). Left panels show the π^+ production, while right panels show the π^- production. In the top right corner of each plot the covered angular range is shown in mrad.

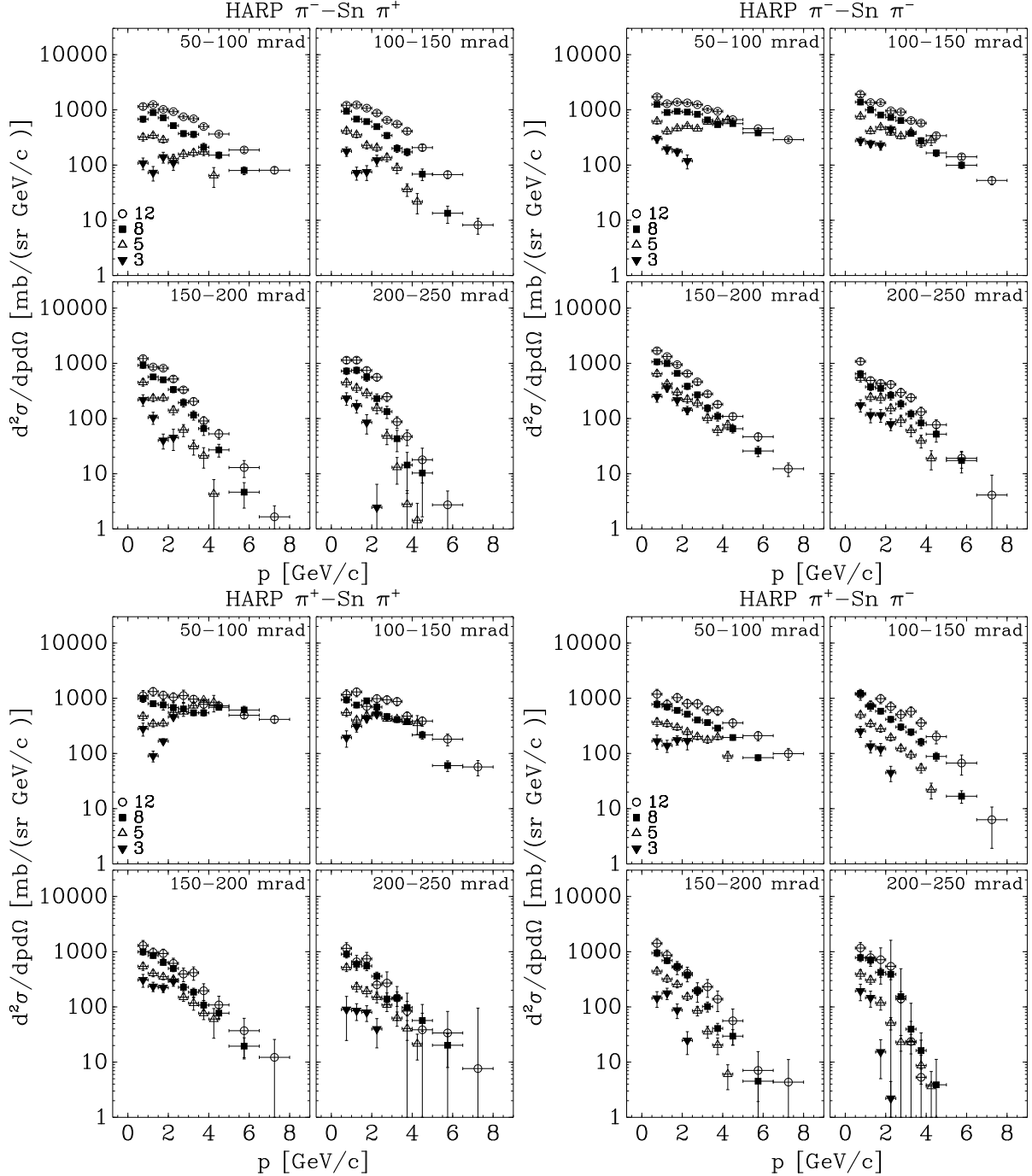


Figure 7: π^- -Sn (top) and π^+ -Sn (bottom) differential cross-sections for different incoming beam momenta (from 3 to 12 GeV/c). Left panels show the π^+ production, while right panels show the π^- production. In the top right corner of each plot the covered angular range is shown in mrad.

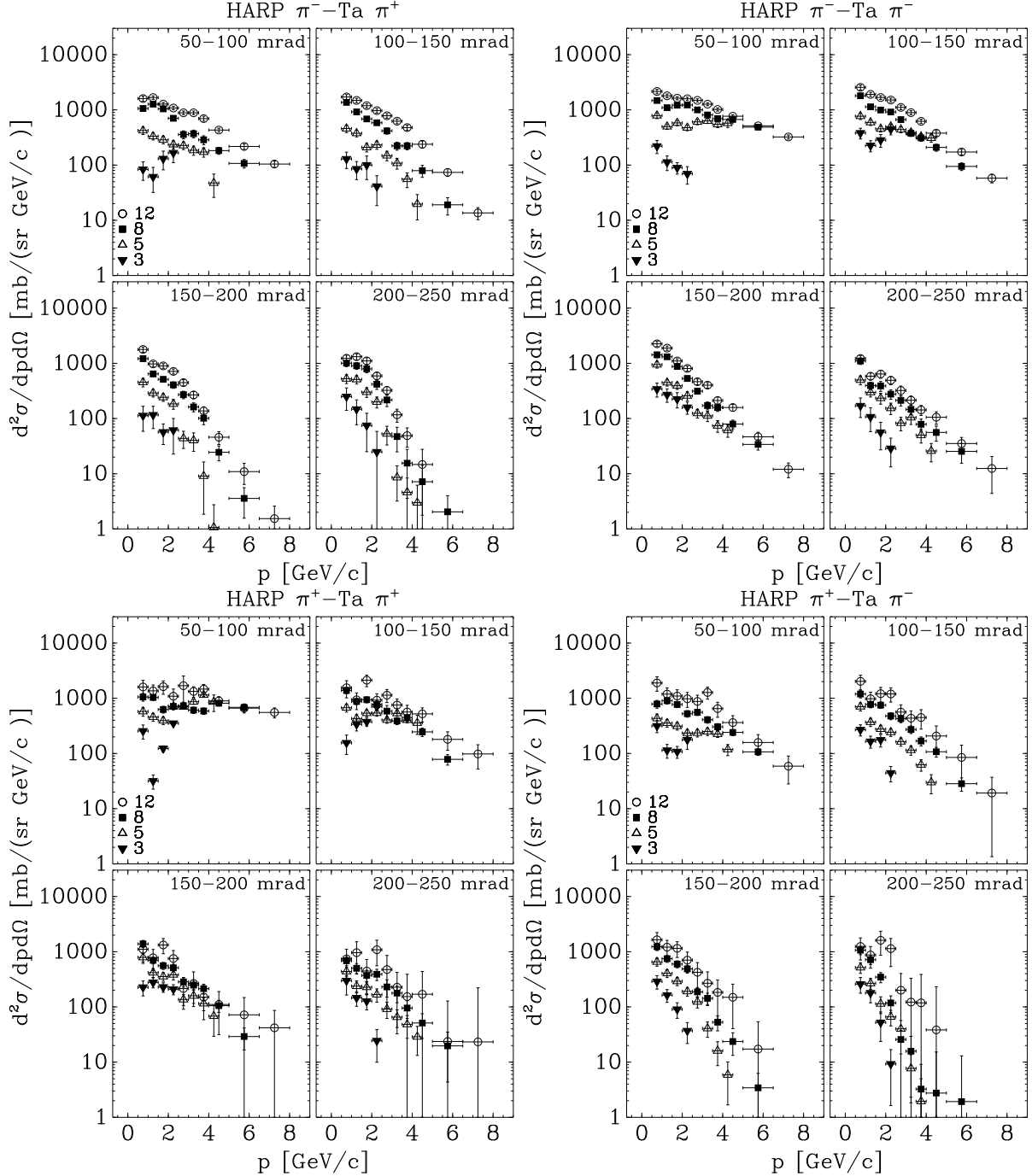


Figure 8: π^- -Ta (top) and π^+ -Ta (bottom) differential cross-sections for different incoming beam momenta (from 3 to 12 GeV/c). Left panels show the π^+ production, while right panels show the π^- production. In the top right corner of each plot the covered angular range is shown in mrad.

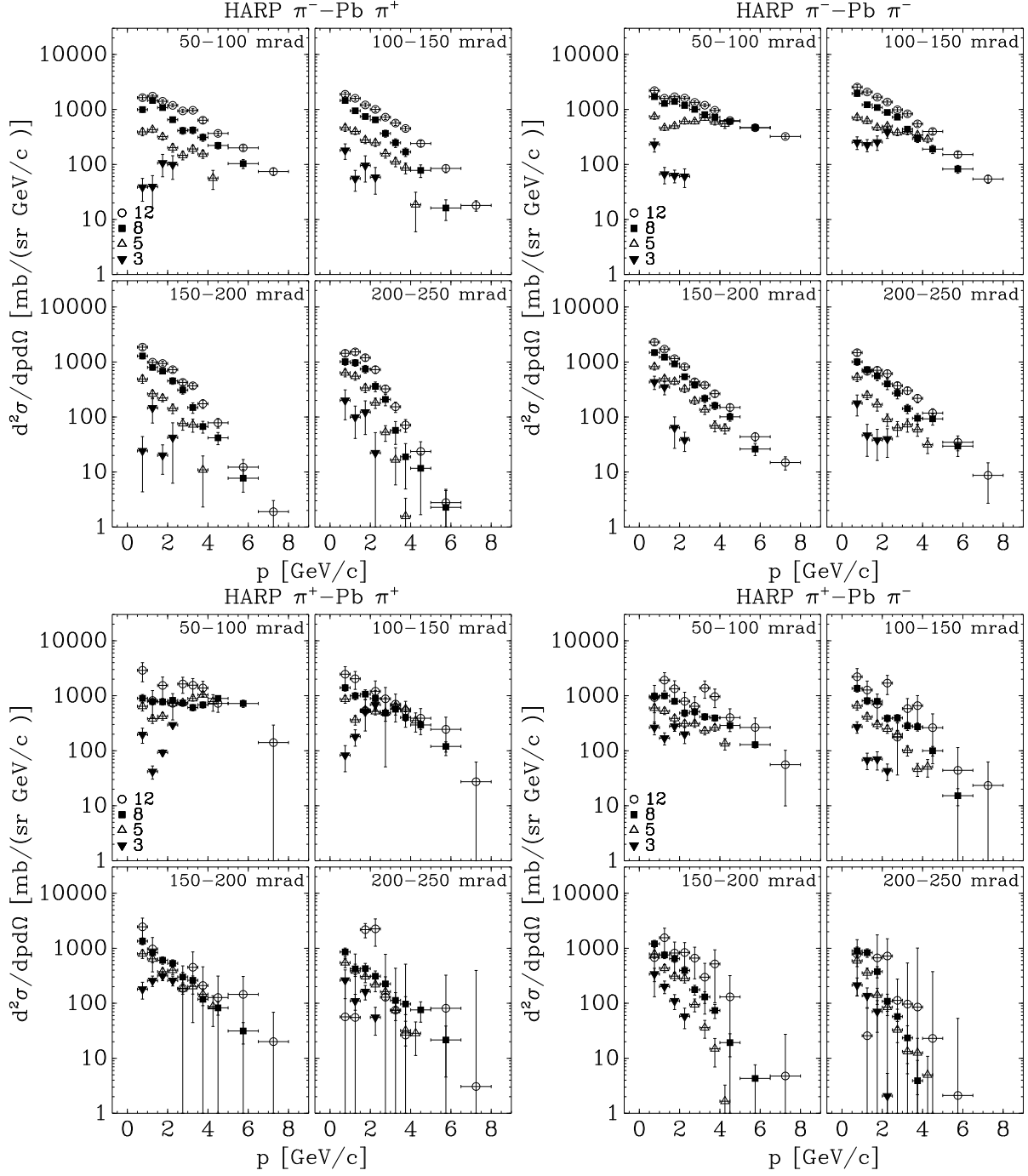


Figure 9: π^- -Pb (top) and π^+ -Pb (bottom) differential cross-sections for different incoming beam momenta (from 3 to 12 GeV/c). Left panels show the π^+ production, while right panels show the π^- production. In the top right corner of each plot the covered angular range is shown in mrad.

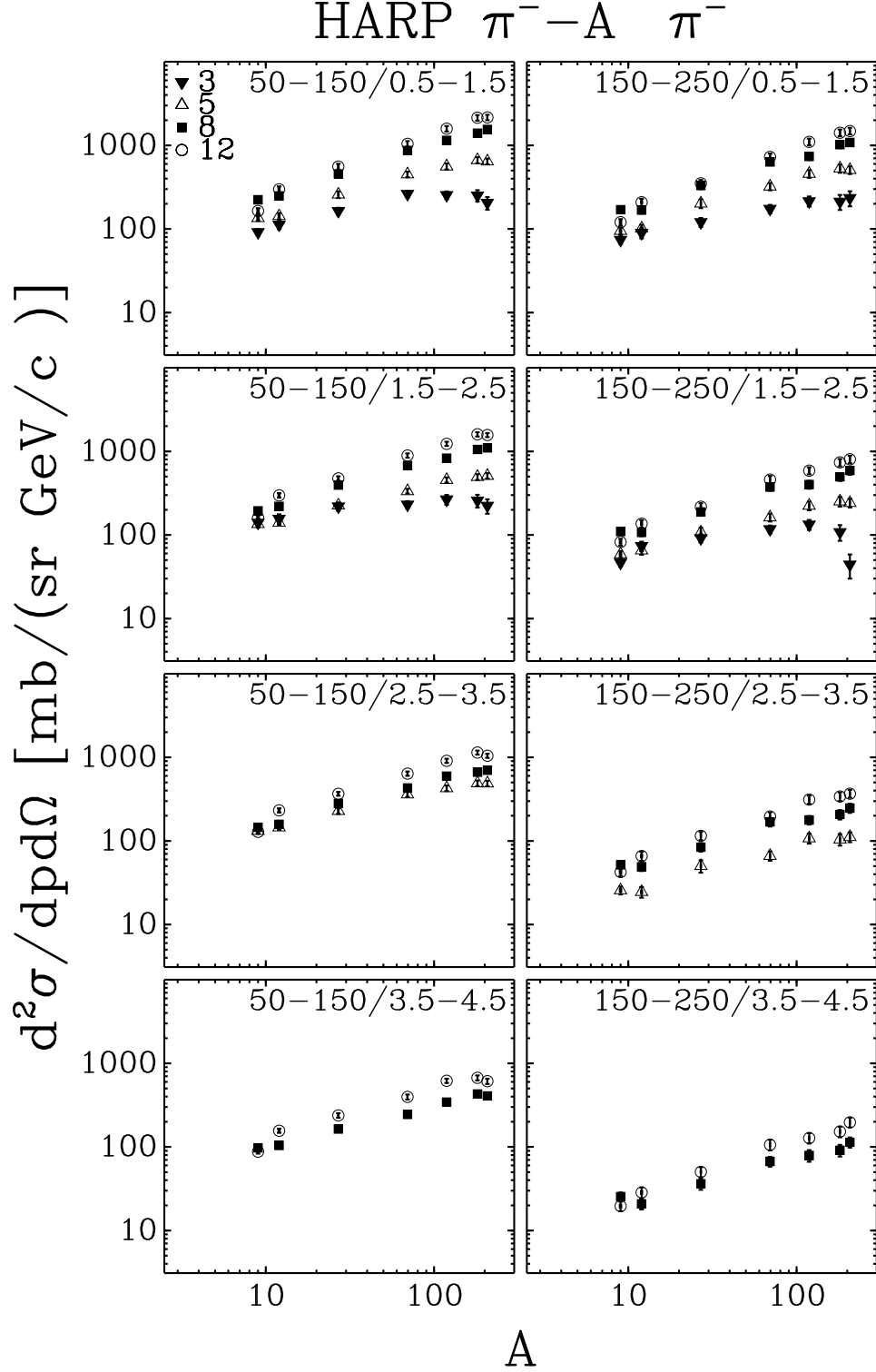


Figure 10: The dependence on the atomic number A of the π^- production yields in π^- -Be, π^- -C, π^- -Al, π^- -Cu, π^- -Sn, π^- -Ta, π^- -Pb interactions averaged over two forward angular region ($0.05 \text{ rad} \leq \theta < 0.15 \text{ rad}$ and $0.15 \text{ rad} \leq \theta < 0.25 \text{ rad}$) and four momentum regions ($0.5 \text{ GeV}/c \leq p < 1.5 \text{ GeV}/c$, $1.5 \text{ GeV}/c \leq p < 2.5 \text{ GeV}/c$, $2.5 \text{ GeV}/c \leq p < 3.5 \text{ GeV}/c$ and $3.5 \text{ GeV}/c \leq p < 4.5 \text{ GeV}/c$), for the four different incoming beam momenta (from $3 \text{ GeV}/c$ to $12 \text{ GeV}/c$).

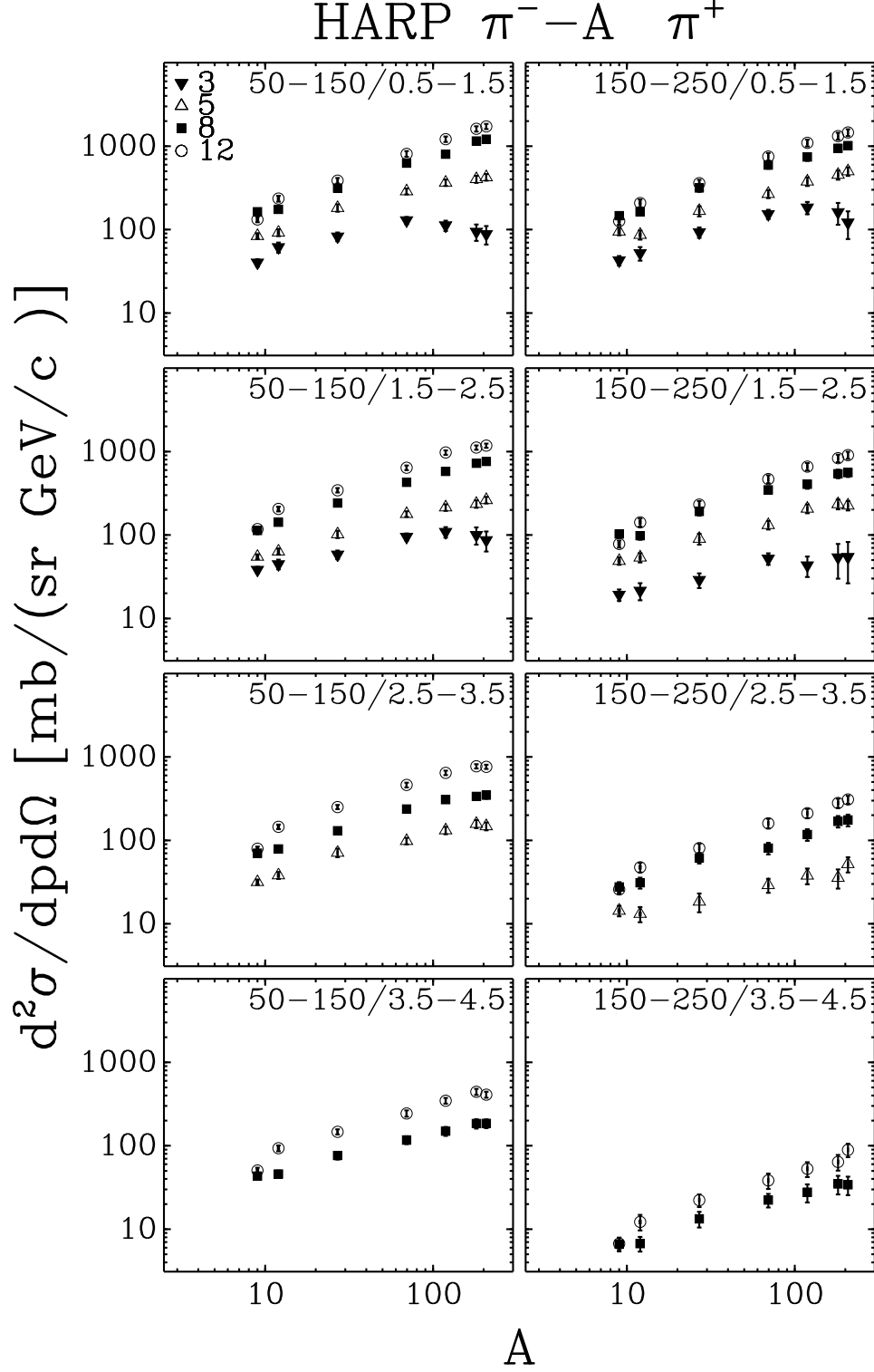


Figure 11: The dependence on the atomic number A of the π^+ production yields in π^- -Be, π^- -C, π^- -Al, π^- -Cu, π^- -Sn, π^- -Ta, π^- -Pb interactions averaged over two forward angular region ($0.05 \text{ rad} \leq \theta < 0.15 \text{ rad}$ and $0.15 \text{ rad} \leq \theta < 0.25 \text{ rad}$) and four momentum regions ($0.5 \text{ GeV}/c \leq p < 1.5 \text{ GeV}/c$, $1.5 \text{ GeV}/c \leq p < 2.5 \text{ GeV}/c$, $2.5 \text{ GeV}/c \leq p < 3.5 \text{ GeV}/c$ and $3.5 \text{ GeV}/c \leq p < 4.5 \text{ GeV}/c$), for the four different incoming beam momenta (from $3 \text{ GeV}/c$ to $12 \text{ GeV}/c$).

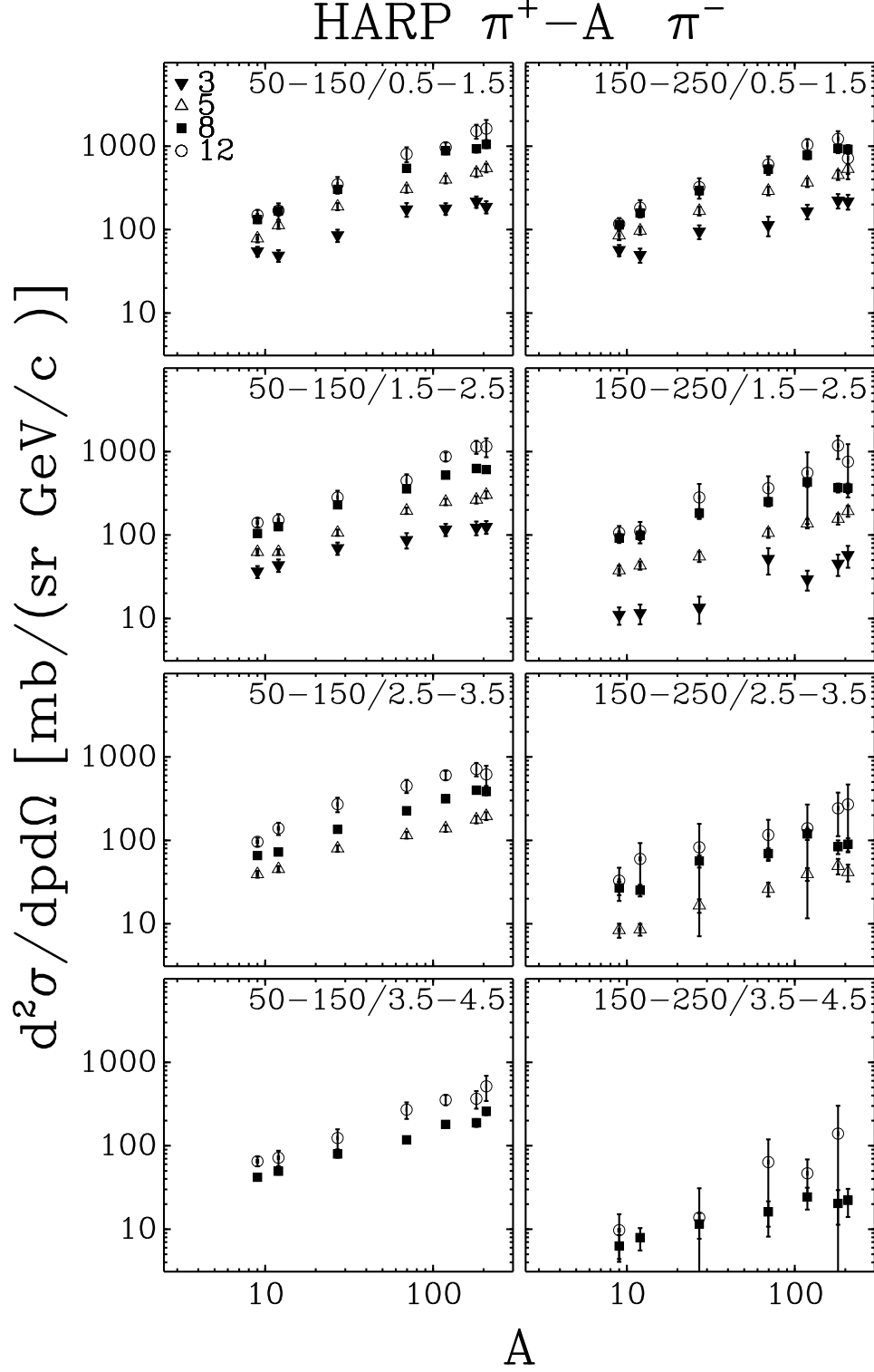


Figure 12: The dependence on the atomic number A of the π^- production yields in π^+ -Be, π^+ -C, π^+ -Al, π^+ -Cu, π^+ -Sn, π^+ -Ta, π^+ -Pb interactions averaged over two forward angular region ($0.05 \text{ rad} \leq \theta < 0.15 \text{ rad}$ and $0.15 \text{ rad} \leq \theta < 0.25 \text{ rad}$) and four momentum regions ($0.5 \text{ GeV}/c \leq p < 1.5 \text{ GeV}/c$, $1.5 \text{ GeV}/c \leq p < 2.5 \text{ GeV}/c$, $2.5 \text{ GeV}/c \leq p < 3.5 \text{ GeV}/c$ and $3.5 \text{ GeV}/c \leq p < 4.5 \text{ GeV}/c$), for the four different incoming beam momenta (from 3 GeV/c to 12 GeV/c).

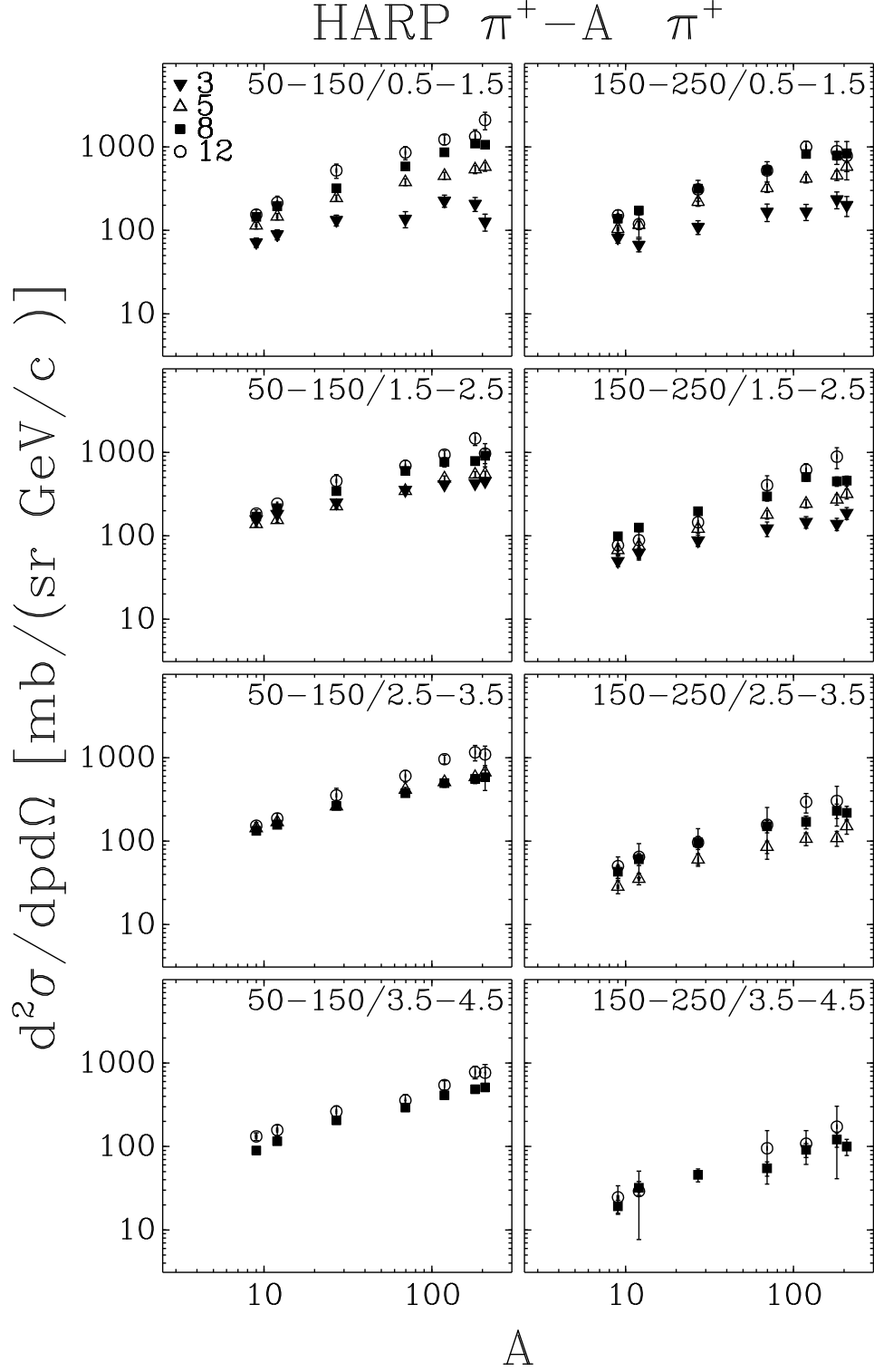


Figure 13: The dependence on the atomic number A of the π^+ production yields in π^+ -Be, π^+ -C, π^+ -Al, π^+ -Cu, π^+ -Sn, π^+ -Ta, π^+ -Pb interactions averaged over two forward angular region ($0.05 \text{ rad} \leq \theta < 0.15 \text{ rad}$ and $0.15 \text{ rad} \leq \theta < 0.25 \text{ rad}$) and four momentum regions ($0.5 \text{ GeV}/c \leq p < 1.5 \text{ GeV}/c$, $1.5 \text{ GeV}/c \leq p < 2.5 \text{ GeV}/c$, $2.5 \text{ GeV}/c \leq p < 3.5 \text{ GeV}/c$ and $3.5 \text{ GeV}/c \leq p < 4.5 \text{ GeV}/c$), for the four different incoming beam momenta (from 3 GeV/c to 12 GeV/c).

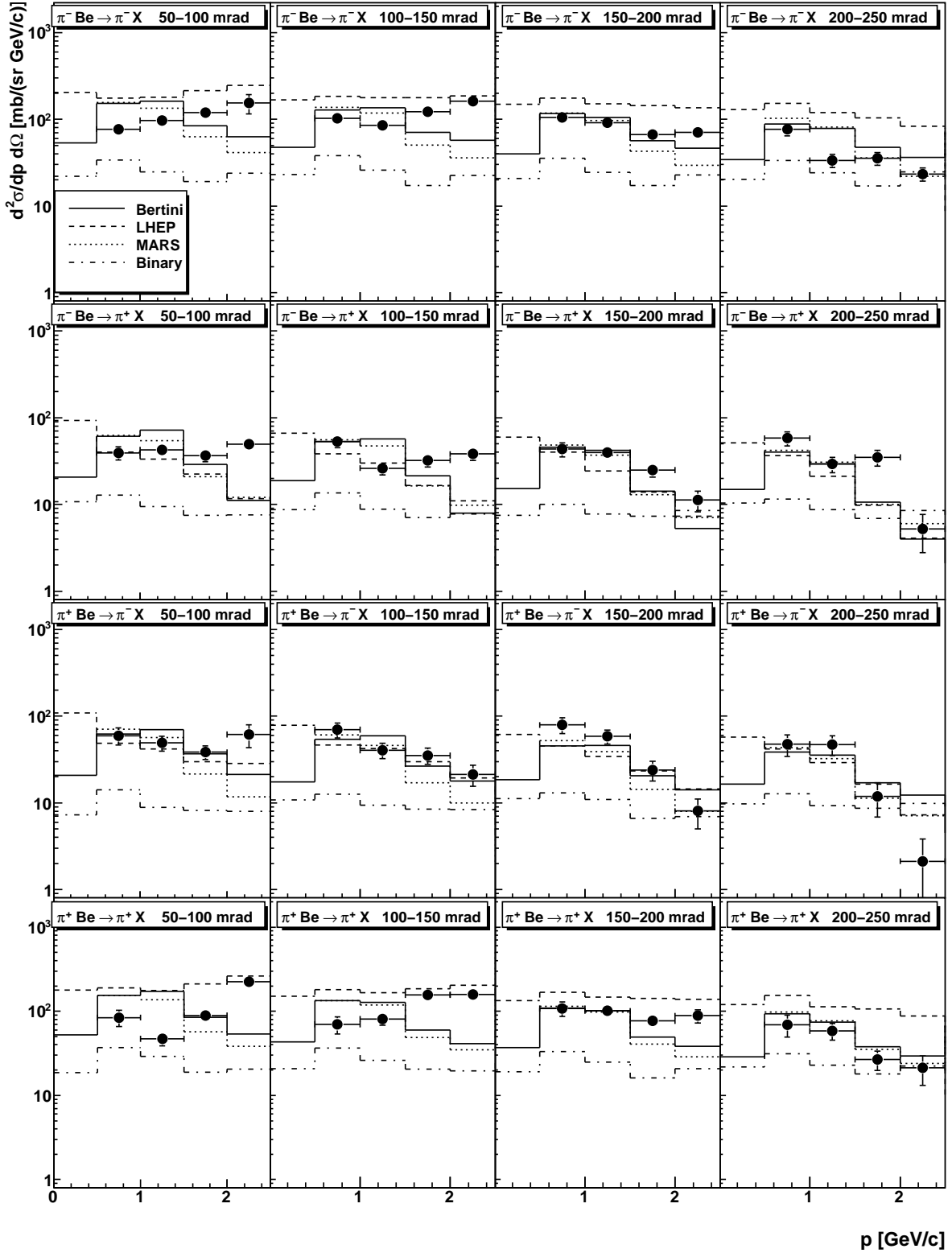


Figure 14: Comparison of HARP double-differential π^\pm cross-sections for π -Be at 3 GeV/c with GEANT4 and MARS MC predictions, using several generator models.

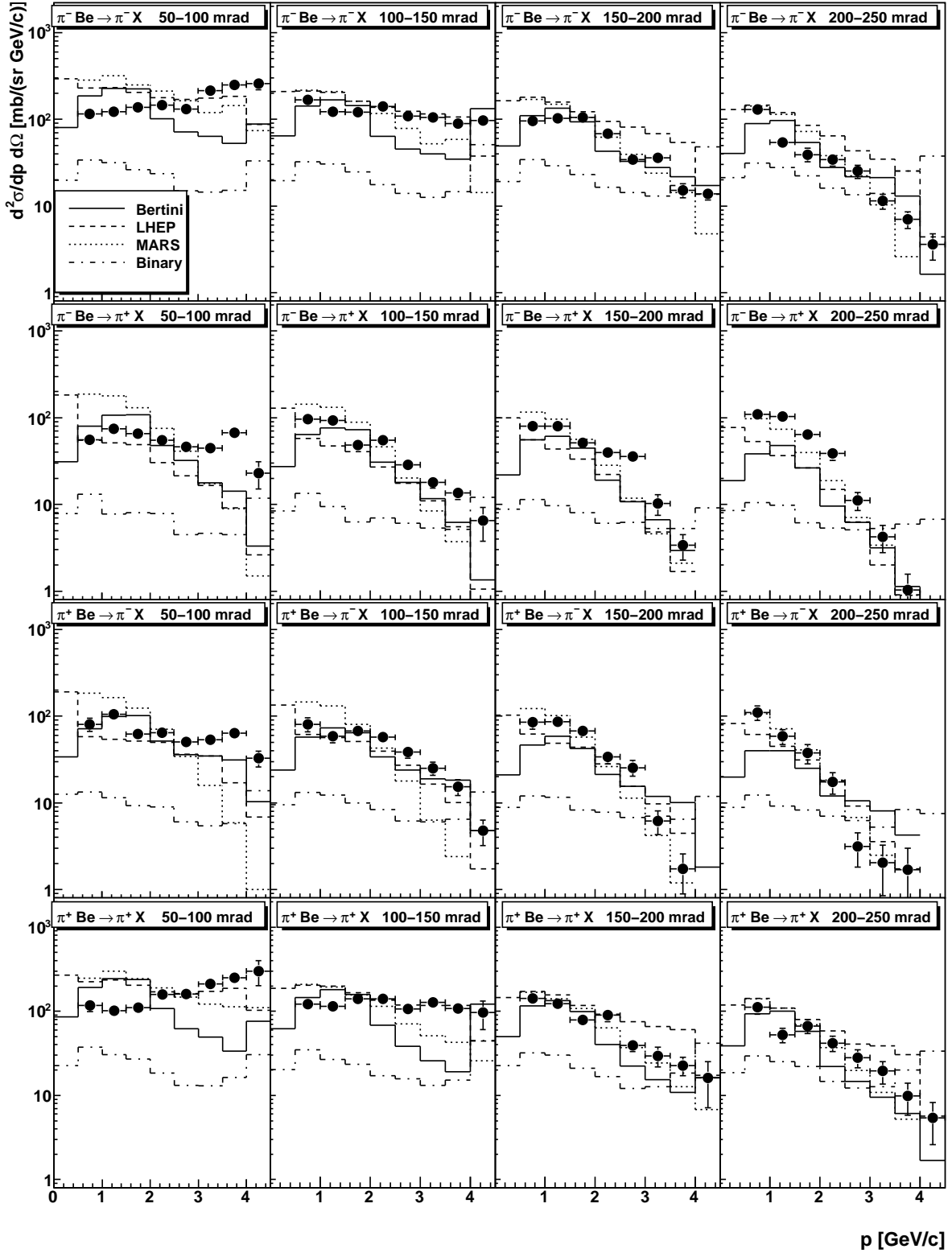


Figure 15: Comparison of HARP double-differential π^\pm cross-sections for π -Be at 5 GeV/c with GEANT4 and MARS MC predictions, using several generator models.

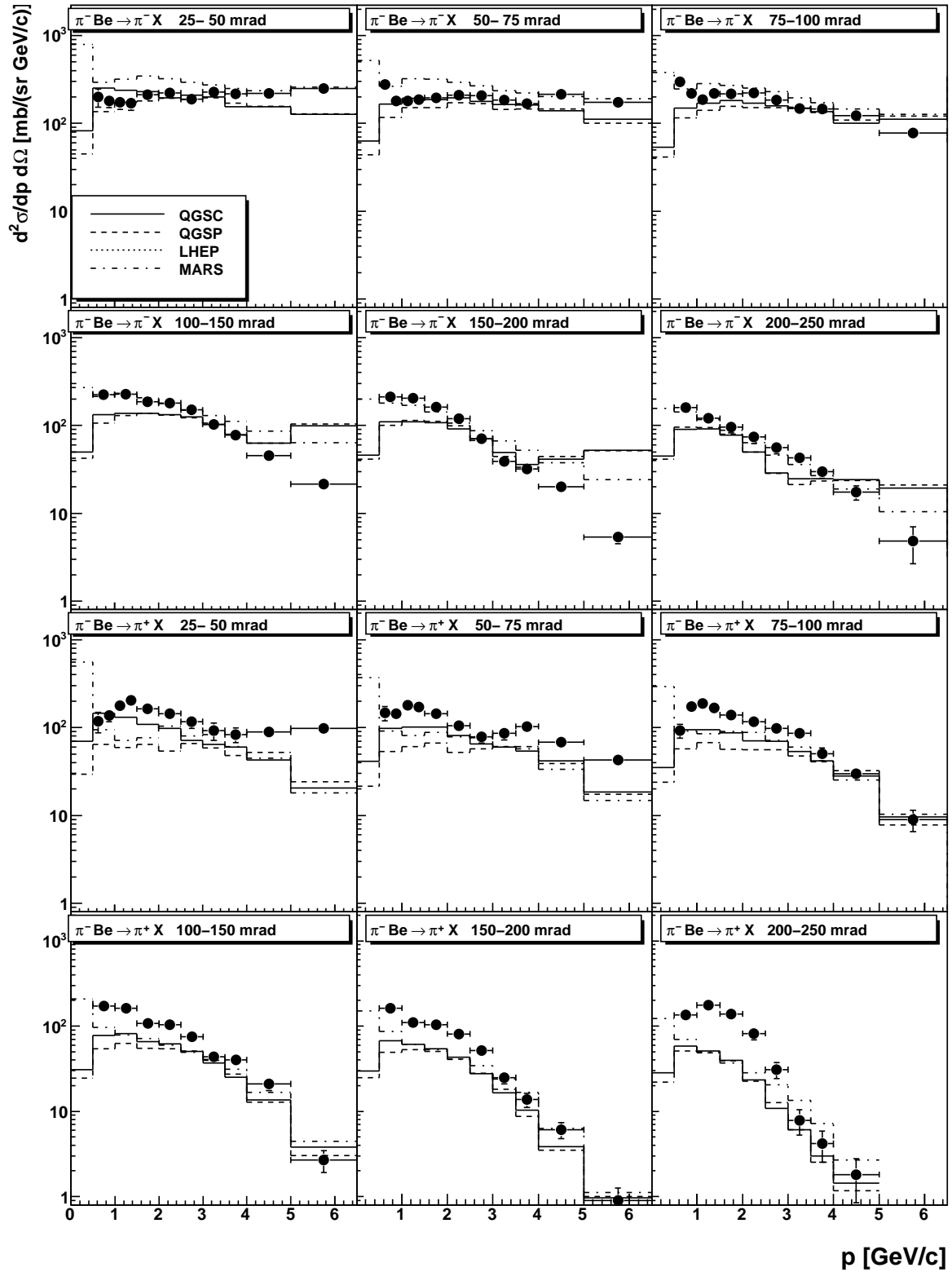


Figure 16: Comparison of HARP double-differential π^\pm cross-sections for π^- -Be at 8 GeV/c with GEANT4 and MARS MC predictions, using several generator models.

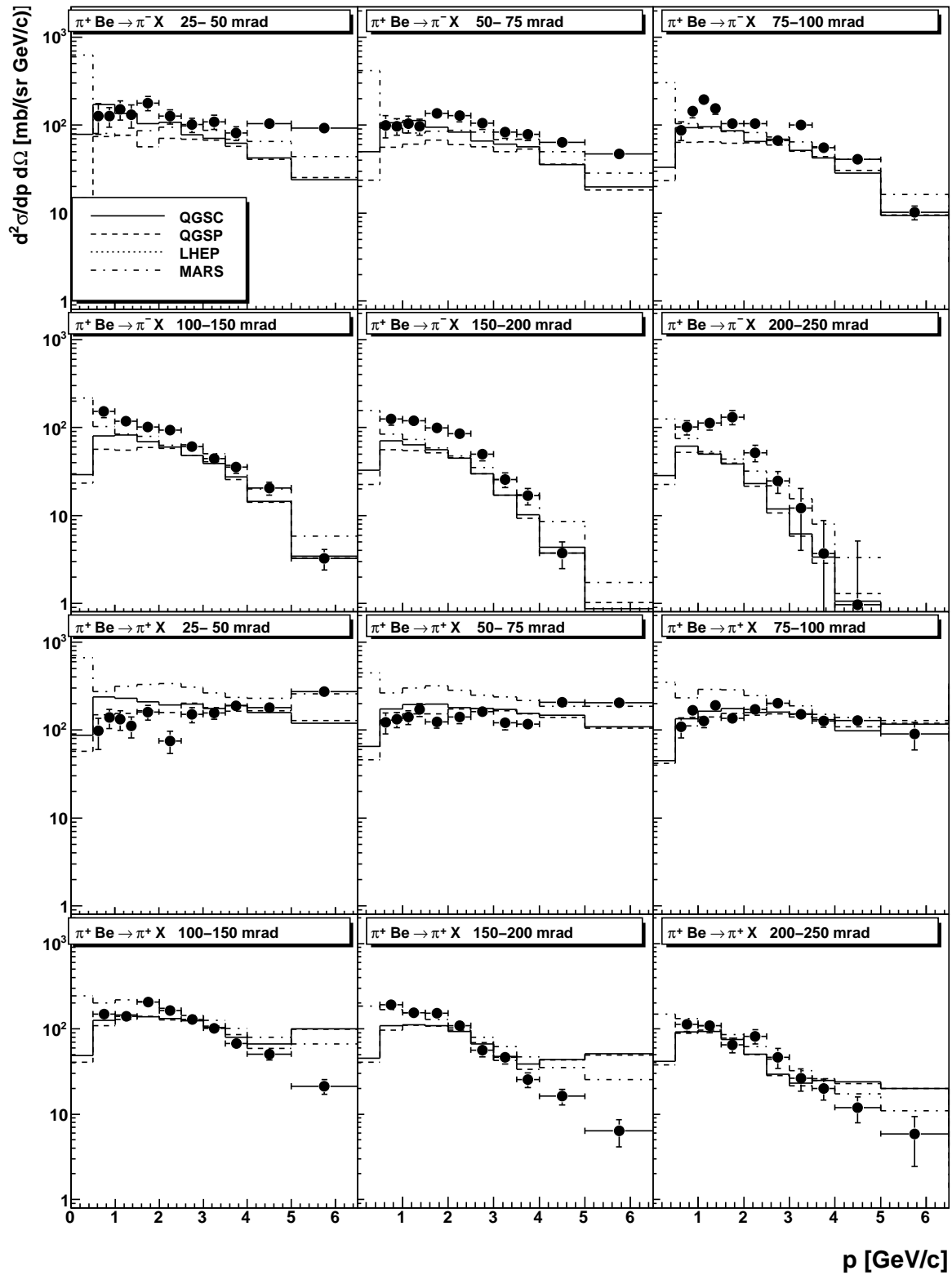


Figure 17: Comparison of HARP double-differential π^\pm cross-sections for π^+ -Be at 8 GeV/c with GEANT4 and MARS MC predictions, using several generator models.

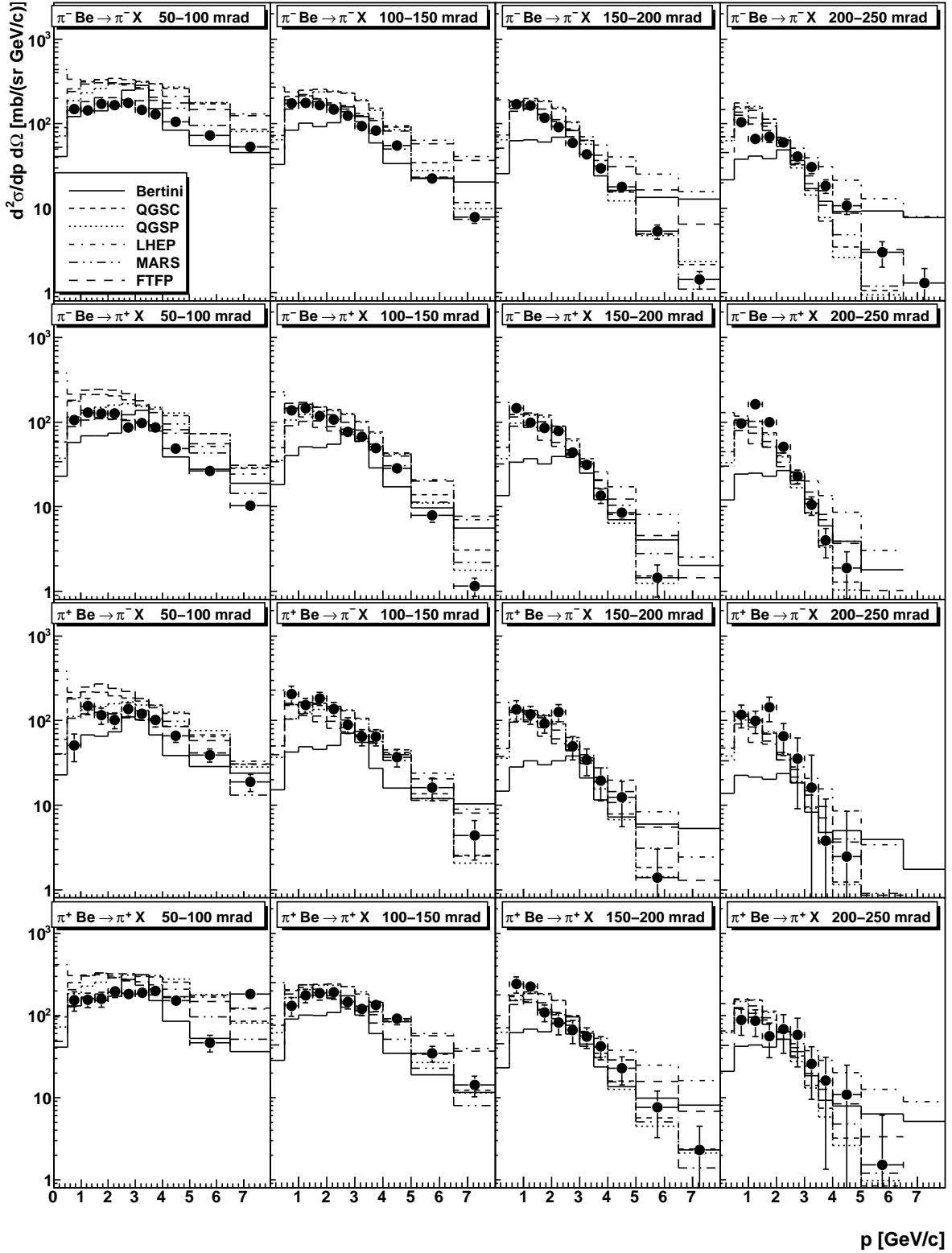


Figure 18: Comparison of HARP double-differential π^\pm cross-sections for π -Be at 12 GeV/c with GEANT4 and MARS MC predictions, using several generator models.

The MARS code system [25] uses as basic model an inclusive approach to multiparticle production originated by R. Feynman in 1974. At each interaction vertex, a particle cascade tree is constructed by using a fixed number of particles with weights that in the simplest case are equal to the partial mean multiplicity of that event. Above 3 GeV phenomenological particle production models are used, while below 5 GeV a cascade-exciton model [33] combined with the Fermi break-up model, the coalescence model, an evaporation model and a multifragmentation extension are used instead.

HARP measurements have been compared to the available models, first renormalizing MC predictions to data and then computing the χ^2 between models and data themselves. Normalization factors are shown in Tables 2 and 3. An absolute comparison yields χ^2 values that are too large to be meaningful. Over the full energy range covered by the HARP experiment, the best comparison is obtained with the MARS Monte Carlo which is on average 10% below the data, with a maximum shift of 30%. This may be owing to the fact that MARS is using different models in different energy regions, equivalent to use a collection of models as implemented in the “physics lists” of GEANT4. Unfortunately, all models have very bad χ^2 compared with the data, showing significant inconsistencies in the shape distribution. This is worse than the situation with incident protons and may be explained by the fact that in the latter case some experimental data were available for tuning of the Monte Carlo simulations. This was not the case with incident pions in the momentum range studied here (below 15 GeV/c).

At higher energies the FTP model (from GEANT4) and the MARS model describe the data better, while at the lowest energies the Bertini and binary cascade models (from GEANT4) seem more appropriate. Parametrized models, such as LHEP from GEANT4, show important discrepancies.

Table 2: Normalization factors data over MC for some models, incident π^+ .

Generator	Be		Ta		Be		Ta		Be		Ta		Be		Ta	
	3 GeV/c		3 GeV/c		5 GeV/c		5 GeV/c		8 GeV/c		8 GeV/c		12 GeV/c		12 GeV/c	
	π^+	π^-	π^+	π^-	π^+	π^-	π^+	π^-	π^+	π^-	π^+	π^-	π^+	π^-	π^+	π^-
Bertini	1.1	1.1	0.9	0.6	1.3	1.3	1.1	1.1	1.7	1.4	1.5	1.4	2.0	1.4	1.9	1.6
LHEP	1.3	0.6	2.8	1.0	1.5	0.8	2.5	1.1	1.3	0.8	1.0	0.5	1.0	0.8	0.7	0.5
QGSC	-	-	-	-	-	-	-	-	1.6	1.0	1.2	0.7	0.8	0.7	1.0	0.8
QGSP	-	-	-	-	-	-	-	-	1.9	1.0	1.2	0.6	0.9	0.8	0.8	0.6
FTFP	-	-	-	-	-	-	-	-	-	-	0.8	0.7	1.1	1.0	0.9	0.8
MARS	1.3	1.2	1.2	0.9	0.9	1.0	0.7	0.6	1.0	1.1	0.8	0.6	0.8	1.0	0.8	0.7

Table 3: Normalization factors data over MC for some models, incident π^- .

Generator	Be		Ta		Be		Ta		Be		Ta		Be		Ta	
	3 GeV/c		3 GeV/c		5 GeV/c		5 GeV/c		8 GeV/c		8 GeV/c		12 GeV/c		12 GeV/c	
	π^+	π^-	π^+	π^-	π^+	π^-	π^+	π^-	π^+	π^-	π^+	π^-	π^+	π^-	π^+	π^-
Bertini	1.0	1.1	0.5	0.6	1.2	1.4	0.9	1.2	1.6	2.1	1.4	1.9	1.2	1.6	1.6	2.1
LHEP	0.5	1.6	0.7	2.9	0.8	1.9	1.0	2.6	0.9	1.7	0.6	1.2	0.6	1.0	0.5	0.7
QGSC	-	-	-	-	-	-	-	-	1.1	1.8	0.7	1.3	0.6	0.7	0.8	1.1
QGSP	-	-	-	-	-	-	-	-	1.2	2.2	0.7	1.4	0.6	0.8	0.6	0.9
FTFP	-	-	-	-	-	-	-	-	-	-	0.7	1.1	0.7	1.0	0.8	1.1
MARS	1.1	1.2	0.7	1.0	0.9	0.9	0.6	0.6	1.2	1.2	0.7	0.9	0.8	0.7	0.7	0.9

The full set of HARP data, taken with targets spanning the full periodic table of elements, with small total errors and full coverage of the solid angle in a single detector will definitely help the validation of models used in hadronic simulations in the difficult energy range between 3 GeV/c and 15 GeV/c of incident momentum with incident pions, where data were previously missing.

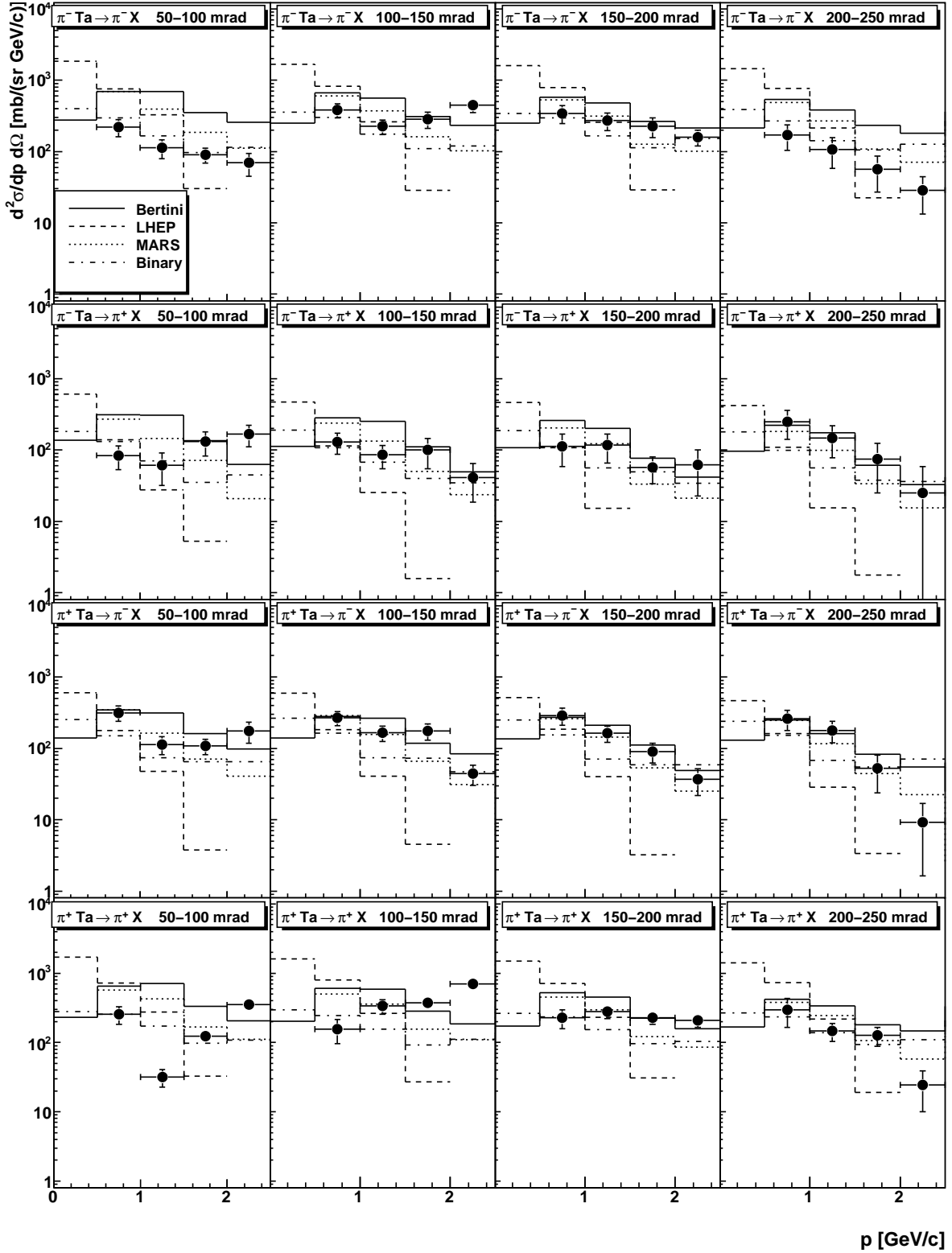


Figure 19: Comparison of HARP double-differential π^\pm cross-sections for π^- -Ta at 3 GeV/c with GEANT4 and MARS MC predictions, using several generator models.

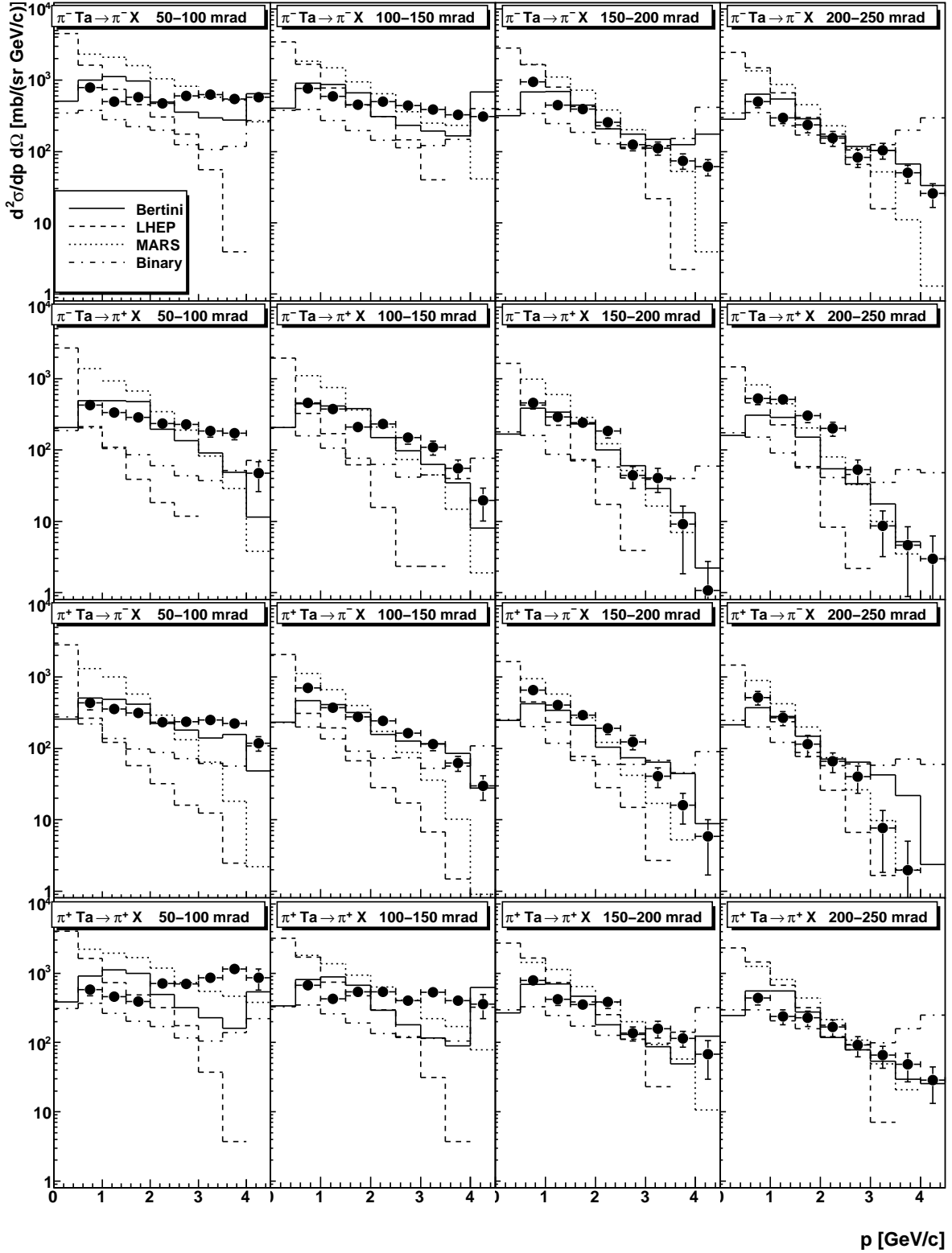


Figure 20: Comparison of HARP double-differential π^\pm cross-sections for π^- -Ta at 5 GeV/c with GEANT4 and MARS MC predictions, using several generator models.

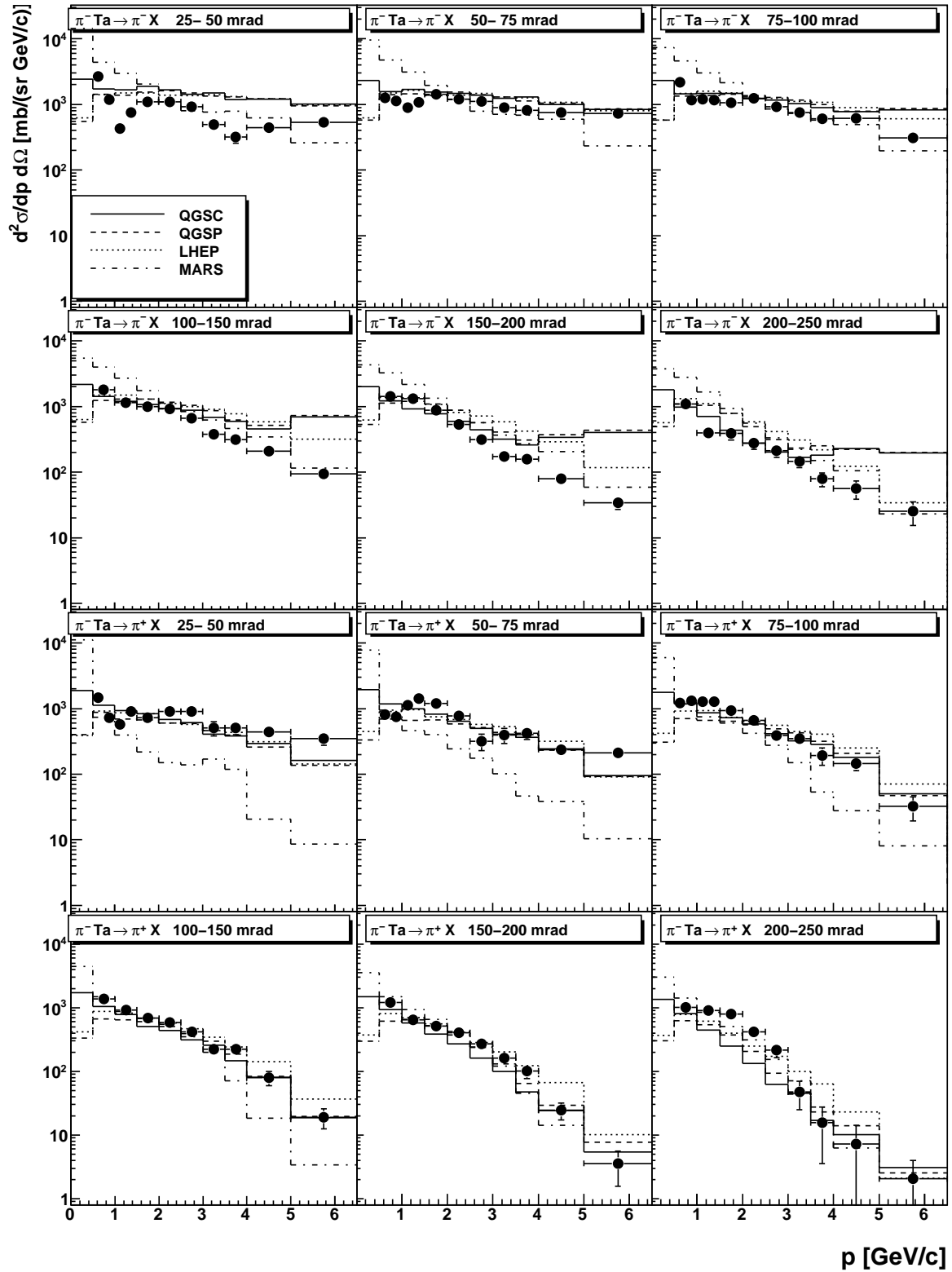


Figure 21: Comparison of HARP double-differential π^\pm cross-sections for π^- -Ta at 8 GeV/c with GEANT4 and MARS MC predictions, using several generator models.

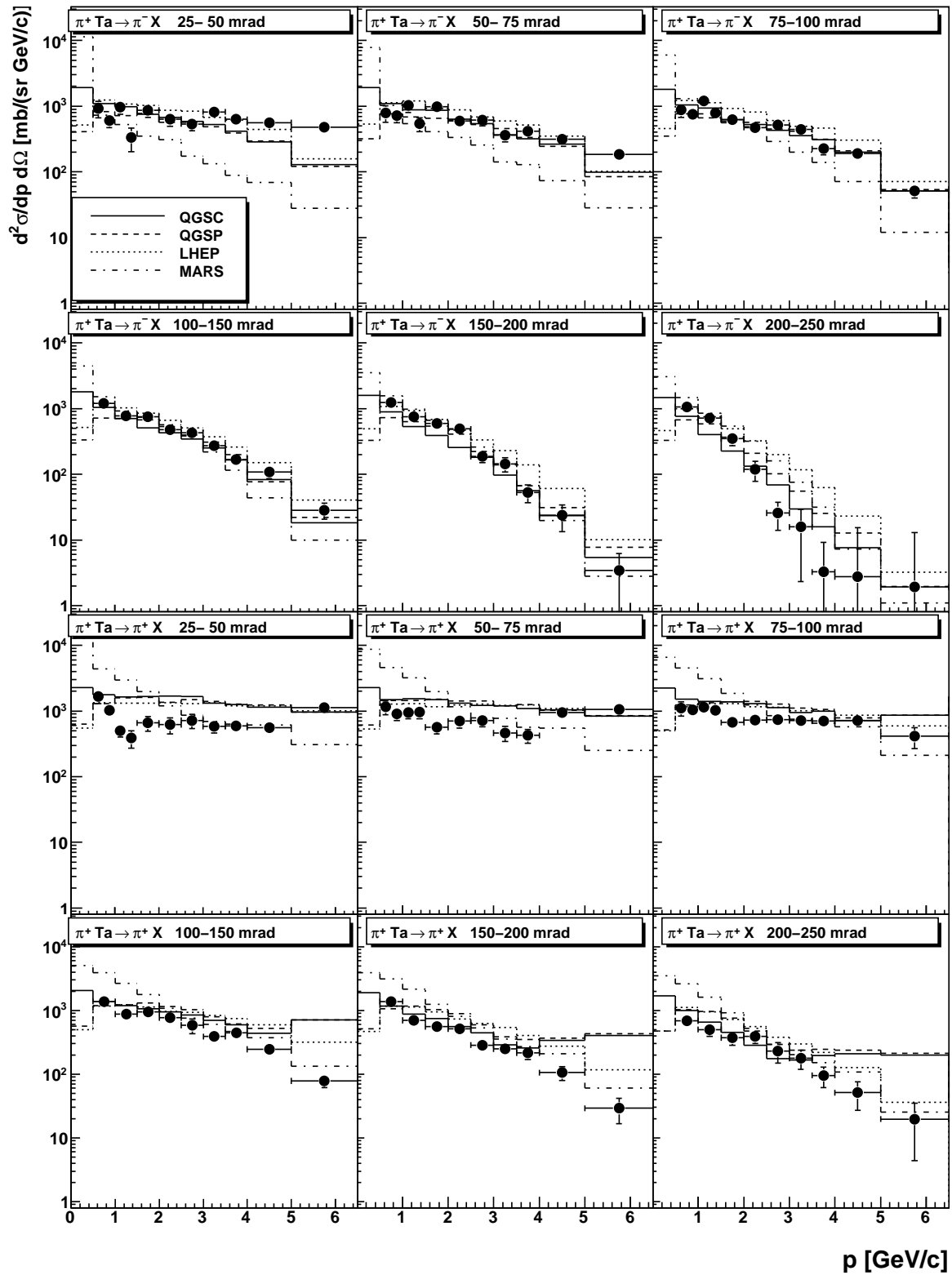


Figure 22: Comparison of HARP double-differential π^\pm cross-sections for π^\pm -Ta at 8 GeV/c with GEANT4 and MARS MC predictions, using several generator models.

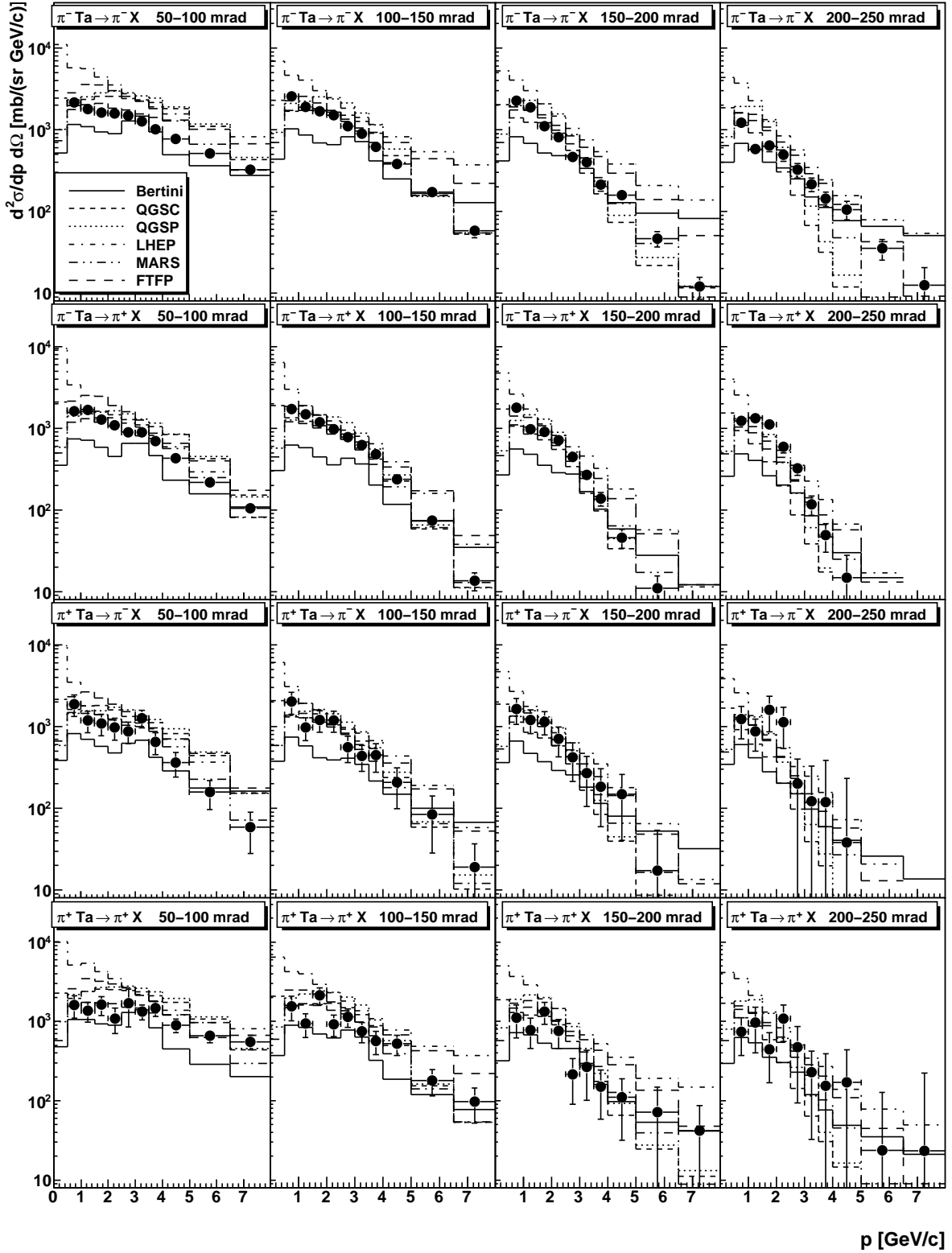


Figure 23: Comparison of HARP double-differential π^\pm cross-sections for π -Ta at 12 GeV/c with GEANT4 and MARS MC predictions, using several generator models.

4 Summary and conclusions

Double-differential cross-sections for the production of positive and negative pions in the kinematic range $0.5 \text{ GeV}/c \leq p_\pi \leq 8 \text{ GeV}/c$ and $0.025 \text{ rad} \leq \theta_\pi \leq 0.25 \text{ rad}$ from the interactions of 3, 5, 8 and 12 GeV/c π^\pm on beryllium, carbon, aluminium, copper, tin, tantalum and lead targets of 5% interaction length thickness have been reported.

We should stress that the HARP data are the first precision measurements with incoming charged pion beams in this kinematic region and may have a major impact on the tuning of Monte Carlo generators at low energies. Quantitative comparisons with a variety of generators currently in use have been presented.

The pion yield averaged over different momentum and angular ranges increase smoothly with the atomic number A of the target and with the energy of the incoming pion beam.

5 Acknowledgments

We gratefully acknowledge the help and support of the PS beam staff and of the numerous technical collaborators who contributed to the detector design, construction, commissioning and operation. In particular, we would like to thank G. Barichello, R. Brocard, K. Burin, V. Carassiti, F. Chignoli, D. Conventi, G. Decreuse, M. Delattre, C. Detraz, A. Domeniconi, M. Dwuznik, F. Evangelisti, B. Friend, A. Iacifano, I. Krasin, D. Lacroix, J.-C. Legrand, M. Lobello, M. Lollo, J. Loquet, F. Marinilli, R. Mazza, J. Mulon, L. Musa, R. Nicholson, A. Pepato, P. Petev, X. Pons, I. Rusinov, M. Scandurra, E. Usenko, R. van der Vlugt, for their support in the construction of the detector and P. Dini for his contribution to Monte Carlo production. The collaboration acknowledges the major contributions and advice of M. Baldo-Ceolin, L. Linssen, M.T. Muciaccia and A. Pullia during the construction of the experiment. The collaboration is indebted to V. Ableev, F. Bergsma, P. Binko, E. Boter, M. Calvi, C. Cavion, M. Chizov, A. Chukanov, A. DeSanto, A. DeMin, M. Doucet, D. Düllmann, V. Ermilova, W. Flegel, Y. Hayato, A. Ichikawa, O. Klimov, T. Kobayashi, D. Kustov, M. Laveder, M. Mass, H. Meinhard, A. Menegolli, T. Nakaya, K. Nishikawa, M. Paganoni, F. Paleari, M. Pasquali, M. Placentino, V. Serdiouk, S. Simone, P.J. Soler, S. Troquereau, S. Ueda, A. Valassi and R. Veenhof for their contributions to the experiment.

We acknowledge the contributions of V. Ammosov, G. Chelkov, D. Dedovich, F. Dydak, M. Gostkin, A. Guskov, D. Khartchenko, V. Koreshev, Z. Kroumchtein, I. Nefedov, A. Semak, J. Wotschack, V. Zaets and A. Zhemchugov to the work described in this paper.

The experiment was made possible by grants from the Institut Interuniversitaire des Sciences Nucléaires and the Interuniversitair Instituut voor Kernwetenschappen (Belgium), Ministerio de Educacion y Ciencia, Grant FPA2003-06921-c02-02 and Generalitat Valenciana, grant GV00-054-1, CERN (Geneva, Switzerland), the German Bundesministerium für Bildung und Forschung (Germany), the Istituto Nazionale di Fisica Nucleare (Italy), INR RAS (Moscow), the Russian Foundation for Basic Research (grant 08-02-00018), the Particle Physics and Astronomy Research Council (UK) and the Swiss National Science Foundation, in the framework of the SCOPES programme. We gratefully acknowledge their support.

References

- [1] M. G. Catanesi *et al.*, HARP Collaboration, “Proposal to study hadron production for the neutrino factory and for the atmospheric neutrino flux”, CERN-SPSC/99-35 (1999).
- [2] G. Ambrosini *et al.* [NA56 Collaboration], *Eur. Phys. J. C* **10** (1999) 605;
G. Ambrosini *et al.* [NA56 Collaboration], *Phys. Lett. B* **420** (1998) 225;
G. Ambrosini *et al.* [NA56 Collaboration], *Phys. Lett. B* **425** (1998) 208.
- [3] H.W. Atherton, CERN 80-07, August 1980.

- [4] M. Bonesini and A. Guglielmi, Phys. Rep. 433 (2006) 66.
- [5] M. G. Catanesi *et al.* [HARP Collaboration], “Measurement of the production cross-section of positive pions in p-Al collisions at 12.9 GeV/ c ”, Nucl. Phys. B **732** (2006) 1 [arXiv:hep-ex/0510039].
- [6] M. G. Catanesi *et al.* [HARP Collaboration], “Measurement of the production cross-section of positive pions in the collision of 8.9 GeV/ c protons on beryllium”, Eur. Phys. J. C **52** (2007) 29 [arXiv:hep-ex/0702024].
- [7] M. G. Catanesi *et al.* [HARP Collaboration], “Measurement of the production cross-sections of π^\pm in p-C and π^\pm -C interactions at 12 GeV/ c ”, Astroparticle Physics 29/4 (2008) 257, arXiv:0802.0657 [astro-ph].
- [8] M. G. Catanesi *et al.* [HARP Collaboration], “Forward π^\pm production in p-O₂ and p-N₂ interactions at 12 GeV/ c ”, Astroparticle Physics 30/3 (2008) 124, arXiv:0807.1025 [hep-ex].
- [9] H.R. Blieden *et al.*, Phys. ReV. **D11**, 14 (1975).
- [10] MIPP Collaboration, <http://ppd.fnal.gov/experiments/2907/>;
R. Raja, “The Main Injector particle production Experiment (MIPP) at Fermilab”, Jour. Phys. Conf. Series **9** (2005) 303.
- [11] D. Isenhower *et al.*, Proposal to update the MIPP experiment, Fermilab Proposal P-960.
- [12] M. G. Catanesi *et al.* [HARP Collaboration], “The HARP Detector at the CERN PS”, Nucl. Instrum. Meth. A **571** (2007) 527.
- [13] M. Anfreville *et al.*, “The drift chambers of the NOMAD experiment”, Nucl. Instrum. Meth. A **481** (2002) 339 [arXiv:hep-ex/0104012].
- [14] M. Baldo-Ceolin *et al.*, “The Time-Of-Flight TOFW Detector Of The HARP Experiment: Construction And Performance”, Nucl. Instrum. Meth. A **532** (2004) 548;
M. Bonesini *et al.*, “Construction of a Fast-laser Calibration System for the HARP TOF counter wall”, IEEE Trans. Nucl. Science **50** (2003) 541.
- [15] L. Durieu, A. Mueller and M. Martini, PAC-2001-TPAH142 *Presented at IEEE Particle Accelerator Conference (PAC2001), Chicago, Illinois, 18-22 Jun 2001*;
L. Durieu *et al.*, Proceedings of PAC’97, Vancouver, (1997);
L. Durieu, O. Fernando, CERN PS/PA Note 96-38.
- [16] K. Pretzl *et al.*, Invited talk at the “International Symposium on Strangeness and Quark Matter”, Crete, (1999) 230.
- [17] M. G. Catanesi *et al.* [HARP Collaboration], “Particle identification algorithms for the HARP forward spectrometer”, Nucl. Instrum. Meth. A **572** (2007) 899.
- [18] G. D’Agostini, DESY 94-099, ISSN 0418-9833, 1994.
G. D’Agostini, Nucl. Instrum. Meth. A **362** (1995) 487.
- [19] M. G. Catanesi *et al.*, [HARP Collaboration], “Measurement of the Production of charged Pions by Protons on a Tantalum Target”, Eur. Phys. J. C **51** (2007) 787, arXiv:0706.1600 [hep-ex]
- [20] M. G. Catanesi *et al.*, [HARP Collaboration], “Large-angle production of charged pions by 3 GeV/ c –12 GeV/ c protons on carbon, copper and tin targets”, Eur. Phys. C **53** (2008) 177, arXiv:0709.3464 [hep-ex],
- [21] M. G. Catanesi *et al.*, [HARP Collaboration], “Large-angle production of charged pions by 3 GeV/ c –12.9 GeV/ c protons on beryllium, aluminium and lead targets”, Eur. Phys. C **54** (2008) 37, arXiv:0709.3458 [hep-ex].
- [22] M. G. Catanesi *et al.*, [HARP Collaboration], “Large-angle production of charged pions with incident protons on nuclear targets as measured in the HARP experiment”, Phys. ReV. **C77** (2008) 055207.

- [23] S. Agostinelli *et al.* [GEANT4 Collaboration], Nucl. Instrum. Meth. A **506** (2003) 250.
- [24] V. Ivanchenko, "Simulation and recent results of the HARP experiment", NSS Conference Record, 2006, IEEE, Vol3, pp.1660-1665
- [25] N.V. Mokhov, S.I. Striganov, "MARS overview", FERMILAB-CONF-07-008-AD, 2007.
- [26] D.H. Wright *et al.*, AIP Conf. Proc. 867 (2006) 479.
- [27] D.H. Wright *et al.*, AIP Conf. Proc. 896 (2007) 11.
- [28] A. Heikkinen *et al.* e-print physics/0306008.
- [29] G. Folger, V. Ivanchenko and H.P. Wellisch, Eur. Phys. J. A21 (2004) 407.
- [30] H.W. Bertini, P. Guthrie, Nucl. Phys. **A169** (1971).
- [31] G. Folger and H.P. Wellisch, e-print physics/0306007.
- [32] H. Fesefeld, Technical report PITHA 85-02, Aachen, 1985.
- [33] S.G. Mashnik *et al.*, LANL report LA-UR-05-7321, 2005.

A Cross-section data

The following tables report the measured differential cross-section for positive and negative pion production in interactions of 3, 5, 8 and 12 GeV/ c momentum charged pions on different types of nuclear targets. The data are presented in the kinematic range of $0.5 \text{ GeV}/c \leq p_\pi \leq 8 \text{ GeV}/c$ and $0.05 \text{ rad} \leq \theta_\pi \leq 0.25 \text{ rad}$. The overall normalization uncertainty ($\leq 2\%$) is not included in the reported errors.

Results at higher incoming beam momenta, from 8 GeV/ c to 12.9 GeV/ c , are also presented extending to a lower value of the polar angle θ (0.025 rad), using a finer binning. This second set of tables contains additional data for collisions of 12.9 GeV/ c π^\pm on Al and 8.9 GeV/ c π^\pm on Be.

The cross-section values in some bins of the following tables are omitted and replaced by the symbol $* \pm *$, due to instabilities in the unfolding procedure coming from the low statistics available.

Table 4: HARP results for the double-differential π^+ production cross-section in the laboratory system, $d^2\sigma^\pi/(dpd\Omega)$, for π^- -Be interactions at 3,5,8,12 GeV/c. Each row refers to a different ($p_{\min} \leq p < p_{\max}, \theta_{\min} \leq \theta < \theta_{\max}$) bin, where p and θ are the pion momentum and polar angle, respectively. The central value as well as the square-root of the diagonal elements of the covariance matrix are given.

θ_{\min} (rad)	θ_{\max} (rad)	p_{\min} (GeV/c)	p_{\max} (GeV/c)	$d^2\sigma^{\pi^+}/(dpd\Omega)$ (barn/(GeV/c sr))			
				3 GeV/c	5 GeV/c	8 GeV/c	12 GeV/c
0.05	0.10	0.50	1.00	0.038±0.007	0.054±0.007	0.14±0.02	0.106±0.012
		1.00	1.50	0.042±0.006	0.073±0.007	0.177±0.011	0.130±0.010
		1.50	2.00	0.035±0.005	0.064±0.006	0.141±0.009	0.127±0.010
		2.00	2.50	0.048±0.007	0.053±0.005	0.112±0.008	0.127±0.008
		2.50	3.00	±	0.045±0.004	0.090±0.008	0.086±0.006
		3.00	3.50	±	0.044±0.005	0.086±0.008	0.097±0.008
		3.50	4.00	±	0.066±0.005	0.072±0.007	0.087±0.007
		4.00	5.00	±	0.022±0.008	0.046±0.004	0.049±0.004
		5.00	6.50	±	±	0.023±0.003	0.027±0.002
		6.50	8.00	±	±	±	0.010±0.001
0.10	0.15	0.50	1.00	0.052±0.008	0.094±0.011	0.17±0.02	0.137±0.015
		1.00	1.50	0.026±0.004	0.091±0.009	0.162±0.013	0.145±0.012
		1.50	2.00	0.032±0.005	0.047±0.005	0.107±0.010	0.117±0.010
		2.00	2.50	0.037±0.006	0.054±0.006	0.104±0.009	0.107±0.010
		2.50	3.00	±	0.028±0.004	0.075±0.007	0.077±0.007
		3.00	3.50	±	0.018±0.003	0.044±0.005	0.068±0.006
		3.50	4.00	±	0.013±0.002	0.040±0.004	0.049±0.005
		4.00	5.00	±	0.006±0.003	0.021±0.004	0.028±0.003
		5.00	6.50	±	±	0.003±0.001	0.008±0.001
		6.50	8.00	±	±	±	0.001±0.000
0.15	0.20	0.50	1.00	0.042±0.008	0.078±0.010	0.16±0.02	0.15±0.02
		1.00	1.50	0.039±0.005	0.078±0.008	0.110±0.010	0.099±0.009
		1.50	2.00	0.024±0.004	0.050±0.005	0.104±0.009	0.085±0.008
		2.00	2.50	0.011±0.003	0.039±0.005	0.081±0.008	0.078±0.008
		2.50	3.00	±	0.035±0.005	0.052±0.007	0.044±0.006
		3.00	3.50	±	0.010±0.003	0.025±0.004	0.031±0.004
		3.50	4.00	±	0.003±0.001	0.014±0.003	0.014±0.003
		4.00	5.00	±	0.001±0.000	0.006±0.001	0.008±0.001
		5.00	6.50	±	±	0.001±0.000	0.001±0.001
		6.50	8.00	±	±	±	±
0.20	0.25	0.50	1.00	0.057±0.010	0.107±0.014	0.13±0.02	0.097±0.013
		1.00	1.50	0.028±0.006	0.101±0.013	0.18±0.02	0.16±0.02
		1.50	2.00	0.034±0.007	0.063±0.009	0.14±0.02	0.099±0.014
		2.00	2.50	0.005±0.002	0.038±0.006	0.082±0.013	0.051±0.008
		2.50	3.00	±	0.011±0.003	0.031±0.007	0.023±0.004
		3.00	3.50	±	0.004±0.001	0.008±0.003	0.011±0.003
		3.50	4.00	±	0.001±0.001	0.004±0.002	0.004±0.002
		4.00	5.00	±	±	0.002±0.001	0.002±0.001
		5.00	6.50	±	±	±	±
		6.50	8.00	±	±	±	0.000±0.001

Table 5: HARP results for the double-differential π^- production cross-section in the laboratory system, $d^2\sigma^\pi/(dpd\Omega)$, for π^- -Be interactions at 3,5,8,12 GeV/c. Each row refers to a different ($p_{\min} \leq p < p_{\max}, \theta_{\min} \leq \theta < \theta_{\max}$) bin, where p and θ are the pion momentum and polar angle, respectively. The central value as well as the square-root of the diagonal elements of the covariance matrix are given.

θ_{\min} (rad)	θ_{\max} (rad)	p_{\min} (GeV/c)	p_{\max} (GeV/c)	$d^2\sigma^{\pi^-}/(dpd\Omega)$ (barn/(GeV/c sr))					
				3 GeV/c	5 GeV/c	8 GeV/c	12 GeV/c		
0.05	0.10	0.50	1.00	0.075±0.010	0.113±0.012	0.25±0.02	0.15±0.02		
		1.00	1.50	0.094±0.010	0.119±0.009	0.195±0.014	0.144±0.012		
		1.50	2.00	0.116±0.009	0.134±0.009	0.208±0.013	0.172±0.011		
		2.00	2.50	0.15±0.04	0.142±0.010	0.217±0.014	0.167±0.011		
		2.50	3.00	±	0.128±0.009	0.194±0.011	0.176±0.011		
		3.00	3.50	±	0.21±0.02	0.163±0.011	0.145±0.008		
		3.50	4.00	±	0.241±0.013	0.155±0.011	0.129±0.007		
		4.00	5.00	±	0.25±0.04	0.161±0.009	0.105±0.006		
		5.00	6.50	±	±	0.118±0.006	0.073±0.004		
		6.50	8.00	±	±	±	0.053±0.003		
		0.10	0.15	0.50	1.00	0.100±0.012	0.16±0.02	0.22±0.02	0.17±0.02
				1.00	1.50	0.083±0.009	0.119±0.010	0.23±0.02	0.177±0.014
				1.50	2.00	0.119±0.012	0.118±0.011	0.186±0.014	0.165±0.013
				2.00	2.50	0.16±0.02	0.137±0.011	0.180±0.014	0.147±0.012
2.50	3.00			±	0.107±0.009	0.150±0.012	0.124±0.010		
3.00	3.50			±	0.103±0.008	0.103±0.009	0.093±0.007		
3.50	4.00			±	0.087±0.007	0.078±0.008	0.083±0.006		
4.00	5.00			±	0.094±0.009	0.045±0.005	0.055±0.005		
5.00	6.50			±	±	0.022±0.003	0.023±0.002		
6.50	8.00			±	±	±	0.008±0.001		
0.15	0.20			0.50	1.00	0.103±0.014	0.093±0.012	0.21±0.02	0.17±0.02
				1.00	1.50	0.089±0.010	0.099±0.010	0.20±0.02	0.163±0.014
				1.50	2.00	0.065±0.008	0.103±0.010	0.163±0.014	0.118±0.011
				2.00	2.50	0.069±0.009	0.067±0.007	0.120±0.011	0.091±0.008
		2.50	3.00	±	0.034±0.004	0.071±0.007	0.059±0.006		
		3.00	3.50	±	0.035±0.004	0.039±0.005	0.043±0.004		
		3.50	4.00	±	0.015±0.003	0.032±0.003	0.030±0.003		
		4.00	5.00	±	0.013±0.002	0.020±0.003	0.018±0.002		
		5.00	6.50	±	±	0.005±0.001	0.005±0.001		
		6.50	8.00	±	±	±	0.001±0.000		
		0.20	0.25	0.50	1.00	0.075±0.012	0.13±0.02	0.16±0.02	0.104±0.014
				1.00	1.50	0.033±0.006	0.053±0.008	0.120±0.014	0.066±0.009
				1.50	2.00	0.035±0.006	0.038±0.007	0.096±0.014	0.070±0.011
				2.00	2.50	0.023±0.004	0.033±0.005	0.074±0.012	0.060±0.009
2.50	3.00			±	0.025±0.004	0.056±0.009	0.041±0.006		
3.00	3.50			±	0.011±0.002	0.043±0.006	0.031±0.005		
3.50	4.00			±	0.007±0.002	0.030±0.005	0.018±0.003		
4.00	5.00			±	0.003±0.001	0.017±0.003	0.011±0.002		
5.00	6.50			±	±	0.005±0.002	0.003±0.001		
6.50	8.00			±	±	±	0.001±0.001		

Table 6: HARP results for the double-differential π^+ production cross-section in the laboratory system, $d^2\sigma^\pi/(dpd\Omega)$, for π^+ -Be interactions at 3,5,8,12 GeV/c. Each row refers to a different ($p_{\min} \leq p < p_{\max}, \theta_{\min} \leq \theta < \theta_{\max}$) bin, where p and θ are the pion momentum and polar angle, respectively. The central value as well as the square-root of the diagonal elements of the covariance matrix are given.

θ_{\min} (rad)	θ_{\max} (rad)	p_{\min} (GeV/c)	p_{\max} (GeV/c)	$d^2\sigma^{\pi^+}/(dpd\Omega)$ (barn/(GeV/c sr))			
				3 GeV/c	5 GeV/c	8 GeV/c	12 GeV/c
0.050	0.100	0.50	1.00	0.08±0.02	0.12±0.02	0.13±0.02	0.15±0.04
		1.00	1.50	0.047±0.008	0.102±0.013	0.16±0.02	0.16±0.03
		1.50	2.00	0.089±0.009	0.110±0.012	0.131±0.013	0.16±0.03
		2.00	2.50	0.22±0.02	0.158±0.014	0.158±0.015	0.20±0.03
		2.50	3.00	±	0.161±0.012	0.18±0.02	0.18±0.03
		3.00	3.50	±	0.21±0.02	0.138±0.014	0.19±0.03
		3.50	4.00	±	0.251±0.014	0.122±0.012	0.20±0.03
		4.00	5.00	±	0.30±0.10	0.161±0.010	0.15±0.02
		5.00	6.50	±	±	0.14±0.02	0.047±0.011
		6.50	8.00	±	±	±	0.18±0.02
0.100	0.150	0.50	1.00	0.07±0.02	0.12±0.02	0.15±0.02	0.13±0.03
		1.00	1.50	0.081±0.013	0.114±0.014	0.14±0.02	0.18±0.03
		1.50	2.00	0.16±0.02	0.14±0.02	0.21±0.02	0.19±0.03
		2.00	2.50	0.16±0.02	0.14±0.02	0.16±0.02	0.19±0.03
		2.50	3.00	±	0.107±0.012	0.130±0.014	0.15±0.02
		3.00	3.50	±	0.128±0.013	0.102±0.011	0.12±0.02
		3.50	4.00	±	0.108±0.011	0.067±0.008	0.13±0.02
		4.00	5.00	±	0.10±0.04	0.051±0.008	0.091±0.014
		5.00	6.50	±	±	0.021±0.004	0.034±0.008
		6.50	8.00	±	±	±	0.014±0.004
0.150	0.200	0.50	1.00	0.11±0.02	0.14±0.02	0.19±0.03	0.24±0.05
		1.00	1.50	0.101±0.015	0.122±0.015	0.16±0.02	0.23±0.04
		1.50	2.00	0.077±0.011	0.079±0.010	0.15±0.02	0.11±0.02
		2.00	2.50	0.09±0.02	0.090±0.015	0.109±0.013	0.08±0.02
		2.50	3.00	±	0.039±0.006	0.056±0.009	0.07±0.02
		3.00	3.50	±	0.030±0.008	0.046±0.008	0.06±0.02
		3.50	4.00	±	0.023±0.006	0.026±0.005	0.042±0.013
		4.00	5.00	±	0.016±0.009	0.016±0.003	0.023±0.009
		5.00	6.50	±	±	0.006±0.002	0.008±0.004
		6.50	8.00	±	±	±	0.002±0.002
0.200	0.250	0.50	1.00	0.07±0.02	0.11±0.02	0.11±0.02	0.09±0.03
		1.00	1.50	0.059±0.013	0.053±0.010	0.11±0.02	0.09±0.03
		1.50	2.00	0.027±0.007	0.067±0.013	0.065±0.013	0.06±0.03
		2.00	2.50	0.021±0.008	0.042±0.009	0.08±0.02	0.07±0.03
		2.50	3.00	±	0.028±0.007	0.047±0.012	0.06±0.03
		3.00	3.50	±	0.019±0.006	0.026±0.008	0.03±0.02
		3.50	4.00	±	0.010±0.004	0.020±0.005	0.016±0.015
		4.00	5.00	±	0.005±0.003	0.012±0.004	0.011±0.014
		5.00	6.50	±	±	0.006±0.003	0.002±0.005
		6.50	8.00	±	±	±	0.000±0.011

Table 7: HARP results for the double-differential π^- production cross-section in the laboratory system, $d^2\sigma^\pi/(dpd\Omega)$, for π^+ -Be interactions at 3,5,8,12 GeV/c. Each row refers to a different ($p_{\min} \leq p < p_{\max}, \theta_{\min} \leq \theta < \theta_{\max}$) bin, where p and θ are the pion momentum and polar angle, respectively. The central value as well as the square-root of the diagonal elements of the covariance matrix are given.

θ_{\min} (rad)	θ_{\max} (rad)	p_{\min} (GeV/c)	p_{\max} (GeV/c)	$d^2\sigma^{\pi^-}/(dpd\Omega)$ (barn/(GeV/c sr))					
				3 GeV/c	5 GeV/c	8 GeV/c	12 GeV/c		
0.050	0.100	0.50	1.00	0.060±0.013	0.081±0.014	0.11±0.02	0.05±0.02		
		1.00	1.50	0.049±0.010	0.106±0.013	0.14±0.02	0.15±0.03		
		1.50	2.00	0.038±0.007	0.062±0.008	0.118±0.013	0.12±0.02		
		2.00	2.50	0.06±0.02	0.064±0.008	0.114±0.012	0.10±0.02		
		2.50	3.00	±	0.050±0.007	0.083±0.009	0.14±0.02		
		3.00	3.50	±	0.054±0.008	0.093±0.009	0.12±0.02		
		3.50	4.00	±	0.063±0.007	0.065±0.007	0.10±0.02		
		4.00	5.00	±	0.033±0.007	0.050±0.005	0.066±0.011		
		5.00	6.50	±	±	0.026±0.003	0.039±0.007		
		6.50	8.00	±	±	±	0.019±0.004		
		0.100	0.150	0.50	1.00	0.070±0.014	0.081±0.015	0.15±0.02	0.20±0.05
				1.00	1.50	0.041±0.008	0.059±0.009	0.118±0.014	0.15±0.03
				1.50	2.00	0.035±0.007	0.067±0.010	0.101±0.012	0.18±0.03
				2.00	2.50	0.021±0.006	0.057±0.008	0.093±0.011	0.14±0.03
2.50	3.00			±	0.038±0.006	0.061±0.008	0.09±0.02		
3.00	3.50			±	0.025±0.004	0.044±0.006	0.064±0.014		
3.50	4.00			±	0.015±0.003	0.036±0.005	0.064±0.014		
4.00	5.00			±	0.005±0.002	0.020±0.004	0.037±0.009		
5.00	6.50			±	±	0.003±0.001	0.016±0.005		
6.50	8.00			±	±	±	0.004±0.002		
0.150	0.200			0.50	1.00	0.08±0.02	0.086±0.014	0.13±0.02	0.14±0.04
				1.00	1.50	0.059±0.011	0.086±0.012	0.12±0.02	0.12±0.03
				1.50	2.00	0.024±0.006	0.068±0.010	0.099±0.013	0.09±0.02
				2.00	2.50	0.008±0.003	0.034±0.006	0.085±0.012	0.13±0.03
		2.50	3.00	±	0.025±0.005	0.050±0.008	0.05±0.02		
		3.00	3.50	±	0.006±0.002	0.026±0.005	0.034±0.012		
		3.50	4.00	±	0.002±0.001	0.017±0.004	0.019±0.008		
		4.00	5.00	±	0.001±0.001	0.004±0.001	0.012±0.007		
		5.00	6.50	±	±	*±*	0.001±0.002		
		6.50	8.00	±	±	±	0.000±0.001		
		0.200	0.250	0.50	1.00	0.048±0.013	0.11±0.02	0.10±0.02	0.12±0.04
				1.00	1.50	0.047±0.012	0.059±0.011	0.11±0.02	0.10±0.03
				1.50	2.00	0.012±0.005	0.038±0.010	0.13±0.02	0.14±0.05
				2.00	2.50	0.002±0.002	0.017±0.005	0.052±0.011	0.07±0.03
2.50	3.00			±	0.003±0.001	0.025±0.007	0.04±0.03		
3.00	3.50			±	0.002±0.001	0.012±0.008	0.016±0.023		
3.50	4.00			±	0.002±0.001	0.004±0.005	0.004±0.008		
4.00	5.00			±	0.001±0.001	0.001±0.004	0.002±0.006		
5.00	6.50			±	±	0.000±0.004	0.000±0.001		
6.50	8.00			±	±	±	0.000±0.006		

Table 8: HARP results for the double-differential π^+ production cross-section in the laboratory system, $d^2\sigma^\pi/(dpd\Omega)$, for π^- -C interactions at 3,5,8,12 GeV/c. Each row refers to a different ($p_{\min} \leq p < p_{\max}, \theta_{\min} \leq \theta < \theta_{\max}$) bin, where p and θ are the pion momentum and polar angle, respectively. The central value as well as the square-root of the diagonal elements of the covariance matrix are given.

θ_{\min} (rad)	θ_{\max} (rad)	p_{\min} (GeV/c)	p_{\max} (GeV/c)	$d^2\sigma^{\pi^+}/(dpd\Omega)$ (barn/(GeV/c sr))					
				3 GeV/c	5 GeV/c	8 GeV/c	12 GeV/c		
0.05	0.10	0.50	1.00	0.044±0.012	0.078±0.013	0.14±0.02	0.21±0.03		
		1.00	1.50	0.046±0.010	0.099±0.012	0.204±0.014	0.26±0.02		
		1.50	2.00	0.057±0.011	0.060±0.009	0.174±0.011	0.23±0.02		
		2.00	2.50	0.058±0.012	0.070±0.009	0.126±0.011	0.20±0.02		
		2.50	3.00	±	0.049±0.007	0.094±0.010	0.175±0.014		
		3.00	3.50	±	0.050±0.007	0.094±0.010	0.171±0.014		
		3.50	4.00	±	0.059±0.008	0.068±0.009	0.150±0.013		
		4.00	5.00	±	0.030±0.009	0.050±0.005	0.082±0.008		
		5.00	6.50	±	±	0.023±0.003	0.053±0.005		
		6.50	8.00	±	±	±	0.016±0.003		
		0.10	0.15	0.50	1.00	0.09±0.02	0.090±0.014	0.19±0.02	0.20±0.03
				1.00	1.50	0.054±0.011	0.098±0.012	0.167±0.015	0.27±0.03
1.50	2.00			0.039±0.009	0.073±0.010	0.146±0.013	0.21±0.02		
2.00	2.50			0.035±0.009	0.052±0.008	0.130±0.012	0.19±0.02		
2.50	3.00			±	0.039±0.006	0.086±0.010	0.145±0.015		
3.00	3.50			±	0.024±0.005	0.053±0.007	0.113±0.012		
3.50	4.00			±	0.013±0.003	0.050±0.006	0.102±0.011		
4.00	5.00			±	0.007±0.003	0.019±0.004	0.048±0.007		
5.00	6.50			±	±	0.003±0.001	0.014±0.003		
6.50	8.00			±	±	±	0.002±0.000		
0.15	0.20			0.50	1.00	0.06±0.02	0.09±0.02	0.19±0.02	0.20±0.03
				1.00	1.50	0.034±0.008	0.066±0.010	0.130±0.013	0.19±0.02
		1.50	2.00	0.028±0.008	0.056±0.008	0.115±0.011	0.16±0.02		
		2.00	2.50	0.022±0.008	0.042±0.007	0.091±0.010	0.16±0.02		
		2.50	3.00	±	0.022±0.005	0.050±0.007	0.073±0.010		
		3.00	3.50	±	0.010±0.004	0.031±0.005	0.068±0.010		
		3.50	4.00	±	0.001±0.001	0.016±0.003	0.026±0.005		
		4.00	5.00	±	0.001±0.001	0.009±0.002	0.011±0.003		
		5.00	6.50	±	±	0.001±0.000	0.002±0.001		
		6.50	8.00	±	±	±	±		
		0.20	0.25	0.50	1.00	0.06±0.02	0.10±0.02	0.14±0.02	0.19±0.03
				1.00	1.50	0.06±0.02	0.08±0.02	0.19±0.02	0.25±0.03
1.50	2.00			0.027±0.010	0.077±0.014	0.12±0.02	0.15±0.03		
2.00	2.50			0.010±0.006	0.039±0.008	0.069±0.012	0.10±0.02		
2.50	3.00			±	0.018±0.005	0.036±0.008	0.044±0.011		
3.00	3.50			±	0.004±0.002	0.011±0.005	0.015±0.005		
3.50	4.00			±	0.001±0.001	0.002±0.002	0.008±0.004		
4.00	5.00			±	±	0.001±0.001	0.003±0.003		
5.00	6.50			±	±	±	±		
6.50	8.00			±	±	±	0.000±0.003		

Table 9: HARP results for the double-differential π^- production cross-section in the laboratory system, $d^2\sigma^\pi/(dpd\Omega)$, for π^- -C interactions at 3,5,8,12 GeV/c. Each row refers to a different ($p_{\min} \leq p < p_{\max}, \theta_{\min} \leq \theta < \theta_{\max}$) bin, where p and θ are the pion momentum and polar angle, respectively. The central value as well as the square-root of the diagonal elements of the covariance matrix are given.

θ_{\min} (rad)	θ_{\max} (rad)	p_{\min} (GeV/c)	p_{\max} (GeV/c)	$d^2\sigma^{\pi^-}/(dpd\Omega)$ (barn/(GeV/c sr))					
				3 GeV/c	5 GeV/c	8 GeV/c	12 GeV/c		
0.05	0.10	0.50	1.00	0.11±0.02	0.14±0.02	0.27±0.03	0.28±0.03		
		1.00	1.50	0.080±0.014	0.122±0.013	0.23±0.02	0.29±0.03		
		1.50	2.00	0.14±0.02	0.123±0.013	0.25±0.02	0.32±0.02		
		2.00	2.50	0.15±0.04	0.138±0.014	0.24±0.02	0.32±0.02		
		2.50	3.00	±	0.17±0.02	0.222±0.013	0.30±0.02		
		3.00	3.50	±	0.22±0.02	0.183±0.014	0.26±0.02		
		3.50	4.00	±	0.19±0.02	0.177±0.014	0.23±0.02		
		4.00	5.00	±	0.27±0.05	0.172±0.011	0.194±0.013		
		5.00	6.50	±	±	0.116±0.008	0.134±0.007		
		6.50	8.00	±	±	±	0.089±0.007		
		0.10	0.15	0.50	1.00	0.16±0.03	0.17±0.02	0.25±0.03	0.31±0.04
				1.00	1.50	0.087±0.013	0.133±0.015	0.24±0.02	0.30±0.03
				1.50	2.00	0.15±0.02	0.15±0.02	0.21±0.02	0.31±0.03
				2.00	2.50	0.17±0.03	0.140±0.014	0.20±0.02	0.26±0.02
2.50	3.00			±	0.126±0.013	0.167±0.014	0.23±0.02		
3.00	3.50			±	0.110±0.012	0.097±0.010	0.18±0.02		
3.50	4.00			±	0.100±0.011	0.076±0.008	0.140±0.014		
4.00	5.00			±	0.10±0.02	0.046±0.006	0.090±0.009		
5.00	6.50			±	±	0.020±0.003	0.040±0.005		
6.50	8.00			±	±	±	0.014±0.003		
0.15	0.20			0.50	1.00	0.09±0.02	0.16±0.02	0.22±0.03	0.31±0.04
				1.00	1.50	0.14±0.02	0.12±0.02	0.23±0.02	0.25±0.03
				1.50	2.00	0.12±0.02	0.112±0.013	0.18±0.02	0.23±0.02
				2.00	2.50	0.095±0.014	0.074±0.010	0.120±0.013	0.15±0.02
		2.50	3.00	±	0.041±0.007	0.077±0.008	0.087±0.011		
		3.00	3.50	±	0.024±0.004	0.042±0.006	0.060±0.008		
		3.50	4.00	±	0.018±0.003	0.029±0.004	0.050±0.007		
		4.00	5.00	±	0.022±0.004	0.017±0.003	0.030±0.005		
		5.00	6.50	±	±	0.005±0.001	0.009±0.002		
		6.50	8.00	±	±	±	0.003±0.001		
		0.20	0.25	0.50	1.00	0.08±0.02	0.10±0.02	0.15±0.02	0.19±0.03
				1.00	1.50	0.056±0.013	0.046±0.009	0.099±0.013	0.12±0.02
				1.50	2.00	0.07±0.02	0.048±0.010	0.076±0.014	0.12±0.02
				2.00	2.50	0.027±0.007	0.040±0.008	0.070±0.012	0.075±0.015
2.50	3.00			±	0.024±0.006	0.053±0.009	0.069±0.013		
3.00	3.50			±	0.014±0.003	0.029±0.005	0.052±0.011		
3.50	4.00			±	0.009±0.003	0.020±0.004	0.023±0.006		
4.00	5.00			±	0.005±0.002	0.014±0.003	0.011±0.004		
5.00	6.50			±	±	0.003±0.001	0.006±0.003		
6.50	8.00			±	±	±	0.002±0.002		

Table 10: HARP results for the double-differential π^+ production cross-section in the laboratory system, $d^2\sigma^\pi/(dpd\Omega)$, for π^+ -C interactions at 3,5,8,12 GeV/c. Each row refers to a different ($p_{\min} \leq p < p_{\max}, \theta_{\min} \leq \theta < \theta_{\max}$) bin, where p and θ are the pion momentum and polar angle, respectively. The central value as well as the square-root of the diagonal elements of the covariance matrix are given.

θ_{\min} (rad)	θ_{\max} (rad)	p_{\min} (GeV/c)	p_{\max} (GeV/c)	$d^2\sigma^{\pi^+}/(dpd\Omega)$ (barn/(GeV/c sr))					
				3 GeV/c	5 GeV/c	8 GeV/c	12 GeV/c		
0.050	0.100	0.50	1.00	0.12±0.03	0.14±0.02	0.18±0.03	0.25±0.08		
		1.00	1.50	0.065±0.012	0.112±0.013	0.21±0.02	0.16±0.05		
		1.50	2.00	0.091±0.010	0.137±0.013	0.19±0.02	*±*		
		2.00	2.50	0.25±0.02	0.191±0.014	0.19±0.02	0.36±0.07		
		2.50	3.00	±	0.191±0.012	0.20±0.02	0.20±0.05		
		3.00	3.50	±	0.25±0.02	0.19±0.02	0.28±0.05		
		3.50	4.00	±	0.315±0.015	0.14±0.02	0.27±0.05		
		4.00	5.00	±	0.32±0.10	0.196±0.014	0.14±0.03		
		5.00	6.50	±	±	0.17±0.03	0.12±0.02		
		6.50	8.00	±	±	±	0.09±0.02		
		0.100	0.150	0.50	1.00	0.08±0.02	0.17±0.02	0.18±0.03	0.26±0.08
				1.00	1.50	0.09±0.02	0.15±0.02	0.21±0.02	0.18±0.05
1.50	2.00			0.18±0.02	0.136±0.014	0.25±0.03	0.22±0.06		
2.00	2.50			0.20±0.02	0.160±0.015	0.21±0.03	0.19±0.06		
2.50	3.00			±	0.138±0.013	0.16±0.02	0.16±0.06		
3.00	3.50			±	0.138±0.013	0.110±0.012	0.15±0.04		
3.50	4.00			±	0.115±0.010	0.097±0.011	0.15±0.04		
4.00	5.00			±	0.11±0.04	0.065±0.011	0.07±0.02		
5.00	6.50			±	±	0.022±0.005	0.038±0.014		
6.50	8.00			±	±	±	0.006±0.006		
0.150	0.200			0.50	1.00	0.08±0.02	0.16±0.02	0.20±0.03	0.09±0.05
				1.00	1.50	0.10±0.02	0.119±0.014	0.18±0.02	0.18±0.06
		1.50	2.00	0.12±0.02	0.105±0.011	0.17±0.02	0.13±0.05		
		2.00	2.50	0.09±0.02	0.080±0.010	0.13±0.02	0.12±0.07		
		2.50	3.00	±	0.055±0.007	0.080±0.013	0.10±0.08		
		3.00	3.50	±	0.042±0.010	0.076±0.012	0.11±0.04		
		3.50	4.00	±	0.031±0.007	0.043±0.008	0.06±0.03		
		4.00	5.00	±	0.022±0.012	0.025±0.005	0.022±0.015		
		5.00	6.50	±	±	0.005±0.002	0.015±0.012		
		6.50	8.00	±	±	±	0.002±0.004		
		0.200	0.250	0.50	1.00	0.05±0.02	0.12±0.02	0.19±0.03	0.15±0.08
				1.00	1.50	0.049±0.013	0.070±0.012	0.13±0.02	0.05±0.04
1.50	2.00			0.043±0.011	0.071±0.012	0.13±0.02	0.06±0.05		
2.00	2.50			0.018±0.008	0.053±0.009	0.09±0.02	0.06±0.05		
2.50	3.00			±	0.034±0.007	0.055±0.014	0.05±0.05		
3.00	3.50			±	0.016±0.004	0.040±0.011	0.016±0.016		
3.50	4.00			±	0.012±0.005	0.032±0.009	0.010±0.030		
4.00	5.00			±	0.008±0.004	0.023±0.008	0.025±0.050		
5.00	6.50			±	±	0.007±0.004	0.003±0.010		
6.50	8.00			±	±	±	0.000±0.027		

Table 11: HARP results for the double-differential π^- production cross-section in the laboratory system, $d^2\sigma^\pi/(dpd\Omega)$, for π^+-C interactions at 3,5,8,12 GeV/c. Each row refers to a different ($p_{\min} \leq p < p_{\max}, \theta_{\min} \leq \theta < \theta_{\max}$) bin, where p and θ are the pion momentum and polar angle, respectively. The central value as well as the square-root of the diagonal elements of the covariance matrix are given.

θ_{\min} (rad)	θ_{\max} (rad)	p_{\min} (GeV/c)	p_{\max} (GeV/c)	$d^2\sigma^{\pi^-}/(dpd\Omega)$ (barn/(GeV/c sr))					
				3 GeV/c	5 GeV/c	8 GeV/c	12 GeV/c		
0.050	0.100	0.50	1.00	0.031±0.011	0.082±0.013	0.14±0.02	0.11±0.05		
		1.00	1.50	0.052±0.012	0.111±0.012	0.15±0.02	0.18±0.06		
		1.50	2.00	0.041±0.008	0.073±0.008	0.15±0.02	0.21±0.06		
		2.00	2.50	0.06±0.02	0.067±0.007	0.131±0.015	0.11±0.03		
		2.50	3.00	±	0.064±0.007	0.113±0.013	0.16±0.05		
		3.00	3.50	±	0.067±0.008	0.081±0.009	0.20±0.04		
		3.50	4.00	±	0.062±0.006	0.104±0.011	0.08±0.02		
		4.00	5.00	±	0.030±0.006	0.050±0.005	0.09±0.02		
		5.00	6.50	±	±	0.026±0.003	0.059±0.015		
		6.50	8.00	±	±	±	0.021±0.008		
		0.100	0.150	0.50	1.00	0.07±0.02	0.16±0.02	0.21±0.03	0.25±0.08
				1.00	1.50	0.041±0.010	0.082±0.011	0.15±0.02	0.11±0.04
				1.50	2.00	0.040±0.009	0.061±0.008	0.117±0.014	0.15±0.05
				2.00	2.50	0.036±0.009	0.056±0.007	0.120±0.015	0.14±0.04
2.50	3.00			±	0.034±0.004	0.056±0.008	0.12±0.04		
3.00	3.50			±	0.033±0.004	0.060±0.009	0.11±0.03		
3.50	4.00			±	0.013±0.002	0.037±0.006	0.09±0.03		
4.00	5.00			±	0.003±0.001	0.022±0.004	0.04±0.02		
5.00	6.50			±	±	0.006±0.001	0.013±0.008		
6.50	8.00			±	±	±	0.005±0.004		
0.150	0.200			0.50	1.00	0.07±0.02	0.11±0.02	0.20±0.03	0.27±0.09
				1.00	1.50	0.035±0.009	0.073±0.010	0.13±0.02	0.20±0.06
				1.50	2.00	0.021±0.006	0.091±0.011	0.12±0.02	0.18±0.06
				2.00	2.50	0.015±0.006	0.046±0.006	0.095±0.013	0.12±0.04
		2.50	3.00	±	0.023±0.004	0.048±0.008	0.07±0.03		
		3.00	3.50	±	0.007±0.002	0.027±0.005	0.032±0.035		
		3.50	4.00	±	0.004±0.001	0.017±0.004	0.005±0.009		
		4.00	5.00	±	±	0.005±0.002	0.007±0.016		
		5.00	6.50	±	±	0.001±0.001	0.003±0.009		
		6.50	8.00	±	±	±	0.000±0.001		
		0.200	0.250	0.50	1.00	0.07±0.02	0.12±0.02	0.15±0.03	0.14±0.06
				1.00	1.50	0.025±0.009	0.080±0.013	0.16±0.03	0.15±0.07
				1.50	2.00	0.005±0.003	0.031±0.008	0.13±0.02	0.07±0.05
				2.00	2.50	0.008±0.005	0.015±0.004	0.052±0.012	0.08±0.06
2.50	3.00			±	0.005±0.002	0.020±0.006	0.08±0.06		
3.00	3.50			±	0.002±0.001	0.011±0.004	0.051±0.059		
3.50	4.00			±	0.000±0.000	0.006±0.003	0.021±0.038		
4.00	5.00			±	±	0.002±0.003	0.003±0.019		
5.00	6.50			±	±	0.000±0.001	0.002±0.015		
6.50	8.00			±	±	±	0.001±0.018		

Table 12: HARP results for the double-differential π^+ production cross-section in the laboratory system, $d^2\sigma^\pi/(dpd\Omega)$, for π^- -Al interactions at 3,5,8,12 GeV/c. Each row refers to a different ($p_{\min} \leq p < p_{\max}, \theta_{\min} \leq \theta < \theta_{\max}$) bin, where p and θ are the pion momentum and polar angle, respectively. The central value as well as the square-root of the diagonal elements of the covariance matrix are given.

θ_{\min} (rad)	θ_{\max} (rad)	p_{\min} (GeV/c)	p_{\max} (GeV/c)	$d^2\sigma^{\pi^+}/(dpd\Omega)$ (barn/(GeV/c sr))			
				3 GeV/c	5 GeV/c	8 GeV/c	12 GeV/c
0.05	0.10	0.50	1.00	0.066±0.015	0.14±0.03	0.29±0.03	0.32±0.04
		1.00	1.50	0.086±0.015	0.18±0.02	0.36±0.03	0.44±0.03
		1.50	2.00	0.063±0.012	0.13±0.02	0.30±0.02	0.37±0.03
		2.00	2.50	0.090±0.015	0.12±0.02	0.22±0.02	0.32±0.02
		2.50	3.00	±	0.092±0.015	0.14±0.02	0.29±0.02
		3.00	3.50	±	0.078±0.014	0.17±0.02	0.29±0.02
		3.50	4.00	±	0.080±0.014	0.13±0.02	0.22±0.02
		4.00	5.00	±	0.038±0.011	0.083±0.009	0.138±0.011
		5.00	6.50	±	±	0.039±0.005	0.071±0.006
		6.50	8.00	±	±	±	0.030±0.004
0.10	0.15	0.50	1.00	0.12±0.02	0.22±0.03	0.32±0.04	0.34±0.04
		1.00	1.50	0.052±0.011	0.17±0.02	0.29±0.03	0.44±0.04
		1.50	2.00	0.047±0.010	0.10±0.02	0.24±0.02	0.35±0.03
		2.00	2.50	0.047±0.011	0.074±0.014	0.23±0.02	0.33±0.03
		2.50	3.00	±	0.08±0.02	0.14±0.02	0.25±0.02
		3.00	3.50	±	0.048±0.013	0.094±0.013	0.21±0.02
		3.50	4.00	±	0.011±0.005	0.079±0.011	0.150±0.015
		4.00	5.00	±	0.002±0.002	0.029±0.006	0.084±0.011
		5.00	6.50	±	±	0.006±0.002	0.021±0.004
		6.50	8.00	±	±	±	0.004±0.001
0.15	0.20	0.50	1.00	0.10±0.02	0.17±0.03	0.34±0.04	0.44±0.05
		1.00	1.50	0.082±0.014	0.10±0.02	0.25±0.03	0.32±0.03
		1.50	2.00	0.043±0.009	0.10±0.02	0.20±0.02	0.27±0.03
		2.00	2.50	0.024±0.008	0.08±0.02	0.16±0.02	0.23±0.03
		2.50	3.00	±	0.034±0.010	0.094±0.013	0.121±0.015
		3.00	3.50	±	0.014±0.005	0.055±0.010	0.093±0.014
		3.50	4.00	±	0.007±0.004	0.028±0.006	0.036±0.007
		4.00	5.00	±	0.001±0.001	0.010±0.003	0.028±0.005
		5.00	6.50	±	±	0.002±0.001	0.004±0.001
		6.50	8.00	±	±	±	0.001±0.000
0.20	0.25	0.50	1.00	0.10±0.02	0.19±0.04	0.29±0.04	0.33±0.05
		1.00	1.50	0.10±0.02	0.19±0.04	0.38±0.05	0.36±0.05
		1.50	2.00	0.039±0.012	0.12±0.03	0.27±0.04	0.25±0.04
		2.00	2.50	0.011±0.006	0.06±0.02	0.13±0.02	0.18±0.03
		2.50	3.00	±	0.019±0.008	0.078±0.015	0.08±0.02
		3.00	3.50	±	0.009±0.005	0.024±0.009	0.038±0.009
		3.50	4.00	±	0.003±0.002	0.008±0.004	0.017±0.006
		4.00	5.00	±	0.002±0.002	0.006±0.003	0.007±0.004
		5.00	6.50	±	±	0.001±0.001	0.001±0.001
		6.50	8.00	±	±	±	0.000±0.004

Table 13: HARP results for the double-differential π^- production cross-section in the laboratory system, $d^2\sigma^\pi/(dpd\Omega)$, for π^- -Al interactions at 3,5,8,12 GeV/c. Each row refers to a different ($p_{\min} \leq p < p_{\max}, \theta_{\min} \leq \theta < \theta_{\max}$) bin, where p and θ are the pion momentum and polar angle, respectively. The central value as well as the square-root of the diagonal elements of the covariance matrix are given.

θ_{\min} (rad)	θ_{\max} (rad)	p_{\min} (GeV/c)	p_{\max} (GeV/c)	$d^2\sigma^{\pi^-}/(dpd\Omega)$ (barn/(GeV/c sr))			
				3 GeV/c	5 GeV/c	8 GeV/c	12 GeV/c
0.05	0.10	0.50	1.00	0.16±0.02	0.27±0.04	0.50±0.05	0.49±0.05
		1.00	1.50	0.14±0.02	0.23±0.03	0.41±0.03	0.46±0.04
		1.50	2.00	0.21±0.02	0.25±0.03	0.43±0.03	0.52±0.03
		2.00	2.50	0.21±0.05	0.28±0.03	0.42±0.03	0.47±0.03
		2.50	3.00	±	0.27±0.03	0.39±0.02	0.46±0.03
		3.00	3.50	±	0.31±0.03	0.30±0.02	0.48±0.03
		3.50	4.00	±	0.36±0.03	0.28±0.02	0.42±0.02
		4.00	5.00	±	0.39±0.06	0.27±0.02	0.26±0.02
		5.00	6.50	±	±	0.204±0.013	0.199±0.010
		6.50	8.00	±	±	±	0.136±0.009
0.10	0.15	0.50	1.00	0.18±0.03	0.30±0.04	0.49±0.05	0.62±0.07
		1.00	1.50	0.17±0.02	0.23±0.03	0.42±0.04	0.59±0.05
		1.50	2.00	0.22±0.03	0.19±0.02	0.39±0.03	0.47±0.04
		2.00	2.50	0.23±0.04	0.22±0.03	0.36±0.03	0.46±0.04
		2.50	3.00	±	0.21±0.03	0.30±0.03	0.35±0.03
		3.00	3.50	±	0.17±0.02	0.18±0.02	0.26±0.02
		3.50	4.00	±	0.15±0.02	0.12±0.02	0.20±0.02
		4.00	5.00	±	0.14±0.02	0.068±0.009	0.140±0.013
		5.00	6.50	±	±	0.040±0.005	0.070±0.007
		6.50	8.00	±	±	±	0.025±0.004
0.15	0.20	0.50	1.00	0.19±0.03	0.26±0.04	0.46±0.05	0.55±0.06
		1.00	1.50	0.15±0.02	0.22±0.03	0.42±0.04	0.42±0.04
		1.50	2.00	0.14±0.02	0.14±0.02	0.29±0.03	0.35±0.03
		2.00	2.50	0.12±0.02	0.12±0.02	0.21±0.02	0.25±0.03
		2.50	3.00	±	0.09±0.02	0.12±0.02	0.19±0.02
		3.00	3.50	±	0.031±0.008	0.079±0.011	0.131±0.015
		3.50	4.00	±	0.035±0.008	0.053±0.010	0.081±0.010
		4.00	5.00	±	0.029±0.007	0.025±0.004	0.052±0.007
		5.00	6.50	±	±	0.010±0.002	0.018±0.003
		6.50	8.00	±	±	±	0.004±0.001
0.20	0.25	0.50	1.00	0.10±0.02	0.21±0.04	0.30±0.04	0.32±0.04
		1.00	1.50	0.069±0.015	0.14±0.03	0.18±0.03	0.18±0.03
		1.50	2.00	0.08±0.02	0.10±0.02	0.14±0.03	0.16±0.03
		2.00	2.50	0.036±0.008	0.07±0.02	0.14±0.02	0.15±0.03
		2.50	3.00	±	0.06±0.02	0.09±0.02	0.09±0.02
		3.00	3.50	±	0.025±0.007	0.056±0.010	0.067±0.013
		3.50	4.00	±	0.022±0.007	0.041±0.008	0.046±0.010
		4.00	5.00	±	0.011±0.006	0.024±0.006	0.023±0.006
		5.00	6.50	±	±	0.009±0.004	0.007±0.002
		6.50	8.00	±	±	±	0.002±0.002

Table 14: HARP results for the double-differential π^+ production cross-section in the laboratory system, $d^2\sigma^\pi/(dpd\Omega)$, for π^+ -Al interactions at 3,5,8,12 GeV/c. Each row refers to a different ($p_{\min} \leq p < p_{\max}, \theta_{\min} \leq \theta < \theta_{\max}$) bin, where p and θ are the pion momentum and polar angle, respectively. The central value as well as the square-root of the diagonal elements of the covariance matrix are given.

θ_{\min} (rad)	θ_{\max} (rad)	p_{\min} (GeV/c)	p_{\max} (GeV/c)	$d^2\sigma^{\pi^+}/(dpd\Omega)$ (barn/(GeV/c sr))			
				3 GeV/c	5 GeV/c	8 GeV/c	12 GeV/c
0.050	0.100	0.50	1.00	0.14±0.04	0.23±0.03	0.30±0.05	0.60±0.21
		1.00	1.50	0.09±0.02	0.22±0.03	0.33±0.04	0.47±0.14
		1.50	2.00	0.118±0.014	0.21±0.02	0.32±0.03	0.46±0.13
		2.00	2.50	0.32±0.03	0.24±0.02	0.35±0.03	0.59±0.18
		2.50	3.00	±	0.29±0.02	0.33±0.03	0.36±0.21
		3.00	3.50	±	0.38±0.04	0.35±0.03	0.39±0.09
		3.50	4.00	±	0.40±0.02	0.30±0.03	0.52±0.12
		4.00	5.00	±	0.43±0.14	0.36±0.02	0.29±0.06
		5.00	6.50	±	±	0.26±0.04	0.20±0.04
		6.50	8.00	±	±	±	0.16±0.04
0.100	0.150	0.50	1.00	0.10±0.03	0.27±0.04	0.31±0.04	0.53±0.18
		1.00	1.50	0.19±0.03	0.24±0.03	0.33±0.04	0.50±0.15
		1.50	2.00	0.22±0.03	0.22±0.03	0.34±0.04	0.40±0.12
		2.00	2.50	0.31±0.04	0.23±0.02	0.35±0.04	0.43±0.14
		2.50	3.00	±	0.25±0.03	0.24±0.03	0.30±0.12
		3.00	3.50	±	0.19±0.02	0.20±0.02	0.38±0.10
		3.50	4.00	±	0.16±0.02	0.14±0.02	0.22±0.06
		4.00	5.00	±	0.14±0.05	0.11±0.02	0.14±0.04
		5.00	6.50	±	±	0.037±0.007	0.07±0.03
		6.50	8.00	±	±	±	0.023±0.014
0.150	0.200	0.50	1.00	0.17±0.04	0.30±0.04	0.47±0.06	0.29±0.13
		1.00	1.50	0.13±0.02	0.21±0.03	0.35±0.04	0.50±0.16
		1.50	2.00	0.14±0.02	0.15±0.02	0.26±0.03	0.15±0.07
		2.00	2.50	0.17±0.03	0.13±0.02	0.20±0.03	0.24±0.11
		2.50	3.00	±	0.069±0.011	0.12±0.02	0.25±0.10
		3.00	3.50	±	0.06±0.02	0.10±0.02	0.11±0.06
		3.50	4.00	±	0.055±0.013	0.08±0.02	0.02±0.02
		4.00	5.00	±	0.04±0.02	0.043±0.009	0.03±0.03
		5.00	6.50	±	±	0.014±0.005	0.05±0.04
		6.50	8.00	±	±	±	0.005±0.009
0.200	0.250	0.50	1.00	0.10±0.04	0.22±0.03	0.32±0.05	0.35±0.18
		1.00	1.50	0.06±0.02	0.16±0.03	0.17±0.03	0.13±0.09
		1.50	2.00	0.042±0.014	0.10±0.02	0.17±0.03	0.17±0.19
		2.00	2.50	0.031±0.015	0.11±0.02	0.16±0.03	0.042±0.048
		2.50	3.00	±	0.08±0.02	0.11±0.03	0.046±0.101
		3.00	3.50	±	0.034±0.010	0.07±0.02	0.015±0.027
		3.50	4.00	±	0.018±0.007	0.035±0.012	0.014±0.074
		4.00	5.00	±	0.014±0.007	0.021±0.008	0.014±0.098
		5.00	6.50	±	±	0.007±0.004	0.007±0.038
		6.50	8.00	±	±	±	0.003±0.077

Table 15: HARP results for the double-differential π^- production cross-section in the laboratory system, $d^2\sigma^\pi/(dpd\Omega)$, for π^+ -Al interactions at 3,5,8,12 GeV/c. Each row refers to a different ($p_{\min} \leq p < p_{\max}, \theta_{\min} \leq \theta < \theta_{\max}$) bin, where p and θ are the pion momentum and polar angle, respectively. The central value as well as the square-root of the diagonal elements of the covariance matrix are given.

θ_{\min} (rad)	θ_{\max} (rad)	p_{\min} (GeV/c)	p_{\max} (GeV/c)	$d^2\sigma^{\pi^-}/(dpd\Omega)$ (barn/(GeV/c sr))			
				3 GeV/c	5 GeV/c	8 GeV/c	12 GeV/c
0.050	0.100	0.50	1.00	0.05±0.02	0.16±0.03	0.25±0.04	0.19±0.12
		1.00	1.50	0.07±0.02	0.16±0.02	0.27±0.03	0.38±0.13
		1.50	2.00	0.09±0.02	0.12±0.02	0.25±0.03	0.31±0.10
		2.00	2.50	0.09±0.03	0.120±0.014	0.26±0.03	0.27±0.09
		2.50	3.00	±	0.107±0.013	0.15±0.02	0.39±0.11
		3.00	3.50	±	0.102±0.014	0.16±0.02	0.26±0.08
		3.50	4.00	±	0.095±0.011	0.13±0.02	0.25±0.08
		4.00	5.00	±	0.050±0.010	0.081±0.009	0.13±0.04
		5.00	6.50	±	±	0.048±0.006	0.06±0.02
		6.50	8.00	±	±	±	0.024±0.013
0.100	0.150	0.50	1.00	0.13±0.03	0.24±0.04	0.35±0.05	0.28±0.12
		1.00	1.50	0.06±0.02	0.17±0.02	0.31±0.04	0.49±0.14
		1.50	2.00	0.08±0.02	0.11±0.02	0.26±0.03	0.31±0.10
		2.00	2.50	0.025±0.009	0.090±0.012	0.17±0.02	0.25±0.09
		2.50	3.00	±	0.084±0.012	0.14±0.02	0.20±0.08
		3.00	3.50	±	0.047±0.007	0.109±0.015	0.27±0.09
		3.50	4.00	±	0.023±0.005	0.077±0.012	0.12±0.06
		4.00	5.00	±	0.013±0.004	0.038±0.007	0.03±0.02
		5.00	6.50	±	±	0.006±0.002	0.02±0.02
		6.50	8.00	±	±	±	0.004±0.005
0.150	0.200	0.50	1.00	0.15±0.04	0.21±0.03	0.38±0.06	0.61±0.22
		1.00	1.50	0.06±0.02	0.12±0.02	0.26±0.03	0.33±0.12
		1.50	2.00	0.016±0.007	0.087±0.014	0.19±0.03	0.34±0.12
		2.00	2.50	0.012±0.007	0.065±0.011	0.18±0.02	0.23±0.10
		2.50	3.00	±	0.037±0.008	0.085±0.015	0.09±0.05
		3.00	3.50	±	0.022±0.006	0.043±0.009	0.14±0.10
		3.50	4.00	±	0.005±0.002	0.020±0.005	0.02±0.02
		4.00	5.00	±	0.004±0.002	0.011±0.004	0.03±0.03
		5.00	6.50	±	±	0.002±0.001	*±*
		6.50	8.00	±	±	±	0.001±0.005
0.200	0.250	0.50	1.00	0.06±0.02	0.23±0.04	0.31±0.05	0.15±0.09
		1.00	1.50	0.11±0.03	0.11±0.02	0.23±0.04	0.27±0.15
		1.50	2.00	0.018±0.010	0.06±0.02	0.24±0.04	0.30±0.19
		2.00	2.50	0.007±0.006	0.018±0.005	0.13±0.03	0.257±0.275
		2.50	3.00	±	0.010±0.004	0.07±0.02	0.10±0.19
		3.00	3.50	±	0.003±0.002	0.027±0.010	0.016±0.075
		3.50	4.00	±	0.002±0.002	0.009±0.005	0.000±0.014
		4.00	5.00	±	±	0.003±0.005	0.000±0.016
		5.00	6.50	±	±	0.002±0.003	0.000±0.003
		6.50	8.00	±	±	±	0.000±0.037

Table 16: HARP results for the double-differential π^+ production cross-section in the laboratory system, $d^2\sigma^\pi/(dpd\Omega)$, for π^- -Cu interactions at 3,5,8,12 GeV/c. Each row refers to a different ($p_{\min} \leq p < p_{\max}, \theta_{\min} \leq \theta < \theta_{\max}$) bin, where p and θ are the pion momentum and polar angle, respectively. The central value as well as the square-root of the diagonal elements of the covariance matrix are given.

θ_{\min} (rad)	θ_{\max} (rad)	p_{\min} (GeV/c)	p_{\max} (GeV/c)	$d^2\sigma^{\pi^+}/(dpd\Omega)$ (barn/(GeV/c sr))					
				3 GeV/c	5 GeV/c	8 GeV/c	12 GeV/c		
0.05	0.10	0.50	1.00	0.11±0.02	0.24±0.03	0.63±0.06	0.70±0.08		
		1.00	1.50	0.09±0.02	0.26±0.03	0.62±0.04	0.79±0.07		
		1.50	2.00	0.10±0.02	0.20±0.02	0.53±0.03	0.69±0.06		
		2.00	2.50	0.13±0.02	0.16±0.02	0.39±0.03	0.69±0.05		
		2.50	3.00	±	0.13±0.02	0.27±0.03	0.54±0.04		
		3.00	3.50	±	0.11±0.02	0.29±0.03	0.53±0.04		
		3.50	4.00	±	0.13±0.02	0.19±0.03	0.40±0.04		
		4.00	5.00	±	0.06±0.02	0.143±0.014	0.26±0.02		
		5.00	6.50	±	±	0.066±0.010	0.124±0.014		
		6.50	8.00	±	±	±	0.062±0.008		
		0.10	0.15	0.50	1.00	0.19±0.03	0.35±0.04	0.70±0.07	0.91±0.10
				1.00	1.50	0.11±0.02	0.27±0.03	0.55±0.05	0.79±0.08
1.50	2.00			0.09±0.02	0.21±0.02	0.45±0.04	0.69±0.07		
2.00	2.50			0.081±0.014	0.15±0.02	0.37±0.03	0.54±0.06		
2.50	3.00			±	0.095±0.014	0.27±0.03	0.42±0.05		
3.00	3.50			±	0.073±0.013	0.15±0.02	0.41±0.04		
3.50	4.00			±	0.040±0.008	0.11±0.02	0.25±0.03		
4.00	5.00			±	0.010±0.006	0.051±0.010	0.13±0.02		
5.00	6.50			±	±	0.010±0.003	0.043±0.008		
6.50	8.00			±	±	±	0.006±0.002		
0.15	0.20			0.50	1.00	0.12±0.02	0.32±0.04	0.70±0.07	0.95±0.11
				1.00	1.50	0.11±0.02	0.22±0.03	0.45±0.04	0.57±0.06
		1.50	2.00	0.055±0.010	0.13±0.02	0.36±0.03	0.46±0.05		
		2.00	2.50	0.052±0.011	0.13±0.02	0.29±0.03	0.39±0.05		
		2.50	3.00	±	0.051±0.011	0.12±0.02	0.27±0.04		
		3.00	3.50	±	0.028±0.007	0.067±0.012	0.16±0.02		
		3.50	4.00	±	0.005±0.004	0.050±0.009	0.068±0.015		
		4.00	5.00	±	±	0.021±0.005	0.045±0.010		
		5.00	6.50	±	±	0.002±0.001	0.006±0.003		
		6.50	8.00	±	±	±	0.000±0.001		
		0.20	0.25	0.50	1.00	0.22±0.04	0.27±0.04	0.51±0.07	0.76±0.11
				1.00	1.50	0.14±0.03	0.26±0.04	0.71±0.08	0.72±0.10
1.50	2.00			0.07±0.02	0.17±0.03	0.46±0.06	0.65±0.10		
2.00	2.50			0.035±0.012	0.09±0.02	0.27±0.04	0.35±0.06		
2.50	3.00			±	0.039±0.011	0.11±0.02	0.18±0.04		
3.00	3.50			±	0.003±0.002	0.028±0.010	0.06±0.02		
3.50	4.00			±	±	0.011±0.006	0.028±0.013		
4.00	5.00			±	±	0.005±0.003	0.008±0.009		
5.00	6.50			±	±	±	0.000±0.001		
6.50	8.00			±	±	±	0.000±0.009		

Table 17: HARP results for the double-differential π^- production cross-section in the laboratory system, $d^2\sigma^\pi/(dpd\Omega)$, for π^- -Cu interactions at 3,5,8,12 GeV/c. Each row refers to a different ($p_{\min} \leq p < p_{\max}, \theta_{\min} \leq \theta < \theta_{\max}$) bin, where p and θ are the pion momentum and polar angle, respectively. The central value as well as the square-root of the diagonal elements of the covariance matrix are given.

θ_{\min} (rad)	θ_{\max} (rad)	p_{\min} (GeV/c)	p_{\max} (GeV/c)	$d^2\sigma^{\pi^-}/(dpd\Omega)$ (barn/(GeV/c sr))			
				3 GeV/c	5 GeV/c	8 GeV/c	12 GeV/c
0.05	0.10	0.50	1.00	0.24±0.03	0.45±0.05	0.91±0.08	1.12±0.12
		1.00	1.50	0.21±0.03	0.32±0.03	0.71±0.05	0.96±0.08
		1.50	2.00	0.26±0.03	0.34±0.03	0.75±0.04	0.94±0.07
		2.00	2.50	0.15±0.04	0.36±0.03	0.68±0.04	1.03±0.07
		2.50	3.00	±	0.41±0.03	0.63±0.04	0.76±0.06
		3.00	3.50	±	0.43±0.04	0.47±0.04	0.78±0.06
		3.50	4.00	±	0.53±0.04	0.41±0.03	0.68±0.05
		4.00	5.00	±	0.51±0.08	0.42±0.03	0.48±0.03
		5.00	6.50	±	±	0.30±0.02	0.34±0.02
		6.50	8.00	±	±	±	0.21±0.02
0.10	0.15	0.50	1.00	0.33±0.04	0.58±0.06	1.01±0.11	1.10±0.12
		1.00	1.50	0.24±0.03	0.40±0.04	0.80±0.06	1.00±0.09
		1.50	2.00	0.26±0.03	0.34±0.03	0.67±0.05	0.85±0.08
		2.00	2.50	0.22±0.04	0.31±0.03	0.63±0.05	0.82±0.07
		2.50	3.00	±	0.31±0.03	0.40±0.03	0.63±0.06
		3.00	3.50	±	0.34±0.03	0.31±0.03	0.49±0.05
		3.50	4.00	±	0.21±0.03	0.18±0.03	0.33±0.03
		4.00	5.00	±	0.21±0.04	0.118±0.014	0.25±0.03
		5.00	6.50	±	±	0.059±0.007	0.100±0.013
		6.50	8.00	±	±	±	0.035±0.006
0.15	0.20	0.50	1.00	0.22±0.04	0.42±0.05	0.88±0.09	1.05±0.13
		1.00	1.50	0.21±0.03	0.33±0.04	0.76±0.07	0.86±0.09
		1.50	2.00	0.15±0.02	0.27±0.03	0.51±0.05	0.65±0.07
		2.00	2.50	0.17±0.02	0.19±0.02	0.35±0.03	0.50±0.05
		2.50	3.00	±	0.12±0.02	0.20±0.02	0.32±0.04
		3.00	3.50	±	0.073±0.012	0.114±0.015	0.19±0.03
		3.50	4.00	±	0.039±0.008	0.097±0.012	0.15±0.02
		4.00	5.00	±	0.036±0.007	0.049±0.007	0.088±0.013
		5.00	6.50	±	±	0.019±0.003	0.037±0.007
		6.50	8.00	±	±	±	0.009±0.003
0.20	0.25	0.50	1.00	0.17±0.03	0.39±0.06	0.59±0.07	0.72±0.10
		1.00	1.50	0.11±0.02	0.18±0.03	0.39±0.05	0.38±0.06
		1.50	2.00	0.11±0.02	0.14±0.03	0.31±0.05	0.42±0.07
		2.00	2.50	0.056±0.011	0.07±0.02	0.35±0.05	0.31±0.06
		2.50	3.00	±	0.047±0.011	0.23±0.04	0.16±0.04
		3.00	3.50	±	0.040±0.009	0.13±0.02	0.13±0.03
		3.50	4.00	±	0.032±0.007	0.070±0.013	0.11±0.02
		4.00	5.00	±	0.026±0.006	0.041±0.008	0.08±0.02
		5.00	6.50	±	±	0.013±0.004	0.029±0.010
		6.50	8.00	±	±	±	0.006±0.006

Table 18: HARP results for the double-differential π^+ production cross-section in the laboratory system, $d^2\sigma^\pi/(dpd\Omega)$, for π^+ -Cu interactions at 3,5,8,12 GeV/c. Each row refers to a different ($p_{\min} \leq p < p_{\max}, \theta_{\min} \leq \theta < \theta_{\max}$) bin, where p and θ are the pion momentum and polar angle, respectively. The central value as well as the square-root of the diagonal elements of the covariance matrix are given.

θ_{\min} (rad)	θ_{\max} (rad)	p_{\min} (GeV/c)	p_{\max} (GeV/c)	$d^2\sigma^{\pi^+}/(dpd\Omega)$ (barn/(GeV/c sr))			
				3 GeV/c	5 GeV/c	8 GeV/c	12 GeV/c
0.050	0.100	0.50	1.00	0.16±0.06	0.32±0.05	0.58±0.09	0.74±0.25
		1.00	1.50	0.08±0.02	0.32±0.04	0.60±0.06	0.81±0.21
		1.50	2.00	0.15±0.02	0.27±0.03	0.57±0.06	0.75±0.20
		2.00	2.50	0.43±0.05	0.34±0.03	0.56±0.06	0.68±0.18
		2.50	3.00	±	0.49±0.04	0.54±0.05	0.77±0.19
		3.00	3.50	±	0.60±0.06	0.43±0.05	0.68±0.15
		3.50	4.00	±	0.73±0.04	0.46±0.05	0.71±0.16
		4.00	5.00	±	0.68±0.22	0.48±0.03	0.55±0.10
		5.00	6.50	±	±	0.41±0.06	0.41±0.07
		6.50	8.00	±	±	±	0.18±0.05
0.100	0.150	0.50	1.00	0.12±0.05	0.45±0.06	0.64±0.08	0.86±0.27
		1.00	1.50	0.18±0.05	0.38±0.05	0.51±0.06	0.95±0.25
		1.50	2.00	0.28±0.05	0.40±0.05	0.68±0.07	0.79±0.20
		2.00	2.50	0.51±0.07	0.34±0.04	0.56±0.06	0.56±0.16
		2.50	3.00	±	0.34±0.04	0.31±0.04	0.65±0.16
		3.00	3.50	±	0.33±0.03	0.31±0.04	0.42±0.13
		3.50	4.00	±	0.27±0.03	0.21±0.03	0.23±0.07
		4.00	5.00	±	0.27±0.10	0.16±0.03	0.23±0.07
		5.00	6.50	±	±	0.066±0.014	0.07±0.03
		6.50	8.00	±	±	±	0.03±0.02
0.150	0.200	0.50	1.00	0.21±0.07	0.50±0.07	0.74±0.10	0.85±0.30
		1.00	1.50	0.22±0.05	0.32±0.04	0.55±0.06	0.58±0.19
		1.50	2.00	0.23±0.05	0.26±0.03	0.39±0.05	0.68±0.19
		2.00	2.50	0.14±0.04	0.19±0.03	0.30±0.04	0.72±0.21
		2.50	3.00	±	0.13±0.02	0.24±0.04	0.28±0.11
		3.00	3.50	±	0.09±0.02	0.15±0.03	0.23±0.11
		3.50	4.00	±	0.07±0.02	0.069±0.015	0.16±0.08
		4.00	5.00	±	0.05±0.03	0.043±0.010	0.14±0.07
		5.00	6.50	±	±	0.017±0.007	0.021±0.024
		6.50	8.00	±	±	±	0.007±0.010
0.200	0.250	0.50	1.00	0.18±0.09	0.28±0.05	0.53±0.08	0.41±0.22
		1.00	1.50	0.07±0.03	0.23±0.04	0.33±0.06	0.34±0.26
		1.50	2.00	0.10±0.04	0.14±0.03	0.26±0.05	0.21±0.17
		2.00	2.50	0.05±0.03	0.15±0.03	0.25±0.05	0.14±0.20
		2.50	3.00	±	0.09±0.02	0.14±0.04	0.124±0.253
		3.00	3.50	±	0.041±0.012	0.10±0.03	0.037±0.087
		3.50	4.00	±	0.021±0.009	0.06±0.02	0.034±0.108
		4.00	5.00	±	0.021±0.011	0.038±0.014	0.037±0.124
		5.00	6.50	±	±	0.018±0.011	0.012±0.036
		6.50	8.00	±	±	±	0.003±0.102

Table 19: HARP results for the double-differential π^- production cross-section in the laboratory system, $d^2\sigma^\pi/(dpd\Omega)$, for π^+ -Cu interactions at 3,5,8,12 GeV/c. Each row refers to a different ($p_{\min} \leq p < p_{\max}, \theta_{\min} \leq \theta < \theta_{\max}$) bin, where p and θ are the pion momentum and polar angle, respectively. The central value as well as the square-root of the diagonal elements of the covariance matrix are given.

θ_{\min} (rad)	θ_{\max} (rad)	p_{\min} (GeV/c)	p_{\max} (GeV/c)	$d^2\sigma^{\pi^+}/(dpd\Omega)$ (barn/(GeV/c sr))					
				3 GeV/c	5 GeV/c	8 GeV/c	12 GeV/c		
0.050	0.100	0.50	1.00	0.11±0.04	0.27±0.04	0.51±0.07	0.33±0.16		
		1.00	1.50	0.13±0.04	0.24±0.03	0.54±0.06	0.72±0.21		
		1.50	2.00	0.13±0.03	0.20±0.03	0.41±0.05	0.68±0.19		
		2.00	2.50	0.11±0.04	0.19±0.02	0.38±0.04	0.47±0.14		
		2.50	3.00	±	0.16±0.02	0.27±0.03	0.83±0.20		
		3.00	3.50	±	0.16±0.02	0.25±0.03	0.29±0.09		
		3.50	4.00	±	0.18±0.02	0.18±0.02	0.41±0.12		
		4.00	5.00	±	0.07±0.02	0.17±0.02	0.29±0.08		
		5.00	6.50	±	±	0.065±0.008	0.12±0.04		
		6.50	8.00	±	±	±	0.09±0.04		
		0.100	0.150	0.50	1.00	0.27±0.07	0.45±0.06	0.65±0.09	1.10±0.35
				1.00	1.50	0.14±0.04	0.23±0.03	0.46±0.05	0.85±0.22
				1.50	2.00	0.10±0.03	0.21±0.03	0.38±0.04	0.31±0.12
				2.00	2.50	0.04±0.02	0.18±0.02	0.29±0.04	0.43±0.15
2.50	3.00			±	0.100±0.015	0.24±0.03	0.44±0.14		
3.00	3.50			±	0.077±0.013	0.18±0.02	0.34±0.11		
3.50	4.00			±	0.031±0.006	0.082±0.014	0.36±0.12		
4.00	5.00			±	0.022±0.007	0.073±0.012	0.13±0.06		
5.00	6.50			±	±	0.018±0.004	0.04±0.03		
6.50	8.00			±	±	±	0.002±0.003		
0.150	0.200			0.50	1.00	0.11±0.04	0.42±0.06	0.58±0.08	0.79±0.27
				1.00	1.50	0.10±0.04	0.23±0.03	0.42±0.06	0.66±0.23
				1.50	2.00	0.11±0.04	0.23±0.03	0.33±0.04	0.31±0.13
				2.00	2.50	0.019±0.013	0.11±0.02	0.28±0.04	0.23±0.11
		2.50	3.00	±	0.064±0.013	0.16±0.03	0.16±0.09		
		3.00	3.50	±	0.016±0.004	0.08±0.02	0.22±0.10		
		3.50	4.00	±	0.012±0.005	0.037±0.010	0.18±0.09		
		4.00	5.00	±	0.005±0.003	0.020±0.006	0.11±0.07		
		5.00	6.50	±	±	0.004±0.002	0.03±0.03		
		6.50	8.00	±	±	±	±		
		0.200	0.250	0.50	1.00	0.17±0.07	0.33±0.06	0.60±0.09	0.58±0.26
				1.00	1.50	0.06±0.03	0.20±0.04	0.51±0.08	0.44±0.23
				1.50	2.00	0.08±0.04	0.09±0.02	0.29±0.05	0.72±0.37
				2.00	2.50	0.009±0.011	0.024±0.007	0.13±0.03	0.16±0.18
2.50	3.00			±	0.014±0.005	0.043±0.012	0.07±0.11		
3.00	3.50			±	0.017±0.007	0.020±0.009	0.050±0.065		
3.50	4.00			±	0.008±0.004	0.008±0.006	0.010±0.031		
4.00	5.00			±	0.005±0.004	0.005±0.007	0.019±0.109		
5.00	6.50			±	±	0.002±0.004	0.016±0.090		
6.50	8.00			±	±	±	0.003±0.068		

Table 20: HARP results for the double-differential π^+ production cross-section in the laboratory system, $d^2\sigma^\pi/(dpd\Omega)$, for π^- -Sn interactions at 3,5,8,12 GeV/c. Each row refers to a different ($p_{\min} \leq p < p_{\max}, \theta_{\min} \leq \theta < \theta_{\max}$) bin, where p and θ are the pion momentum and polar angle, respectively. The central value as well as the square-root of the diagonal elements of the covariance matrix are given.

θ_{\min} (rad)	θ_{\max} (rad)	p_{\min} (GeV/c)	p_{\max} (GeV/c)	$d^2\sigma^{\pi^+}/(dpd\Omega)$ (barn/(GeV/c sr))					
				3 GeV/c	5 GeV/c	8 GeV/c	12 GeV/c		
0.05	0.10	0.50	1.00	0.11±0.03	0.32±0.05	0.68±0.08	1.15±0.12		
		1.00	1.50	0.07±0.02	0.34±0.04	0.89±0.07	1.25±0.09		
		1.50	2.00	0.14±0.03	0.29±0.04	0.72±0.05	1.02±0.08		
		2.00	2.50	0.11±0.03	0.13±0.02	0.52±0.05	0.93±0.07		
		2.50	3.00	±	0.16±0.03	0.37±0.04	0.75±0.05		
		3.00	3.50	±	0.17±0.02	0.36±0.05	0.69±0.06		
		3.50	4.00	±	0.17±0.02	0.21±0.04	0.50±0.04		
		4.00	5.00	±	0.06±0.03	0.15±0.02	0.36±0.03		
		5.00	6.50	±	±	0.080±0.013	0.19±0.02		
		6.50	8.00	±	±	±	0.081±0.011		
		0.10	0.15	0.50	1.00	0.18±0.03	0.42±0.06	0.94±0.10	1.21±0.12
				1.00	1.50	0.07±0.02	0.35±0.04	0.68±0.07	1.23±0.11
1.50	2.00			0.08±0.02	0.23±0.03	0.61±0.06	1.07±0.09		
2.00	2.50			0.12±0.03	0.21±0.03	0.50±0.05	0.87±0.08		
2.50	3.00			±	0.14±0.02	0.34±0.04	0.65±0.06		
3.00	3.50			±	0.09±0.02	0.20±0.03	0.55±0.05		
3.50	4.00			±	0.036±0.009	0.17±0.03	0.41±0.04		
4.00	5.00			±	0.022±0.009	0.07±0.02	0.21±0.02		
5.00	6.50			±	±	0.013±0.005	0.067±0.011		
6.50	8.00			±	±	±	0.008±0.003		
0.15	0.20			0.50	1.00	0.22±0.05	0.45±0.07	0.92±0.11	1.22±0.13
				1.00	1.50	0.10±0.03	0.24±0.03	0.57±0.06	0.86±0.08
		1.50	2.00	0.040±0.012	0.24±0.03	0.50±0.05	0.82±0.07		
		2.00	2.50	0.05±0.02	0.14±0.03	0.34±0.04	0.52±0.06		
		2.50	3.00	±	0.06±0.02	0.19±0.03	0.33±0.04		
		3.00	3.50	±	0.031±0.010	0.12±0.02	0.20±0.03		
		3.50	4.00	±	0.021±0.008	0.07±0.02	0.09±0.02		
		4.00	5.00	±	0.004±0.004	0.027±0.007	0.053±0.010		
		5.00	6.50	±	±	0.005±0.002	0.013±0.004		
		6.50	8.00	±	±	±	0.002±0.001		
		0.20	0.25	0.50	1.00	0.23±0.06	0.45±0.08	0.73±0.10	1.14±0.15
				1.00	1.50	0.17±0.04	0.36±0.06	0.75±0.10	1.14±0.14
1.50	2.00			0.08±0.03	0.29±0.05	0.56±0.09	0.75±0.11		
2.00	2.50			0.002±0.005	0.15±0.03	0.23±0.05	0.56±0.09		
2.50	3.00			±	0.05±0.02	0.13±0.03	0.25±0.05		
3.00	3.50			±	0.013±0.007	0.04±0.02	0.09±0.02		
3.50	4.00			±	0.003±0.002	0.014±0.010	0.047±0.015		
4.00	5.00			±	0.001±0.001	0.010±0.009	0.018±0.011		
5.00	6.50			±	±	0.001±0.001	0.003±0.002		
6.50	8.00			±	±	±	0.001±0.009		

Table 21: HARP results for the double-differential π^- production cross-section in the laboratory system, $d^2\sigma^\pi/(dpd\Omega)$, for π^- -Sn interactions at 3,5,8,12 GeV/c. Each row refers to a different ($p_{\min} \leq p < p_{\max}, \theta_{\min} \leq \theta < \theta_{\max}$) bin, where p and θ are the pion momentum and polar angle, respectively. The central value as well as the square-root of the diagonal elements of the covariance matrix are given.

θ_{\min} (rad)	θ_{\max} (rad)	p_{\min} (GeV/c)	p_{\max} (GeV/c)	$d^2\sigma^\pi/(dpd\Omega)$ (barn/(GeV/c sr))					
				3 GeV/c	5 GeV/c	8 GeV/c	12 GeV/c		
0.05	0.10	0.50	1.00	0.30±0.05	0.62±0.07	1.26±0.11	1.72±0.16		
		1.00	1.50	0.19±0.04	0.41±0.04	0.90±0.07	1.29±0.10		
		1.50	2.00	0.17±0.03	0.46±0.05	0.94±0.06	1.38±0.09		
		2.00	2.50	0.12±0.03	0.51±0.05	0.91±0.07	1.34±0.09		
		2.50	3.00	±	0.46±0.04	0.83±0.06	1.24±0.08		
		3.00	3.50	±	0.61±0.06	0.66±0.06	1.02±0.07		
		3.50	4.00	±	0.62±0.06	0.54±0.05	0.94±0.07		
		4.00	5.00	±	0.66±0.10	0.56±0.05	0.67±0.05		
		5.00	6.50	±	±	0.38±0.03	0.46±0.03		
		6.50	8.00	±	±	±	0.29±0.02		
		0.10	0.15	0.50	1.00	0.27±0.05	0.76±0.09	1.39±0.15	1.91±0.20
				1.00	1.50	0.25±0.04	0.41±0.05	1.00±0.09	1.35±0.11
				1.50	2.00	0.23±0.04	0.49±0.05	0.81±0.07	1.35±0.11
				2.00	2.50	0.44±0.08	0.39±0.04	0.73±0.06	0.96±0.08
2.50	3.00			±	0.33±0.04	0.64±0.06	0.91±0.08		
3.00	3.50			±	0.40±0.05	0.37±0.04	0.64±0.06		
3.50	4.00			±	0.25±0.04	0.28±0.04	0.57±0.05		
4.00	5.00			±	0.28±0.06	0.17±0.02	0.34±0.03		
5.00	6.50			±	±	0.100±0.013	0.141±0.015		
6.50	8.00			±	±	±	0.053±0.009		
0.15	0.20			0.50	1.00	0.25±0.05	0.65±0.09	1.07±0.13	1.69±0.18
				1.00	1.50	0.36±0.06	0.43±0.05	0.99±0.09	1.33±0.12
				1.50	2.00	0.22±0.04	0.30±0.04	0.66±0.07	0.95±0.09
				2.00	2.50	0.14±0.02	0.22±0.03	0.38±0.05	0.65±0.06
		2.50	3.00	±	0.19±0.03	0.27±0.03	0.46±0.05		
		3.00	3.50	±	0.10±0.02	0.15±0.02	0.28±0.03		
		3.50	4.00	±	0.062±0.012	0.11±0.02	0.18±0.03		
		4.00	5.00	±	0.077±0.015	0.065±0.011	0.11±0.02		
		5.00	6.50	±	±	0.026±0.005	0.047±0.008		
		6.50	8.00	±	±	±	0.012±0.003		
		0.20	0.25	0.50	1.00	0.17±0.04	0.55±0.09	0.65±0.09	1.08±0.14
				1.00	1.50	0.12±0.03	0.24±0.04	0.37±0.05	0.49±0.07
				1.50	2.00	0.12±0.03	0.24±0.05	0.35±0.07	0.43±0.07
				2.00	2.50	0.08±0.02	0.15±0.03	0.26±0.05	0.42±0.07
2.50	3.00			±	0.09±0.02	0.18±0.03	0.30±0.06		
3.00	3.50			±	0.061±0.014	0.12±0.02	0.24±0.04		
3.50	4.00			±	0.040±0.010	0.08±0.02	0.13±0.03		
4.00	5.00			±	0.019±0.007	0.052±0.015	0.08±0.02		
5.00	6.50			±	±	0.017±0.007	0.019±0.006		
6.50	8.00			±	±	±	0.004±0.005		

Table 22: HARP results for the double-differential π^+ production cross-section in the laboratory system, $d^2\sigma^\pi/(dpd\Omega)$, for π^+ -Sn interactions at 3,5,8,12 GeV/c. Each row refers to a different ($p_{\min} \leq p < p_{\max}, \theta_{\min} \leq \theta < \theta_{\max}$) bin, where p and θ are the pion momentum and polar angle, respectively. The central value as well as the square-root of the diagonal elements of the covariance matrix are given.

θ_{\min} (rad)	θ_{\max} (rad)	p_{\min} (GeV/c)	p_{\max} (GeV/c)	$d^2\sigma^{\pi^+}/(dpd\Omega)$ (barn/(GeV/c sr))			
				3 GeV/c	5 GeV/c	8 GeV/c	12 GeV/c
0.050	0.100	0.50	1.00	0.28±0.07	0.48±0.08	0.99±0.14	1.11±0.27
		1.00	1.50	0.09±0.02	0.35±0.05	0.80±0.08	1.32±0.23
		1.50	2.00	0.17±0.02	0.35±0.05	0.76±0.15	1.14±0.21
		2.00	2.50	0.46±0.04	0.55±0.05	0.68±0.21	1.05±0.21
		2.50	3.00	±	0.57±0.04	0.64±0.17	1.12±0.28
		3.00	3.50	±	0.74±0.07	0.55±0.06	0.96±0.15
		3.50	4.00	±	0.93±0.05	0.55±0.07	0.78±0.13
		4.00	5.00	±	0.85±0.28	0.68±0.06	0.73±0.10
		5.00	6.50	±	±	0.61±0.10	0.49±0.07
		6.50	8.00	±	±	±	0.41±0.06
0.100	0.150	0.50	1.00	0.19±0.06	0.55±0.08	0.94±0.12	1.16±0.26
		1.00	1.50	0.31±0.07	0.40±0.06	0.75±0.08	1.30±0.24
		1.50	2.00	0.43±0.06	0.48±0.06	0.90±0.09	0.71±0.15
		2.00	2.50	0.51±0.06	0.53±0.05	0.69±0.09	0.98±0.18
		2.50	3.00	±	0.43±0.05	0.47±0.06	0.94±0.17
		3.00	3.50	±	0.42±0.04	0.41±0.05	0.87±0.15
		3.50	4.00	±	0.37±0.04	0.38±0.04	0.47±0.09
		4.00	5.00	±	0.35±0.13	0.22±0.03	0.39±0.07
		5.00	6.50	±	±	0.060±0.013	0.18±0.04
		6.50	8.00	±	±	±	0.06±0.02
0.150	0.200	0.50	1.00	0.31±0.08	0.54±0.09	0.99±0.13	1.29±0.31
		1.00	1.50	0.23±0.05	0.41±0.05	0.85±0.09	0.97±0.20
		1.50	2.00	0.22±0.04	0.35±0.04	0.64±0.07	0.93±0.18
		2.00	2.50	0.29±0.05	0.31±0.04	0.50±0.06	0.62±0.15
		2.50	3.00	±	0.15±0.02	0.23±0.04	0.40±0.11
		3.00	3.50	±	0.12±0.03	0.18±0.03	0.42±0.11
		3.50	4.00	±	0.08±0.02	0.11±0.02	0.20±0.07
		4.00	5.00	±	0.06±0.03	0.08±0.02	0.11±0.05
		5.00	6.50	±	±	0.019±0.008	0.04±0.03
		6.50	8.00	±	±	±	0.012±0.014
0.200	0.250	0.50	1.00	0.09±0.07	0.52±0.08	0.91±0.14	1.15±0.31
		1.00	1.50	0.09±0.03	0.23±0.05	0.59±0.10	0.66±0.20
		1.50	2.00	0.08±0.03	0.19±0.04	0.55±0.10	0.74±0.23
		2.00	2.50	0.04±0.02	0.15±0.03	0.36±0.07	0.25±0.11
		2.50	3.00	±	0.11±0.03	0.14±0.04	0.27±0.16
		3.00	3.50	±	0.06±0.02	0.14±0.04	0.15±0.09
		3.50	4.00	±	0.04±0.02	0.10±0.03	0.084±0.093
		4.00	5.00	±	0.022±0.011	0.06±0.02	0.039±0.072
		5.00	6.50	±	±	0.020±0.012	0.034±0.049
		6.50	8.00	±	±	±	0.008±0.087

Table 23: HARP results for the double-differential π^- production cross-section in the laboratory system, $d^2\sigma^\pi/(dpd\Omega)$, for π^+ -Sn interactions at 3,5,8,12 GeV/c. Each row refers to a different ($p_{\min} \leq p < p_{\max}, \theta_{\min} \leq \theta < \theta_{\max}$) bin, where p and θ are the pion momentum and polar angle, respectively. The central value as well as the square-root of the diagonal elements of the covariance matrix are given.

θ_{\min} (rad)	θ_{\max} (rad)	p_{\min} (GeV/c)	p_{\max} (GeV/c)	$d^2\sigma^{\pi^-}/(dpd\Omega)$ (barn/(GeV/c sr))					
				3 GeV/c	5 GeV/c	8 GeV/c	12 GeV/c		
0.050	0.100	0.50	1.00	0.17±0.05	0.37±0.06	0.78±0.10	1.18±0.27		
		1.00	1.50	0.14±0.03	0.34±0.04	0.70±0.08	0.78±0.17		
		1.50	2.00	0.18±0.03	0.30±0.04	0.60±0.06	1.03±0.19		
		2.00	2.50	0.17±0.05	0.25±0.03	0.51±0.06	0.80±0.16		
		2.50	3.00	±	0.20±0.03	0.40±0.04	0.80±0.15		
		3.00	3.50	±	0.18±0.02	0.36±0.04	0.62±0.11		
		3.50	4.00	±	0.20±0.02	0.29±0.03	0.60±0.11		
		4.00	5.00	±	0.09±0.02	0.19±0.02	0.36±0.06		
		5.00	6.50	±	±	0.084±0.010	0.21±0.04		
		6.50	8.00	±	±	±	0.10±0.02		
		0.100	0.150	0.50	1.00	0.25±0.06	0.50±0.08	1.22±0.16	1.18±0.26
				1.00	1.50	0.14±0.03	0.34±0.05	0.71±0.08	0.74±0.16
				1.50	2.00	0.12±0.03	0.28±0.04	0.58±0.07	0.98±0.19
				2.00	2.50	0.045±0.014	0.19±0.03	0.42±0.05	0.71±0.15
2.50	3.00			±	0.12±0.02	0.30±0.04	0.51±0.11		
3.00	3.50			±	0.094±0.015	0.24±0.03	0.58±0.12		
3.50	4.00			±	0.055±0.010	0.16±0.03	0.36±0.08		
4.00	5.00			±	0.022±0.007	0.09±0.02	0.20±0.05		
5.00	6.50			±	±	0.017±0.004	0.07±0.03		
6.50	8.00			±	±	±	0.006±0.004		
0.150	0.200			0.50	1.00	0.14±0.05	0.45±0.07	0.95±0.13	1.41±0.32
				1.00	1.50	0.18±0.04	0.32±0.04	0.69±0.08	0.86±0.20
				1.50	2.00	0.09±0.03	0.26±0.04	0.54±0.07	0.52±0.14
				2.00	2.50	0.025±0.011	0.15±0.02	0.38±0.05	0.40±0.12
		2.50	3.00	±	0.09±0.02	0.20±0.03	0.20±0.08		
		3.00	3.50	±	0.036±0.009	0.10±0.02	0.23±0.08		
		3.50	4.00	±	0.021±0.007	0.041±0.010	0.14±0.06		
		4.00	5.00	±	0.006±0.003	0.030±0.009	0.06±0.04		
		5.00	6.50	±	±	0.005±0.003	0.007±0.008		
		6.50	8.00	±	±	±	0.004±0.007		
		0.200	0.250	0.50	1.00	0.19±0.06	0.40±0.08	0.78±0.12	1.17±0.30
				1.00	1.50	0.15±0.05	0.31±0.05	0.70±0.11	0.78±0.24
				1.50	2.00	0.015±0.010	0.12±0.03	0.42±0.08	0.72±0.46
				2.00	2.50	0.002±0.002	0.051±0.013	0.39±0.08	0.54±1.07
2.50	3.00			±	0.023±0.007	0.15±0.04	0.14±0.35		
3.00	3.50			±	0.023±0.009	0.04±0.02	0.02±0.09		
3.50	4.00			±	0.009±0.005	0.016±0.009	0.01±0.03		
4.00	5.00			±	0.004±0.003	0.004±0.007	0.000±0.003		
5.00	6.50			±	±	0.000±0.002	0.000±0.002		
6.50	8.00			±	±	±	0.000±0.036		

Table 24: HARP results for the double-differential π^+ production cross-section in the laboratory system, $d^2\sigma^\pi/(dpd\Omega)$, for π^- -Ta interactions at 3,5,8,12 GeV/c. Each row refers to a different ($p_{\min} \leq p < p_{\max}, \theta_{\min} \leq \theta < \theta_{\max}$) bin, where p and θ are the pion momentum and polar angle, respectively. The central value as well as the square-root of the diagonal elements of the covariance matrix are given.

θ_{\min} (rad)	θ_{\max} (rad)	p_{\min} (GeV/c)	p_{\max} (GeV/c)	$d^2\sigma^{\pi^+}/(dpd\Omega)$ (barn/(GeV/c sr))			
				3 GeV/c	5 GeV/c	8 GeV/c	12 GeV/c
0.05	0.10	0.50	1.00	0.08±0.03	0.42±0.06	1.06±0.11	1.60±0.17
		1.00	1.50	0.06±0.03	0.33±0.05	1.27±0.09	1.67±0.13
		1.50	2.00	0.13±0.05	0.29±0.04	1.04±0.07	1.27±0.09
		2.00	2.50	0.17±0.06	0.24±0.04	0.70±0.07	1.08±0.08
		2.50	3.00	±	0.23±0.04	0.36±0.06	0.89±0.07
		3.00	3.50	±	0.19±0.03	0.37±0.06	0.89±0.07
		3.50	4.00	±	0.17±0.03	0.29±0.05	0.69±0.07
		4.00	5.00	±	0.05±0.02	0.18±0.03	0.43±0.04
		5.00	6.50	±	±	0.11±0.02	0.22±0.03
		6.50	8.00	±	±	±	0.104±0.014
0.10	0.15	0.50	1.00	0.13±0.04	0.46±0.07	1.37±0.14	1.72±0.17
		1.00	1.50	0.09±0.03	0.38±0.05	0.92±0.09	1.48±0.13
		1.50	2.00	0.10±0.05	0.21±0.04	0.68±0.07	1.19±0.10
		2.00	2.50	0.04±0.02	0.23±0.04	0.58±0.06	0.97±0.09
		2.50	3.00	±	0.15±0.03	0.42±0.05	0.78±0.07
		3.00	3.50	±	0.11±0.02	0.22±0.04	0.62±0.06
		3.50	4.00	±	0.06±0.02	0.22±0.03	0.48±0.05
		4.00	5.00	±	0.020±0.010	0.08±0.02	0.24±0.03
		5.00	6.50	±	±	0.019±0.007	0.074±0.012
		6.50	8.00	±	±	±	0.014±0.003
0.15	0.20	0.50	1.00	0.11±0.05	0.45±0.08	1.22±0.14	1.78±0.19
		1.00	1.50	0.12±0.05	0.29±0.05	0.64±0.07	0.98±0.10
		1.50	2.00	0.06±0.02	0.24±0.04	0.51±0.06	0.90±0.09
		2.00	2.50	0.06±0.04	0.18±0.04	0.41±0.05	0.71±0.08
		2.50	3.00	±	0.04±0.02	0.27±0.04	0.45±0.06
		3.00	3.50	±	0.040±0.015	0.16±0.03	0.27±0.04
		3.50	4.00	±	0.009±0.007	0.10±0.02	0.14±0.03
		4.00	5.00	±	0.001±0.002	0.024±0.007	0.046±0.012
		5.00	6.50	±	±	0.004±0.002	0.011±0.005
		6.50	8.00	±	±	±	0.002±0.001
0.20	0.25	0.50	1.00	0.25±0.11	0.53±0.10	1.01±0.14	1.24±0.17
		1.00	1.50	0.15±0.07	0.51±0.09	0.90±0.12	1.32±0.17
		1.50	2.00	0.07±0.05	0.30±0.06	0.79±0.12	1.11±0.16
		2.00	2.50	0.02±0.03	0.20±0.04	0.42±0.08	0.59±0.10
		2.50	3.00	±	0.05±0.02	0.22±0.05	0.32±0.06
		3.00	3.50	±	0.009±0.005	0.05±0.02	0.12±0.03
		3.50	4.00	±	0.005±0.004	0.016±0.012	0.05±0.02
		4.00	5.00	±	0.003±0.003	0.007±0.007	0.015±0.013
		5.00	6.50	±	±	0.002±0.002	0.001±0.001
		6.50	8.00	±	±	±	0.000±0.013

Table 25: HARP results for the double-differential π^- production cross-section in the laboratory system, $d^2\sigma^\pi/(dpd\Omega)$, for π^- -Ta interactions at 3,5,8,12 GeV/c. Each row refers to a different ($p_{\min} \leq p < p_{\max}, \theta_{\min} \leq \theta < \theta_{\max}$) bin, where p and θ are the pion momentum and polar angle, respectively. The central value as well as the square-root of the diagonal elements of the covariance matrix are given.

θ_{\min} (rad)	θ_{\max} (rad)	p_{\min} (GeV/c)	p_{\max} (GeV/c)	$d^2\sigma^\pi/(dpd\Omega)$ (barn/(GeV/c sr))					
				3 GeV/c	5 GeV/c	8 GeV/c	12 GeV/c		
0.05	0.10	0.50	1.00	0.22±0.06	0.79±0.09	1.48±0.13	2.16±0.20		
		1.00	1.50	0.11±0.03	0.50±0.06	1.10±0.09	1.80±0.14		
		1.50	2.00	0.09±0.02	0.58±0.06	1.22±0.08	1.63±0.11		
		2.00	2.50	0.07±0.02	0.48±0.06	1.23±0.10	1.59±0.11		
		2.50	3.00	±	0.61±0.07	1.00±0.07	1.49±0.10		
		3.00	3.50	±	0.63±0.07	0.81±0.08	1.27±0.08		
		3.50	4.00	±	0.55±0.07	0.69±0.07	1.02±0.07		
		4.00	5.00	±	0.57±0.10	0.67±0.06	0.77±0.05		
		5.00	6.50	±	±	0.49±0.05	0.51±0.03		
		6.50	8.00	±	±	±	0.32±0.03		
		0.10	0.15	0.50	1.00	0.38±0.08	0.77±0.10	1.80±0.20	2.56±0.27
				1.00	1.50	0.22±0.05	0.59±0.07	1.14±0.10	1.91±0.16
				1.50	2.00	0.28±0.07	0.45±0.06	0.99±0.09	1.68±0.13
				2.00	2.50	0.45±0.09	0.50±0.06	0.91±0.08	1.51±0.13
2.50	3.00			±	0.44±0.05	0.67±0.06	1.11±0.10		
3.00	3.50			±	0.39±0.05	0.38±0.05	0.89±0.08		
3.50	4.00			±	0.33±0.04	0.31±0.04	0.62±0.06		
4.00	5.00			±	0.31±0.05	0.21±0.03	0.38±0.04		
5.00	6.50			±	±	0.095±0.015	0.17±0.02		
6.50	8.00			±	±	±	0.058±0.010		
0.15	0.20			0.50	1.00	0.34±0.10	0.95±0.13	1.43±0.17	2.25±0.25
				1.00	1.50	0.27±0.07	0.45±0.06	1.31±0.12	1.89±0.17
				1.50	2.00	0.22±0.07	0.39±0.06	0.88±0.09	1.10±0.11
				2.00	2.50	0.16±0.04	0.26±0.05	0.53±0.06	0.81±0.08
		2.50	3.00	±	0.12±0.02	0.31±0.04	0.46±0.05		
		3.00	3.50	±	0.11±0.02	0.17±0.03	0.40±0.05		
		3.50	4.00	±	0.07±0.02	0.16±0.02	0.21±0.03		
		4.00	5.00	±	0.06±0.02	0.079±0.014	0.16±0.02		
		5.00	6.50	±	±	0.034±0.007	0.047±0.010		
		6.50	8.00	±	±	±	0.012±0.004		
		0.20	0.25	0.50	1.00	0.17±0.07	0.50±0.09	1.10±0.14	1.22±0.16
				1.00	1.50	0.11±0.05	0.30±0.05	0.40±0.06	0.58±0.08
				1.50	2.00	0.06±0.03	0.23±0.05	0.39±0.08	0.64±0.10
				2.00	2.50	0.03±0.02	0.15±0.04	0.28±0.05	0.49±0.08
2.50	3.00			±	0.08±0.02	0.21±0.04	0.32±0.07		
3.00	3.50			±	0.10±0.03	0.15±0.03	0.21±0.04		
3.50	4.00			±	0.050±0.014	0.08±0.02	0.14±0.03		
4.00	5.00			±	0.026±0.009	0.06±0.02	0.11±0.03		
5.00	6.50			±	±	0.025±0.010	0.035±0.010		
6.50	8.00			±	±	±	0.012±0.008		

Table 26: HARP results for the double-differential π^+ production cross-section in the laboratory system, $d^2\sigma^\pi/(dpd\Omega)$, for π^+ -Ta interactions at 3,5,8,12 GeV/c. Each row refers to a different ($p_{\min} \leq p < p_{\max}, \theta_{\min} \leq \theta < \theta_{\max}$) bin, where p and θ are the pion momentum and polar angle, respectively. The central value as well as the square-root of the diagonal elements of the covariance matrix are given.

θ_{\min} (rad)	θ_{\max} (rad)	p_{\min} (GeV/c)	p_{\max} (GeV/c)	$d^2\sigma^{\pi^+}/(dpd\Omega)$ (barn/(GeV/c sr))			
				3 GeV/c	5 GeV/c	8 GeV/c	12 GeV/c
0.050	0.100	0.50	1.00	0.26±0.07	0.58±0.10	1.06±0.17	1.60±0.51
		1.00	1.50	0.032±0.009	0.46±0.07	1.03±0.12	1.36±0.38
		1.50	2.00	0.123±0.015	0.39±0.06	0.63±0.09	1.62±0.44
		2.00	2.50	0.35±0.03	0.71±0.07	0.71±0.10	1.09±0.38
		2.50	3.00	±	0.70±0.06	0.73±0.09	1.69±0.84
		3.00	3.50	±	0.87±0.09	0.61±0.08	1.33±0.29
		3.50	4.00	±	1.15±0.07	0.59±0.08	1.46±0.31
		4.00	5.00	±	0.86±0.29	0.81±0.06	0.90±0.17
		5.00	6.50	±	±	0.68±0.10	0.66±0.12
		6.50	8.00	±	±	±	0.55±0.11
0.100	0.150	0.50	1.00	0.16±0.06	0.67±0.11	1.38±0.18	1.55±0.53
		1.00	1.50	0.34±0.08	0.43±0.08	0.88±0.11	0.94±0.31
		1.50	2.00	0.37±0.06	0.54±0.07	0.94±0.12	2.13±0.51
		2.00	2.50	0.70±0.09	0.54±0.07	0.77±0.14	0.92±0.28
		2.50	3.00	±	0.40±0.05	0.58±0.15	1.14±0.30
		3.00	3.50	±	0.53±0.06	0.39±0.06	0.75±0.22
		3.50	4.00	±	0.40±0.05	0.45±0.06	0.56±0.18
		4.00	5.00	±	0.36±0.14	0.25±0.04	0.52±0.15
		5.00	6.50	±	±	0.08±0.02	0.18±0.07
		6.50	8.00	±	±	±	0.10±0.05
0.150	0.200	0.50	1.00	0.23±0.07	0.79±0.13	1.38±0.20	1.11±0.49
		1.00	1.50	0.28±0.06	0.42±0.08	0.70±0.10	0.78±0.32
		1.50	2.00	0.23±0.04	0.36±0.06	0.56±0.08	1.33±0.41
		2.00	2.50	0.21±0.04	0.38±0.07	0.51±0.08	0.75±0.30
		2.50	3.00	±	0.14±0.03	0.28±0.06	0.22±0.13
		3.00	3.50	±	0.16±0.04	0.25±0.04	0.27±0.16
		3.50	4.00	±	0.12±0.03	0.21±0.04	0.15±0.09
		4.00	5.00	±	0.07±0.04	0.11±0.03	0.11±0.08
		5.00	6.50	±	±	0.029±0.012	0.072±0.076
		6.50	8.00	±	±	±	0.042±0.045
0.200	0.250	0.50	1.00	0.30±0.13	0.44±0.09	0.69±0.13	0.74±0.37
		1.00	1.50	0.15±0.04	0.24±0.06	0.50±0.11	0.96±0.56
		1.50	2.00	0.13±0.04	0.23±0.06	0.37±0.09	0.45±0.28
		2.00	2.50	0.024±0.014	0.17±0.05	0.39±0.09	1.09±0.53
		2.50	3.00	±	0.09±0.03	0.23±0.08	0.48±0.38
		3.00	3.50	±	0.07±0.02	0.18±0.06	0.23±0.20
		3.50	4.00	±	0.05±0.02	0.10±0.03	0.154±0.237
		4.00	5.00	±	0.03±0.02	0.05±0.02	0.17±0.27
		5.00	6.50	±	±	0.02±0.02	0.02±0.10
		6.50	8.00	±	±	±	0.02±0.20

Table 27: HARP results for the double-differential π^- production cross-section in the laboratory system, $d^2\sigma^\pi/(dpd\Omega)$, for π^+ -Ta interactions at 3,5,8,12 GeV/c. Each row refers to a different ($p_{\min} \leq p < p_{\max}, \theta_{\min} \leq \theta < \theta_{\max}$) bin, where p and θ are the pion momentum and polar angle, respectively. The central value as well as the square-root of the diagonal elements of the covariance matrix are given.

θ_{\min} (rad)	θ_{\max} (rad)	p_{\min} (GeV/c)	p_{\max} (GeV/c)	$d^2\sigma^{\pi^-}/(dpd\Omega)$ (barn/(GeV/c sr))					
				3 GeV/c	5 GeV/c	8 GeV/c	12 GeV/c		
0.050	0.100	0.50	1.00	0.32±0.08	0.43±0.09	0.79±0.13	1.89±0.55		
		1.00	1.50	0.11±0.03	0.36±0.06	0.90±0.11	1.19±0.35		
		1.50	2.00	0.11±0.03	0.31±0.05	0.77±0.09	1.10±0.33		
		2.00	2.50	0.18±0.06	0.23±0.03	0.53±0.07	0.98±0.30		
		2.50	3.00	±	0.24±0.04	0.56±0.07	0.88±0.26		
		3.00	3.50	±	0.25±0.04	0.41±0.05	1.27±0.31		
		3.50	4.00	±	0.22±0.03	0.30±0.04	0.65±0.20		
		4.00	5.00	±	0.12±0.03	0.24±0.03	0.36±0.12		
		5.00	6.50	±	±	0.107±0.015	0.16±0.06		
		6.50	8.00	±	±	±	0.06±0.03		
		0.100	0.150	0.50	1.00	0.27±0.06	0.70±0.12	1.19±0.18	2.02±0.60
				1.00	1.50	0.17±0.04	0.37±0.06	0.78±0.10	0.98±0.31
				1.50	2.00	0.18±0.04	0.28±0.05	0.75±0.09	1.21±0.36
				2.00	2.50	0.044±0.014	0.24±0.04	0.48±0.07	1.20±0.35
2.50	3.00			±	0.16±0.03	0.43±0.06	0.56±0.20		
3.00	3.50			±	0.11±0.02	0.27±0.04	0.44±0.15		
3.50	4.00			±	0.062±0.015	0.17±0.03	0.45±0.17		
4.00	5.00			±	0.030±0.011	0.11±0.02	0.21±0.11		
5.00	6.50			±	±	0.028±0.008	0.08±0.06		
6.50	8.00			±	±	±	0.02±0.02		
0.150	0.200			0.50	1.00	0.29±0.08	0.65±0.11	1.23±0.18	1.65±0.57
				1.00	1.50	0.16±0.04	0.41±0.06	0.75±0.11	1.21±0.39
				1.50	2.00	0.09±0.03	0.29±0.05	0.60±0.09	1.15±0.37
				2.00	2.50	0.04±0.02	0.19±0.03	0.49±0.08	0.70±0.28
		2.50	3.00	±	0.12±0.03	0.19±0.04	0.42±0.21		
		3.00	3.50	±	0.041±0.013	0.14±0.03	0.27±0.16		
		3.50	4.00	±	0.016±0.007	0.05±0.02	0.18±0.12		
		4.00	5.00	±	0.006±0.004	0.024±0.010	0.15±0.11		
		5.00	6.50	±	±	0.003±0.003	0.017±0.037		
		6.50	8.00	±	±	±	0.000±0.001		
		0.200	0.250	0.50	1.00	0.26±0.08	0.52±0.11	1.07±0.18	1.24±0.54
				1.00	1.50	0.18±0.06	0.27±0.06	0.72±0.13	0.87±0.37
				1.50	2.00	0.05±0.03	0.11±0.04	0.35±0.07	1.61±0.74
				2.00	2.50	0.009±0.008	0.07±0.02	0.12±0.04	1.14±0.60
2.50	3.00			±	0.04±0.02	0.026±0.012	0.20±0.20		
3.00	3.50			±	0.008±0.006	0.016±0.013	0.12±0.21		
3.50	4.00			±	0.00±0.00	0.00±0.01	0.12±0.27		
4.00	5.00			±	0.00±0.00	0.00±0.01	0.04±0.19		
5.00	6.50			±	±	0.00±0.01	0.00±0.04		
6.50	8.00			±	±	±	0.00±0.10		

Table 28: HARP results for the double-differential π^+ production cross-section in the laboratory system, $d^2\sigma^\pi/(dpd\Omega)$, for π^- -Pb interactions at 3,5,8,12 GeV/c. Each row refers to a different ($p_{\min} \leq p < p_{\max}, \theta_{\min} \leq \theta < \theta_{\max}$) bin, where p and θ are the pion momentum and polar angle, respectively. The central value as well as the square-root of the diagonal elements of the covariance matrix are given.

θ_{\min} (rad)	θ_{\max} (rad)	p_{\min} (GeV/c)	p_{\max} (GeV/c)	$d^2\sigma^{\pi^+}/(dpd\Omega)$ (barn/(GeV/c sr))					
				3 GeV/c	5 GeV/c	8 GeV/c	12 GeV/c		
0.05	0.10	0.50	1.00	0.04±0.02	0.39±0.06	0.99±0.11	1.64±0.16		
		1.00	1.50	0.04±0.02	0.42±0.05	1.46±0.10	1.75±0.12		
		1.50	2.00	0.10±0.05	0.32±0.04	1.08±0.07	1.41±0.10		
		2.00	2.50	0.10±0.04	0.20±0.03	0.65±0.07	1.19±0.08		
		2.50	3.00	±	0.14±0.03	0.41±0.06	0.94±0.07		
		3.00	3.50	±	0.19±0.03	0.42±0.06	0.96±0.07		
		3.50	4.00	±	0.15±0.03	0.31±0.05	0.64±0.07		
		4.00	5.00	±	0.06±0.02	0.22±0.03	0.37±0.03		
		5.00	6.50	±	±	0.10±0.02	0.20±0.02		
		6.50	8.00	±	±	±	0.074±0.011		
		0.10	0.15	0.50	1.00	0.18±0.06	0.46±0.07	1.45±0.15	1.89±0.18
				1.00	1.50	0.05±0.02	0.39±0.05	0.95±0.09	1.59±0.13
				1.50	2.00	0.09±0.05	0.27±0.04	0.75±0.08	1.21±0.10
				2.00	2.50	0.06±0.03	0.24±0.04	0.65±0.07	1.00±0.09
2.50	3.00			±	0.16±0.03	0.37±0.05	0.72±0.07		
3.00	3.50			±	0.11±0.02	0.25±0.04	0.57±0.06		
3.50	4.00			±	0.09±0.02	0.17±0.03	0.45±0.04		
4.00	5.00			±	0.018±0.012	0.08±0.02	0.24±0.03		
5.00	6.50			±	±	0.016±0.007	0.085±0.014		
6.50	8.00			±	±	±	0.018±0.004		
0.15	0.20			0.50	1.00	0.02±0.02	0.48±0.08	1.29±0.15	1.86±0.19
				1.00	1.50	0.14±0.07	0.26±0.04	0.80±0.08	0.99±0.09
				1.50	2.00	0.020±0.011	0.22±0.03	0.68±0.07	0.94±0.09
				2.00	2.50	0.04±0.04	0.14±0.03	0.45±0.06	0.73±0.07
		2.50	3.00	±	0.07±0.02	0.31±0.05	0.43±0.05		
		3.00	3.50	±	0.07±0.02	0.15±0.03	0.37±0.04		
		3.50	4.00	±	0.011±0.009	0.07±0.02	0.17±0.03		
		4.00	5.00	±	0.001±0.001	0.042±0.010	0.08±0.02		
		5.00	6.50	±	±	0.008±0.003	0.012±0.005		
		6.50	8.00	±	±	±	0.002±0.001		
		0.20	0.25	0.50	1.00	0.20±0.11	0.63±0.10	1.01±0.14	1.44±0.18
				1.00	1.50	0.10±0.06	0.54±0.08	0.97±0.13	1.53±0.18
				1.50	2.00	0.12±0.07	0.33±0.06	0.75±0.12	1.20±0.16
				2.00	2.50	0.02±0.03	0.18±0.04	0.36±0.07	0.73±0.11
2.50	3.00			±	0.05±0.02	0.21±0.05	0.32±0.05		
3.00	3.50			±	0.016±0.011	0.06±0.03	0.15±0.03		
3.50	4.00			±	0.002±0.002	0.019±0.014	0.07±0.02		
4.00	5.00			±	0.000±0.001	0.012±0.010	0.024±0.012		
5.00	6.50			±	±	0.002±0.002	0.003±0.002		
6.50	8.00			±	±	±	0.001±0.009		

Table 29: HARP results for the double-differential π^- production cross-section in the laboratory system, $d^2\sigma^\pi/(dpd\Omega)$, for π^- -Pb interactions at 3,5,8,12 GeV/c. Each row refers to a different ($p_{\min} \leq p < p_{\max}, \theta_{\min} \leq \theta < \theta_{\max}$) bin, where p and θ are the pion momentum and polar angle, respectively. The central value as well as the square-root of the diagonal elements of the covariance matrix are given.

θ_{\min} (rad)	θ_{\max} (rad)	p_{\min} (GeV/c)	p_{\max} (GeV/c)	$d^2\sigma^{\pi^-}/(dpd\Omega)$ (barn/(GeV/c sr))			
				3 GeV/c	5 GeV/c	8 GeV/c	12 GeV/c
0.05	0.10	0.50	1.00	0.23±0.06	0.73±0.08	1.71±0.15	2.20±0.19
		1.00	1.50	0.07±0.02	0.46±0.05	1.29±0.10	1.60±0.13
		1.50	2.00	0.06±0.02	0.49±0.05	1.40±0.10	1.70±0.11
		2.00	2.50	0.06±0.02	0.60±0.06	1.18±0.08	1.61±0.11
		2.50	3.00	±	0.59±0.06	1.00±0.08	1.34±0.09
		3.00	3.50	±	0.69±0.07	0.81±0.08	1.19±0.08
		3.50	4.00	±	0.59±0.08	0.72±0.08	0.96±0.07
		4.00	5.00	±	0.54±0.09	0.61±0.06	0.63±0.05
		5.00	6.50	±	±	0.47±0.04	0.47±0.03
		6.50	8.00	±	±	±	0.32±0.03
0.10	0.15	0.50	1.00	0.25±0.06	0.70±0.09	1.95±0.21	2.55±0.26
		1.00	1.50	0.22±0.06	0.61±0.07	1.22±0.10	2.08±0.16
		1.50	2.00	0.25±0.07	0.46±0.05	1.09±0.10	1.67±0.13
		2.00	2.50	0.38±0.09	0.49±0.06	0.89±0.08	1.37±0.11
		2.50	3.00	±	0.37±0.05	0.72±0.07	0.99±0.09
		3.00	3.50	±	0.39±0.05	0.44±0.05	0.83±0.07
		3.50	4.00	±	0.34±0.05	0.29±0.04	0.55±0.05
		4.00	5.00	±	0.29±0.04	0.19±0.03	0.40±0.04
		5.00	6.50	±	±	0.083±0.013	0.15±0.02
		6.50	8.00	±	±	±	0.054±0.009
0.15	0.20	0.50	1.00	0.43±0.12	0.81±0.11	1.49±0.17	2.30±0.24
		1.00	1.50	0.34±0.10	0.49±0.06	1.23±0.12	1.71±0.15
		1.50	2.00	0.06±0.04	0.44±0.05	0.92±0.09	1.15±0.11
		2.00	2.50	0.038±0.014	0.32±0.05	0.54±0.06	0.82±0.09
		2.50	3.00	±	0.19±0.03	0.38±0.04	0.44±0.05
		3.00	3.50	±	0.13±0.03	0.22±0.03	0.38±0.04
		3.50	4.00	±	0.07±0.02	0.16±0.02	0.27±0.03
		4.00	5.00	±	0.061±0.013	0.10±0.02	0.15±0.02
		5.00	6.50	±	±	0.026±0.006	0.044±0.008
		6.50	8.00	±	±	±	0.015±0.004
0.20	0.25	0.50	1.00	0.18±0.07	0.52±0.09	1.01±0.14	1.48±0.18
		1.00	1.50	0.05±0.03	0.25±0.04	0.73±0.10	0.68±0.09
		1.50	2.00	0.04±0.02	0.17±0.04	0.56±0.10	0.71±0.10
		2.00	2.50	0.04±0.02	0.09±0.02	0.40±0.09	0.62±0.10
		2.50	3.00	±	0.06±0.02	0.27±0.06	0.37±0.06
		3.00	3.50	±	0.07±0.02	0.14±0.03	0.30±0.05
		3.50	4.00	±	0.058±0.014	0.09±0.02	0.22±0.04
		4.00	5.00	±	0.031±0.010	0.09±0.02	0.12±0.02
		5.00	6.50	±	±	0.030±0.010	0.035±0.011
		6.50	8.00	±	±	±	0.009±0.006

Table 30: HARP results for the double-differential π^+ production cross-section in the laboratory system, $d^2\sigma^\pi/(dpd\Omega)$, for π^+ -Pb interactions at 3,5,8,12 GeV/c. Each row refers to a different ($p_{\min} \leq p < p_{\max}, \theta_{\min} \leq \theta < \theta_{\max}$) bin, where p and θ are the pion momentum and polar angle, respectively. The central value as well as the square-root of the diagonal elements of the covariance matrix are given.

θ_{\min} (rad)	θ_{\max} (rad)	p_{\min} (GeV/c)	p_{\max} (GeV/c)	$d^2\sigma^{\pi^+}/(dpd\Omega)$ (barn/(GeV/c sr))			
				3 GeV/c	5 GeV/c	8 GeV/c	12 GeV/c
0.050	0.100	0.50	1.00	0.20±0.06	0.64±0.12	0.90±0.16	2.89±1.10
			1.50	0.042±0.011	0.38±0.07	0.78±0.10	0.82±0.42
		1.50	2.00	0.093±0.011	0.43±0.07	0.77±0.10	1.54±0.65
			2.50	0.29±0.03	0.72±0.08	0.82±0.11	0.73±0.36
		2.50	3.00	±	0.75±0.07	0.74±0.10	1.64±0.53
			3.50	±	0.89±0.09	0.61±0.08	1.55±0.50
		3.50	4.00	±	1.04±0.07	0.68±0.09	1.38±0.45
			4.00	5.00	±	0.78±0.26	0.89±0.07
		5.00	6.50	±	±	0.72±0.11	*±*
			6.50	8.00	±	±	±
0.100	0.150	0.50	1.00	0.08±0.04	0.87±0.14	1.40±0.19	2.46±0.91
			1.50	0.18±0.06	0.36±0.07	1.00±0.15	2.03±0.73
		1.50	2.00	0.52±0.08	0.55±0.08	1.07±0.21	0.54±0.31
			2.50	0.69±0.09	0.52±0.07	0.89±0.36	1.20±0.65
		2.50	3.00	±	0.49±0.06	0.49±0.43	0.88±0.53
			3.00	3.50	±	0.66±0.08	0.57±0.12
		3.50	4.00	±	0.57±0.06	0.40±0.06	0.53±0.26
			4.00	5.00	±	0.35±0.13	0.29±0.05
		5.00	6.50	±	±	0.12±0.03	0.24±0.16
			6.50	8.00	±	±	±
0.150	0.200	0.50	1.00	0.18±0.06	0.79±0.14	1.35±0.19	2.46±1.08
			1.50	0.26±0.06	0.64±0.10	0.83±0.11	0.97±0.60
		1.50	2.00	0.31±0.06	0.37±0.06	0.61±0.09	*±*
			2.50	0.26±0.05	0.40±0.07	0.53±0.09	*±*
		2.50	3.00	±	0.18±0.04	0.30±0.07	0.19±0.29
			3.00	3.50	±	0.20±0.06	0.26±0.05
		3.50	4.00	±	0.15±0.04	0.12±0.03	0.210±0.250
			4.00	5.00	±	0.09±0.05	0.08±0.02
		5.00	6.50	±	±	0.031±0.013	0.145±0.162
			6.50	8.00	±	±	±
0.200	0.250	0.50	1.00	0.26±0.14	0.55±0.11	0.86±0.15	0.057±0.212
			1.50	0.11±0.04	0.39±0.08	0.42±0.09	0.06±0.73
		1.50	2.00	0.16±0.05	0.31±0.07	0.43±0.10	2.18±0.64
			2.50	0.06±0.03	0.22±0.06	0.31±0.08	2.25±1.17
		2.50	3.00	±	0.16±0.05	0.23±0.08	0.13±0.65
			3.00	3.50	±	0.07±0.03	0.11±0.04
		3.50	4.00	±	0.03±0.02	0.10±0.03	0.026±0.488
			4.00	5.00	±	0.03±0.02	0.08±0.03
		5.00	6.50	±	±	0.02±0.02	0.08±0.24

Table 31: HARP results for the double-differential π^- production cross-section in the laboratory system, $d^2\sigma^\pi/(dpd\Omega)$, for π^+ -Pb interactions at 3,5,8,12 GeV/c. Each row refers to a different ($p_{\min} \leq p < p_{\max}, \theta_{\min} \leq \theta < \theta_{\max}$) bin, where p and θ are the pion momentum and polar angle, respectively. The central value as well as the square-root of the diagonal elements of the covariance matrix are given.

θ_{\min} (rad)	θ_{\max} (rad)	p_{\min} (GeV/c)	p_{\max} (GeV/c)	$d^2\sigma^{\pi^-}/(dpd\theta)$ (barn/(GeV/c rad))					
				3 GeV/c	5 GeV/c	8 GeV/c	12 GeV/c		
0.050	0.100	0.50	1.00	0.26±0.07	0.60±0.11	0.98±0.14	0.93±0.62		
		1.00	1.50	0.17±0.04	0.53±0.07	1.00±0.12	1.92±0.70		
		1.50	2.00	0.28±0.05	0.39±0.06	0.79±0.10	1.34±0.53		
		2.00	2.50	0.20±0.06	0.31±0.04	0.48±0.07	0.79±0.36		
		2.50	3.00	±	0.31±0.05	0.51±0.07	0.64±0.31		
		3.00	3.50	±	0.23±0.04	0.41±0.05	1.38±0.48		
		3.50	4.00	±	0.26±0.04	0.39±0.05	0.96±0.36		
		4.00	5.00	±	0.13±0.03	0.29±0.03	0.40±0.18		
		5.00	6.50	±	±	0.13±0.02	0.27±0.13		
		6.50	8.00	±	±	±	0.06±0.05		
		0.100	0.150	0.50	1.00	0.27±0.06	0.66±0.12	1.36±0.20	2.21±0.90
				1.00	1.50	0.07±0.02	0.42±0.07	0.81±0.10	1.27±0.58
				1.50	2.00	0.07±0.03	0.30±0.05	0.79±0.10	0.70±0.37
				2.00	2.50	0.043±0.014	0.25±0.04	0.39±0.06	1.70±0.65
2.50	3.00			±	0.20±0.03	0.39±0.06	0.18±0.14		
3.00	3.50			±	0.10±0.02	0.28±0.05	0.58±0.31		
3.50	4.00			±	0.046±0.012	0.27±0.05	0.66±0.35		
4.00	5.00			±	0.05±0.02	0.10±0.02	0.26±0.20		
5.00	6.50			±	±	0.015±0.005	0.04±0.07		
6.50	8.00			±	±	±	0.023±0.039		
0.150	0.200			0.50	1.00	0.34±0.09	0.79±0.13	1.21±0.19	0.68±0.55
				1.00	1.50	0.20±0.05	0.43±0.07	0.76±0.11	1.56±0.76
				1.50	2.00	0.11±0.03	0.31±0.05	0.65±0.09	0.82±0.48
				2.00	2.50	0.06±0.02	0.28±0.05	0.40±0.07	0.84±0.43
		2.50	3.00	±	0.09±0.02	0.18±0.04	0.66±0.38		
		3.00	3.50	±	0.036±0.013	0.13±0.03	0.30±0.23		
		3.50	4.00	±	0.015±0.008	0.07±0.02	0.52±0.42		
		4.00	5.00	±	0.002±0.002	0.019±0.009	0.13±0.19		
		5.00	6.50	±	±	0.004±0.003	0.001±0.006		
		6.50	8.00	±	±	±	0.005±0.023		
		0.200	0.250	0.50	1.00	0.21±0.08	0.59±0.13	0.90±0.16	0.78±0.65
				1.00	1.50	0.14±0.05	0.36±0.08	0.83±0.15	0.03±0.06
				1.50	2.00	0.07±0.04	0.14±0.05	0.38±0.09	0.67±1.08
				2.00	2.50	±	0.09±0.03	0.11±0.04	0.72±0.77
2.50	3.00			±	0.033±0.014	0.06±0.02	0.11±0.16		
3.00	3.50			±	0.013±0.008	0.02±0.02	0.10±0.44		
3.50	4.00			±	0.013±0.010	0.00±0.01	0.09±0.93		
4.00	5.00			±	0.00±0.01	0.00±0.01	0.02±0.35		
5.00	6.50			±	±	±	0.00±0.05		
6.50	8.00			±	±	±	0.00±0.20		

chop chop

Table 32: HARP results for the double-differential π^+ and π^- production cross-section in the laboratory system, $d^2\sigma^\pi/(dpd\Omega)$, for π^- -Be interactions at 8 and 12 GeV/c. Each row refers to a different ($p_{\min} \leq p < p_{\max}, \theta_{\min} \leq \theta < \theta_{\max}$) bin, where p and θ are the pion momentum and polar angle, respectively. A finer angular binning than in the previous set of tables is used. The central value as well as the square-root of the diagonal elements of the covariance matrix are given.

θ_{\min} (rad)	θ_{\max} (rad)	p_{\min} (GeV/c)	p_{\max} (GeV/c)	$d^2\sigma^{\pi^+}/(dpd\Omega)$ (barn/(GeV/c rad))		$d^2\sigma^{\pi^-}/(dpd\Omega)$ (barn/(GeV/c rad))	
				8 GeV/c	12 GeV/c	8 GeV/c	12 GeV/c
0.025	0.050	0.50	0.75	0.12±0.03	0.07±0.02	0.20±0.05	0.13±0.03
			0.75	1.00	0.14±0.02	0.11±0.02	0.18±0.03
		1.00	1.25	0.18±0.02	0.09±0.02	0.17±0.03	0.12±0.02
			1.25	1.50	0.20±0.02	0.13±0.03	0.17±0.03
		1.50	2.00	0.16±0.02	0.13±0.02	0.21±0.02	0.17±0.02
			2.00	2.50	0.14±0.02	0.13±0.02	0.22±0.02
		2.50	3.00	0.12±0.02	0.15±0.02	0.19±0.02	0.14±0.02
			3.00	3.50	0.09±0.02	0.12±0.02	0.23±0.02
		3.50	4.00	0.08±0.02	0.094±0.014	0.22±0.02	0.132±0.014
			4.00	5.00	0.089±0.013	0.064±0.009	0.22±0.02
		5.00	6.50	0.098±0.011	0.065±0.007	0.25±0.02	0.117±0.010
			6.50	8.00	±	0.053±0.006	±
		0.050	0.075	0.50	0.75	0.15±0.03	0.08±0.02
0.75	1.00				0.14±0.02	0.10±0.02	0.18±0.02
1.00	1.25			0.18±0.02	0.12±0.02	0.18±0.02	0.13±0.02
	1.25			1.50	0.17±0.02	0.13±0.02	0.19±0.02
1.50	2.00			0.145±0.012	0.119±0.012	0.20±0.02	0.15±0.02
	2.00			2.50	0.105±0.012	0.133±0.012	0.21±0.02
2.50	3.00			0.079±0.012	0.088±0.009	0.21±0.02	0.158±0.014
	3.00			3.50	0.086±0.014	0.106±0.011	0.18±0.02
3.50	4.00			0.103±0.012	0.096±0.010	0.17±0.02	0.135±0.011
	4.00			5.00	0.068±0.007	0.056±0.006	0.21±0.02
5.00	6.50			0.043±0.005	0.037±0.004	0.174±0.012	0.100±0.006
	6.50			8.00	±	0.018±0.003	±
0.075	0.100			0.50	0.75	0.09±0.02	0.10±0.02
		0.75	1.00		0.17±0.02	0.128±0.015	0.22±0.02
		1.00	1.25	0.19±0.02	0.124±0.013	0.19±0.02	0.15±0.02
			1.25	1.50	0.167±0.014	0.141±0.013	0.22±0.02
		1.50	2.00	0.139±0.010	0.133±0.012	0.22±0.02	0.185±0.013
			2.00	2.50	0.117±0.010	0.122±0.010	0.222±0.015
		2.50	3.00	0.098±0.009	0.085±0.007	0.184±0.012	0.189±0.013
			3.00	3.50	0.086±0.008	0.091±0.009	0.147±0.012
		3.50	4.00	0.050±0.009	0.080±0.009	0.146±0.013	0.124±0.008
			4.00	5.00	0.030±0.004	0.043±0.004	0.123±0.009
		5.00	6.50	0.009±0.002	0.019±0.002	0.078±0.005	0.053±0.004
			6.50	8.00	±	0.005±0.001	±

Table 33: HARP results for the double-differential π^+ and π^- production cross-section in the laboratory system, $d^2\sigma^\pi/(dpd\Omega)$, for π^+ -Be interactions at 8 and 8.9 GeV/c. Each row refers to a different ($p_{\min} \leq p < p_{\max}, \theta_{\min} \leq \theta < \theta_{\max}$) bin, where p and θ are the pion momentum and polar angle, respectively. A finer angular binning than in the previous set of tables is used. The central value as well as the square-root of the diagonal elements of the covariance matrix are given.

θ_{\min} (rad)	θ_{\max} (rad)	p_{\min} (GeV/c)	p_{\max} (GeV/c)	$d^2\sigma^{\pi^+}/(dpd\Omega)$ (barn/(GeV/c rad))		$d^2\sigma^{\pi^-}/(dpd\Omega)$ (barn/(GeV/c rad))			
				8 GeV/c	8.9 GeV/c	8 GeV/c	8.9 GeV/c		
0.025	0.050	0.50	0.75	0.10±0.04	0.13±0.04	0.13±0.05	0.10±0.03		
		0.75	1.00	0.14±0.03	0.09±0.03	0.13±0.03	0.12±0.03		
		1.00	1.25	0.13±0.03	0.14±0.03	0.15±0.04	0.11±0.03		
		1.25	1.50	0.11±0.03	0.13±0.03	0.13±0.04	0.16±0.03		
		1.50	2.00	0.16±0.03	0.15±0.03	0.18±0.03	0.13±0.02		
		2.00	2.50	0.08±0.02	0.15±0.02	0.13±0.02	0.12±0.02		
		2.50	3.00	0.15±0.03	0.19±0.02	0.10±0.02	0.07±0.02		
		3.00	3.50	0.16±0.02	0.15±0.02	0.11±0.02	0.10±0.02		
		3.50	4.00	0.19±0.03	0.21±0.02	0.081±0.014	0.081±0.015		
		4.00	5.00	0.18±0.02	0.21±0.02	0.104±0.014	0.085±0.012		
		5.00	6.50	0.27±0.02	0.22±0.02	0.092±0.012	0.079±0.009		
		0.050	0.075	0.50	0.75	0.12±0.03	0.12±0.03	0.10±0.03	0.09±0.02
				0.75	1.00	0.13±0.03	0.10±0.02	0.10±0.02	0.11±0.02
1.00	1.25			0.14±0.03	0.11±0.02	0.10±0.02	0.12±0.02		
1.25	1.50			0.17±0.03	0.16±0.02	0.10±0.02	0.12±0.02		
1.50	2.00			0.12±0.02	0.15±0.02	0.14±0.02	0.14±0.02		
2.00	2.50			0.14±0.02	0.14±0.02	0.13±0.02	0.129±0.014		
2.50	3.00			0.16±0.02	0.14±0.02	0.11±0.02	0.096±0.013		
3.00	3.50			0.12±0.02	0.17±0.02	0.083±0.013	0.106±0.011		
3.50	4.00			0.12±0.02	0.17±0.02	0.079±0.012	0.084±0.009		
4.00	5.00			0.21±0.02	0.173±0.012	0.064±0.009	0.062±0.007		
5.00	6.50			0.203±0.013	0.136±0.010	0.047±0.006	0.035±0.004		
0.075	0.100			0.50	0.75	0.11±0.03	0.15±0.03	0.09±0.02	0.12±0.02
				0.75	1.00	0.17±0.03	0.15±0.02	0.14±0.02	0.08±0.02
		1.00	1.25	0.13±0.02	0.18±0.02	0.20±0.03	0.14±0.02		
		1.25	1.50	0.19±0.03	0.18±0.02	0.16±0.02	0.16±0.02		
		1.50	2.00	0.14±0.02	0.19±0.02	0.104±0.014	0.132±0.012		
		2.00	2.50	0.17±0.02	0.188±0.014	0.105±0.014	0.118±0.010		
		2.50	3.00	0.20±0.02	0.150±0.011	0.067±0.009	0.088±0.008		
		3.00	3.50	0.15±0.02	0.168±0.013	0.100±0.012	0.078±0.008		
		3.50	4.00	0.13±0.02	0.143±0.011	0.055±0.008	0.061±0.006		
		4.00	5.00	0.128±0.010	0.109±0.009	0.041±0.005	0.036±0.004		
		5.00	6.50	0.09±0.03	0.074±0.005	0.010±0.002	0.011±0.002		

Table 34: HARP results for the double-differential π^+ and π^- production cross-section in the laboratory system, $d^2\sigma^\pi/(dpd\Omega)$, for π^- -C interactions at 8 and 12 GeV/c. Each row refers to a different ($p_{\min} \leq p < p_{\max}, \theta_{\min} \leq \theta < \theta_{\max}$) bin, where p and θ are the pion momentum and polar angle, respectively. A finer angular binning than in the previous set of tables is used. The central value as well as the square-root of the diagonal elements of the covariance matrix are given.

θ_{\min} (rad)	θ_{\max} (rad)	p_{\min} (GeV/c)	p_{\max} (GeV/c)	$d^2\sigma^{\pi^+}/(dpd\Omega)$ (barn/(GeV/c rad))		$d^2\sigma^{\pi^-}/(dpd\Omega)$ (barn/(GeV/c rad))			
				8 GeV/c	12 GeV/c	8 GeV/c	12 GeV/c		
0.025	0.050	0.50	0.75	0.06±0.02	0.13±0.04	0.22±0.06	0.21±0.07		
			0.75	1.00	0.15±0.03	0.25±0.05	0.24±0.04	0.30±0.05	
		1.00	1.25	0.20±0.03	0.12±0.03	0.18±0.03	0.24±0.05		
			1.25	1.50	0.24±0.03	0.22±0.05	0.23±0.04	0.22±0.04	
		1.50	2.00	0.17±0.03	0.25±0.04	0.29±0.03	0.31±0.04		
			2.00	2.50	0.16±0.02	0.26±0.04	0.24±0.02	0.34±0.05	
		2.50	3.00	0.15±0.03	0.24±0.03	0.21±0.03	0.25±0.03		
			3.00	3.50	0.05±0.02	0.22±0.03	0.23±0.03	0.33±0.04	
		3.50	4.00	0.11±0.02	0.17±0.03	0.17±0.03	0.24±0.03		
			4.00	5.00	0.08±0.02	0.13±0.02	0.23±0.03	0.24±0.03	
		5.00	6.50	0.098±0.015	0.119±0.014	0.24±0.03	0.27±0.03		
			6.50	8.00	±	0.108±0.015	±	0.30±0.02	
		0.050	0.075	0.50	0.75	0.15±0.03	0.24±0.05	0.30±0.05	0.29±0.06
					0.75	1.00	0.13±0.02	0.22±0.04	0.25±0.03
1.00	1.25			0.23±0.03	0.26±0.04	0.24±0.03	0.29±0.04		
	1.25			1.50	0.19±0.02	0.20±0.03	0.18±0.02	0.23±0.03	
1.50	2.00			0.18±0.02	0.20±0.03	0.25±0.02	0.34±0.04		
	2.00			2.50	0.14±0.02	0.17±0.02	0.25±0.02	0.29±0.03	
2.50	3.00			0.10±0.02	0.17±0.02	0.22±0.02	0.26±0.03		
	3.00			3.50	0.09±0.02	0.18±0.02	0.22±0.02	0.28±0.03	
3.50	4.00			0.090±0.013	0.17±0.02	0.20±0.02	0.24±0.03		
	4.00			5.00	0.083±0.010	0.096±0.012	0.21±0.02	0.23±0.02	
5.00	6.50			0.045±0.006	0.073±0.009	0.17±0.02	0.173±0.013		
	6.50			8.00	±	0.026±0.005	±	0.140±0.012	
0.075	0.100			0.50	0.75	0.12±0.02	0.14±0.03	0.30±0.04	0.37±0.06
					0.75	1.00	0.16±0.02	0.23±0.03	0.22±0.02
		1.00	1.25	0.21±0.02	0.27±0.03	0.25±0.02	0.29±0.03		
			1.25	1.50	0.18±0.02	0.30±0.03	0.25±0.03	0.33±0.04	
		1.50	2.00	0.166±0.013	0.25±0.02	0.25±0.02	0.30±0.03		
			2.00	2.50	0.114±0.012	0.21±0.02	0.24±0.02	0.34±0.03	
		2.50	3.00	0.092±0.010	0.18±0.02	0.23±0.02	0.32±0.03		
			3.00	3.50	0.096±0.010	0.17±0.02	0.16±0.02	0.25±0.02	
		3.50	4.00	0.053±0.012	0.136±0.014	0.16±0.02	0.23±0.02		
			4.00	5.00	0.026±0.005	0.072±0.008	0.144±0.013	0.171±0.014	
		5.00	6.50	0.008±0.003	0.039±0.006	0.078±0.006	0.105±0.008		
			6.50	8.00	±	0.008±0.002	±	0.052±0.006	

Table 35: HARP results for the double-differential π^+ and π^- production cross-section in the laboratory system, $d^2\sigma^\pi/(dpd\Omega)$, for π^+-C interactions at 8 GeV/c. Each row refers to a different ($p_{\min} \leq p < p_{\max}, \theta_{\min} \leq \theta < \theta_{\max}$) bin, where p and θ are the pion momentum and polar angle, respectively. A finer angular binning than in the previous set of tables is used. The central value as well as the square-root of the diagonal elements of the covariance matrix are given.

θ_{\min} (rad)	θ_{\max} (rad)	p_{\min} (GeV/c)	p_{\max} (GeV/c)	$d^2\sigma^{\pi^+}/(dpd\Omega)$ (barn/(GeV/c rad)) 8 GeV/c	$d^2\sigma^{\pi^-}/(dpd\Omega)$ (barn/(GeV/c rad)) 8 GeV/c		
0.025	0.050	0.50	0.75	0.15±0.06	0.27±0.08		
		0.75	1.00	0.19±0.05	0.19±0.05		
		1.00	1.25	0.05±0.02	0.12±0.03		
		1.25	1.50	0.07±0.03	0.18±0.06		
		1.50	2.00	0.11±0.03	0.17±0.04		
		2.00	2.50	0.15±0.04	0.12±0.03		
		2.50	3.00	0.18±0.04	0.09±0.02		
		3.00	3.50	0.23±0.03	0.15±0.05		
		3.50	4.00	0.17±0.02	0.10±0.02		
		4.00	5.00	0.21±0.02	0.11±0.02		
		5.00	6.50	0.36±0.02	0.097±0.014		
		0.050	0.075	0.50	0.75	0.18±0.05	0.16±0.04
				0.75	1.00	0.17±0.03	0.12±0.03
				1.00	1.25	0.14±0.03	0.17±0.04
1.25	1.50			0.25±0.04	0.15±0.03		
1.50	2.00			0.17±0.03	0.15±0.02		
2.00	2.50			0.16±0.03	0.16±0.02		
2.50	3.00			0.22±0.03	0.11±0.02		
3.00	3.50			0.17±0.03	0.081±0.014		
3.50	4.00			0.14±0.02	0.13±0.02		
4.00	5.00			0.26±0.02	0.065±0.010		
5.00	6.50			0.25±0.02	0.046±0.006		
0.075	0.100			0.50	0.75	0.13±0.03	0.17±0.04
				0.75	1.00	0.22±0.04	0.13±0.02
				1.00	1.25	0.23±0.03	0.14±0.03
		1.25	1.50	0.21±0.03	0.15±0.02		
		1.50	2.00	0.20±0.02	0.15±0.02		
		2.00	2.50	0.20±0.03	0.11±0.02		
		2.50	3.00	0.19±0.02	0.12±0.02		
		3.00	3.50	0.20±0.02	0.081±0.011		
		3.50	4.00	0.14±0.02	0.088±0.013		
		4.00	5.00	0.153±0.014	0.039±0.005		
		5.00	6.50	0.12±0.04	0.011±0.002		

Table 36: HARP results for the double-differential π^+ and π^- production cross-section in the laboratory system, $d^2\sigma^\pi/(dpd\Omega)$, for π^- -Al interactions at 8 and 12 GeV/c. Each row refers to a different ($p_{\min} \leq p < p_{\max}, \theta_{\min} \leq \theta < \theta_{\max}$) bin, where p and θ are the pion momentum and polar angle, respectively. A finer angular binning than in the previous set of tables is used. The central value as well as the square-root of the diagonal elements of the covariance matrix are given.

θ_{\min} (rad)	θ_{\max} (rad)	p_{\min} (GeV/c)	p_{\max} (GeV/c)	$d^2\sigma^{\pi^+}/(dpd\Omega)$ (barn/(GeV/c rad))		$d^2\sigma^{\pi^-}/(dpd\Omega)$ (barn/(GeV/c rad))			
				8 GeV/c	12 GeV/c	8 GeV/c	12 GeV/c		
0.025	0.050	0.50	0.75	0.12±0.04	0.32±0.09	0.49±0.11	0.50±0.12		
			0.75	0.27±0.05	0.37±0.06	0.41±0.06	0.42±0.07		
		1.00	1.25	0.22±0.04	0.33±0.06	0.36±0.06	0.38±0.06		
			1.25	0.42±0.07	0.38±0.06	0.34±0.06	0.50±0.09		
		1.50	2.00	0.33±0.05	0.36±0.06	0.45±0.05	0.51±0.06		
			2.00	0.32±0.05	0.48±0.06	0.42±0.05	0.49±0.07		
		2.50	3.00	0.19±0.04	0.45±0.06	0.40±0.05	0.37±0.05		
			3.00	0.15±0.04	0.30±0.04	0.38±0.04	0.43±0.05		
		3.50	4.00	0.17±0.04	0.31±0.04	0.31±0.04	0.41±0.04		
			4.00	0.15±0.03	0.26±0.03	0.32±0.04	0.41±0.04		
		5.00	6.50	0.14±0.02	0.19±0.02	0.35±0.04	0.39±0.03		
			6.50	±	0.16±0.02	±	0.40±0.03		
		0.050	0.075	0.50	0.75	0.28±0.06	0.23±0.05	0.55±0.09	0.48±0.08
					0.75	0.25±0.04	0.38±0.05	0.45±0.05	0.38±0.05
1.00	1.25			0.34±0.04	0.39±0.05	0.32±0.04	0.38±0.05		
	1.25			0.30±0.04	0.43±0.06	0.33±0.05	0.43±0.06		
1.50	2.00			0.33±0.03	0.35±0.04	0.46±0.04	0.48±0.05		
	2.00			0.20±0.03	0.34±0.04	0.40±0.04	0.47±0.05		
2.50	3.00			0.13±0.03	0.28±0.03	0.39±0.04	0.45±0.04		
	3.00			0.18±0.03	0.35±0.04	0.33±0.04	0.48±0.05		
3.50	4.00			0.17±0.02	0.24±0.03	0.33±0.04	0.48±0.04		
	4.00			0.12±0.02	0.16±0.02	0.33±0.03	0.31±0.03		
5.00	6.50			0.073±0.010	0.098±0.011	0.29±0.02	0.27±0.02		
	6.50			±	0.049±0.007	±	0.23±0.02		
0.075	0.100			0.50	0.75	0.26±0.05	0.25±0.04	0.57±0.08	0.63±0.09
					0.75	0.35±0.04	0.40±0.05	0.43±0.04	0.43±0.05
		1.00	1.25	0.36±0.04	0.52±0.05	0.44±0.04	0.49±0.05		
			1.25	0.40±0.04	0.42±0.04	0.50±0.05	0.52±0.06		
		1.50	2.00	0.28±0.02	0.39±0.03	0.41±0.03	0.54±0.04		
			2.00	0.23±0.02	0.31±0.03	0.44±0.04	0.48±0.04		
		2.50	3.00	0.14±0.02	0.30±0.02	0.40±0.03	0.48±0.04		
			3.00	0.17±0.02	0.25±0.02	0.28±0.03	0.47±0.03		
		3.50	4.00	0.10±0.02	0.21±0.02	0.24±0.03	0.38±0.03		
			4.00	0.060±0.009	0.124±0.012	0.23±0.02	0.23±0.02		
		5.00	6.50	0.015±0.005	0.052±0.006	0.140±0.011	0.146±0.011		
			6.50	±	0.016±0.003	±	0.071±0.007		

Table 37: HARP results for the double-differential π^+ and π^- production cross-section in the laboratory system, $d^2\sigma^\pi/(dpd\Omega)$, for π^+ -Al interactions at 8 and 12.9 GeV/c. Each row refers to a different ($p_{\min} \leq p < p_{\max}, \theta_{\min} \leq \theta < \theta_{\max}$) bin, where p and θ are the pion momentum and polar angle, respectively. A finer angular binning than in the previous set of tables is used. The central value as well as the square-root of the diagonal elements of the covariance matrix are given.

θ_{\min} (rad)	θ_{\max} (rad)	p_{\min} (GeV/c)	p_{\max} (GeV/c)	$d^2\sigma^{\pi^+}/(dpd\Omega)$ (barn/(GeV/c rad))		$d^2\sigma^{\pi^-}/(dpd\Omega)$ (barn/(GeV/c rad))			
				8 GeV/c	12.9 GeV/c	8 GeV/c	12.9 GeV/c		
0.025	0.050	0.50	0.75	0.37±0.11	0.51±0.16	0.15±0.06	0.35±0.16		
			0.75	0.38±0.08	0.43±0.13	0.37±0.09	0.38±0.12		
		1.00	1.25	0.24±0.07	0.36±0.12	0.27±0.07	0.36±0.14		
			1.25	0.11±0.04	0.27±0.10	0.48±0.12	0.13±0.08		
		1.50	2.00	0.23±0.05	0.54±0.10	0.26±0.06	0.30±0.09		
			2.00	0.27±0.06	0.42±0.09	0.24±0.05	0.34±0.11		
		2.50	3.00	0.35±0.06	0.63±0.10	0.21±0.04	0.27±0.07		
			3.00	0.31±0.05	0.47±0.08	0.25±0.04	0.35±0.08		
		3.50	4.00	0.38±0.05	0.49±0.09	0.21±0.04	0.40±0.08		
			4.00	0.37±0.04	0.39±0.06	0.19±0.03	0.21±0.04		
		5.00	6.50	0.50±0.03	0.41±0.05	0.19±0.03	0.14±0.03		
			6.50	±	0.42±0.05	±	0.16±0.03		
		0.050	0.075	0.50	0.75	0.38±0.09	0.48±0.11	0.22±0.06	0.21±0.08
					0.75	0.33±0.06	0.64±0.10	0.15±0.04	0.27±0.07
1.00	1.25			0.33±0.06	0.36±0.08	0.24±0.05	0.40±0.09		
	1.25			0.21±0.05	0.36±0.08	0.18±0.04	0.39±0.09		
1.50	2.00			0.28±0.04	0.43±0.07	0.23±0.04	0.43±0.06		
	2.00			0.37±0.05	0.52±0.07	0.24±0.04	0.33±0.06		
2.50	3.00			0.34±0.05	0.45±0.06	0.16±0.03	0.24±0.05		
	3.00			0.33±0.05	0.46±0.06	0.21±0.03	0.32±0.06		
3.50	4.00			0.29±0.04	0.42±0.06	0.18±0.03	0.29±0.05		
	4.00			0.42±0.04	0.41±0.04	0.13±0.02	0.17±0.03		
5.00	6.50			0.40±0.03	0.29±0.03	0.080±0.011	0.14±0.02		
	6.50			±	0.21±0.03	±	0.052±0.012		
0.075	0.100			0.50	0.75	0.26±0.06	0.35±0.09	0.32±0.07	0.24±0.08
					0.75	0.26±0.05	0.59±0.08	0.26±0.04	0.30±0.07
		1.00	1.25	0.34±0.05	0.47±0.07	0.33±0.05	0.41±0.07		
			1.25	0.40±0.06	0.45±0.07	0.28±0.04	0.41±0.07		
		1.50	2.00	0.35±0.04	0.43±0.06	0.26±0.03	0.36±0.05		
			2.00	0.34±0.04	0.54±0.06	0.27±0.03	0.36±0.04		
		2.50	3.00	0.33±0.04	0.34±0.04	0.15±0.02	0.29±0.04		
			3.00	0.36±0.04	0.48±0.05	0.12±0.02	0.27±0.03		
		3.50	4.00	0.31±0.05	0.36±0.04	0.09±0.02	0.29±0.03		
			4.00	0.31±0.02	0.25±0.03	0.043±0.007	0.12±0.02		
		5.00	6.50	0.16±0.05	0.14±0.02	0.025±0.005	0.051±0.010		
			6.50	±	0.080±0.012	±	0.015±0.004		

Table 38: HARP results for the double-differential π^+ and π^- production cross-section in the laboratory system, $d^2\sigma^\pi/(dpd\Omega)$, for π^- -Cu interactions at 8 and 12 GeV/c. Each row refers to a different ($p_{\min} \leq p < p_{\max}, \theta_{\min} \leq \theta < \theta_{\max}$) bin, where p and θ are the pion momentum and polar angle, respectively. A finer angular binning than in the previous set of tables is used. The central value as well as the square-root of the diagonal elements of the covariance matrix are given.

θ_{\min} (rad)	θ_{\max} (rad)	p_{\min} (GeV/c)	p_{\max} (GeV/c)	$d^2\sigma^{\pi^+}/(dpd\Omega)$ (barn/(GeV/c rad))		$d^2\sigma^{\pi^-}/(dpd\Omega)$ (barn/(GeV/c rad))	
				8 GeV/c	12 GeV/c	8 GeV/c	12 GeV/c
				0.025	0.050	0.50	0.75
		0.75	1.00	0.47±0.06	0.68±0.12	0.55±0.07	1.08±0.16
		1.00	1.25	0.42±0.05	0.64±0.11	0.46±0.06	0.54±0.10
		1.25	1.50	0.70±0.09	0.80±0.14	0.55±0.09	0.89±0.17
		1.50	2.00	0.55±0.07	0.71±0.11	0.78±0.07	0.93±0.12
		2.00	2.50	0.50±0.07	0.54±0.09	0.68±0.06	0.80±0.11
		2.50	3.00	0.46±0.07	0.73±0.11	0.57±0.06	0.73±0.10
		3.00	3.50	0.24±0.06	0.76±0.11	0.42±0.05	0.79±0.10
		3.50	4.00	0.24±0.05	0.61±0.09	0.35±0.05	0.63±0.08
		4.00	5.00	0.29±0.05	0.33±0.05	0.37±0.05	0.61±0.07
		5.00	6.50	0.24±0.04	0.34±0.04	0.41±0.05	0.57±0.06
		6.50	8.00	±	0.27±0.04	±	0.61±0.05
0.050	0.075	0.50	0.75	0.55±0.09	0.81±0.15	1.12±0.15	1.25±0.22
		0.75	1.00	0.63±0.07	0.72±0.11	0.77±0.07	1.09±0.14
		1.00	1.25	0.59±0.06	0.85±0.12	0.61±0.06	0.99±0.13
		1.25	1.50	0.67±0.07	0.83±0.12	0.62±0.07	0.81±0.11
		1.50	2.00	0.61±0.05	0.63±0.08	0.76±0.06	0.92±0.10
		2.00	2.50	0.37±0.05	0.60±0.07	0.70±0.06	0.93±0.10
		2.50	3.00	0.24±0.04	0.49±0.06	0.62±0.05	0.67±0.08
		3.00	3.50	0.29±0.05	0.56±0.07	0.50±0.06	0.70±0.08
		3.50	4.00	0.25±0.04	0.47±0.07	0.43±0.06	0.63±0.09
		4.00	5.00	0.23±0.03	0.28±0.04	0.55±0.06	0.59±0.05
		5.00	6.50	0.12±0.02	0.17±0.02	0.43±0.04	0.48±0.04
		6.50	8.00	±	0.12±0.02	±	0.34±0.03
0.075	0.100	0.50	0.75	0.55±0.09	0.72±0.12	1.08±0.13	1.42±0.19
		0.75	1.00	0.75±0.07	0.59±0.08	0.70±0.06	0.74±0.09
		1.00	1.25	0.67±0.06	0.87±0.10	0.82±0.07	1.10±0.12
		1.25	1.50	0.58±0.05	0.65±0.07	0.75±0.07	0.89±0.10
		1.50	2.00	0.48±0.04	0.73±0.08	0.74±0.05	0.96±0.08
		2.00	2.50	0.40±0.04	0.75±0.07	0.67±0.05	1.10±0.09
		2.50	3.00	0.29±0.03	0.58±0.05	0.63±0.05	0.83±0.07
		3.00	3.50	0.30±0.03	0.51±0.05	0.45±0.05	0.84±0.08
		3.50	4.00	0.16±0.04	0.35±0.04	0.39±0.04	0.71±0.08
		4.00	5.00	0.082±0.014	0.24±0.03	0.33±0.03	0.40±0.03
		5.00	6.50	0.024±0.007	0.089±0.014	0.21±0.02	0.24±0.02
		6.50	8.00	±	0.018±0.005	±	0.122±0.013

Table 39: HARP results for the double-differential π^+ and π^- production cross-section in the laboratory system, $d^2\sigma^\pi/(dpd\Omega)$, for π^+ -Cu interactions at 8 GeV/c. Each row refers to a different ($p_{\min} \leq p < p_{\max}, \theta_{\min} \leq \theta < \theta_{\max}$) bin, where p and θ are the pion momentum and polar angle, respectively. A finer angular binning than in the previous set of tables is used. The central value as well as the square-root of the diagonal elements of the covariance matrix are given.

θ_{\min} (rad)	θ_{\max} (rad)	p_{\min} (GeV/c)	p_{\max} (GeV/c)	$d^2\sigma^{\pi^+}/(dpd\Omega)$ (barn/(GeV/c rad)) 8 GeV/c	$d^2\sigma^{\pi^-}/(dpd\Omega)$ (barn/(GeV/c rad)) 8 GeV/c		
0.025	0.050	0.50	0.75	0.22±0.08	0.45±0.15		
		0.75	1.00	0.32±0.08	0.45±0.11		
		1.00	1.25	0.26±0.07	0.37±0.10		
		1.25	1.50	0.49±0.12	0.31±0.11		
		1.50	2.00	0.32±0.08	0.64±0.12		
		2.00	2.50	0.34±0.09	0.36±0.08		
		2.50	3.00	0.61±0.12	0.27±0.06		
		3.00	3.50	0.32±0.06	0.40±0.07		
		3.50	4.00	0.47±0.07	0.31±0.05		
		4.00	5.00	0.40±0.05	0.32±0.04		
		5.00	6.50	0.76±0.05	0.30±0.04		
		0.050	0.075	0.50	0.75	0.57±0.14	0.44±0.11
				0.75	1.00	0.59±0.11	0.49±0.09
				1.00	1.25	0.49±0.09	0.48±0.10
1.25	1.50			0.66±0.11	0.56±0.10		
1.50	2.00			0.60±0.08	0.44±0.07		
2.00	2.50			0.59±0.09	0.36±0.06		
2.50	3.00			0.51±0.08	0.31±0.05		
3.00	3.50			0.45±0.08	0.30±0.05		
3.50	4.00			0.44±0.07	0.22±0.04		
4.00	5.00			0.58±0.06	0.23±0.03		
5.00	6.50			0.62±0.04	0.12±0.02		
0.075	0.100			0.50	0.75	0.64±0.15	0.61±0.12
				0.75	1.00	0.53±0.09	0.47±0.08
				1.00	1.25	0.66±0.10	0.46±0.08
		1.25	1.50	0.59±0.08	0.64±0.09		
		1.50	2.00	0.55±0.07	0.39±0.05		
		2.00	2.50	0.54±0.07	0.40±0.05		
		2.50	3.00	0.56±0.07	0.24±0.03		
		3.00	3.50	0.41±0.05	0.22±0.03		
		3.50	4.00	0.47±0.07	0.15±0.03		
		4.00	5.00	0.41±0.04	0.13±0.02		
		5.00	6.50	0.27±0.09	0.024±0.005		

Table 40: HARP results for the double-differential π^+ and π^- production cross-section in the laboratory system, $d^2\sigma^\pi/(dpd\Omega)$, for π^- -Sn interactions at 8 and 12 GeV/c. Each row refers to a different ($p_{\min} \leq p < p_{\max}, \theta_{\min} \leq \theta < \theta_{\max}$) bin, where p and θ are the pion momentum and polar angle, respectively. A finer angular binning than in the previous set of tables is used. The central value as well as the square-root of the diagonal elements of the covariance matrix are given.

θ_{\min} (rad)	θ_{\max} (rad)	p_{\min} (GeV/c)	p_{\max} (GeV/c)	$d^2\sigma^{\pi^+}/(dpd\Omega)$ (barn/(GeV/c rad))		$d^2\sigma^{\pi^-}/(dpd\Omega)$ (barn/(GeV/c rad))			
				8 GeV/c	12 GeV/c	8 GeV/c	12 GeV/c		
0.025	0.050	0.50	0.75	0.64±0.14	1.56±0.30	1.39±0.21	1.86±0.34		
			0.75	0.53±0.07	1.16±0.19	0.70±0.08	1.53±0.17		
		1.00	1.25	0.36±0.05	0.94±0.13	0.29±0.04	0.93±0.12		
			1.25	0.55±0.09	1.15±0.17	0.55±0.10	1.34±0.20		
		1.50	2.00	0.63±0.10	1.01±0.76	0.80±0.08	1.38±0.15		
			2.00	0.84±0.12	1.07±0.36	0.75±0.09	1.19±0.16		
		2.50	3.00	0.53±0.11	0.88±0.15	0.70±0.09	1.08±0.12		
			3.00	0.24±0.08	0.92±0.16	0.45±0.07	1.04±0.11		
		3.50	4.00	0.37±0.09	0.81±0.10	0.27±0.05	0.95±0.13		
			4.00	0.36±0.07	0.58±0.07	0.43±0.07	0.91±0.09		
		5.00	6.50	0.25±0.05	0.43±0.05	0.63±0.09	0.73±0.07		
			6.50	±	0.39±0.05	±	0.84±0.07		
		0.050	0.075	0.50	0.75	0.55±0.11	0.84±0.16	1.19±0.17	1.98±0.28
					0.75	0.57±0.09	0.99±0.13	1.01±0.11	1.13±0.14
1.00	1.25			0.79±0.10	1.01±0.13	0.82±0.10	1.20±0.14		
	1.25			0.96±0.12	1.24±0.17	0.88±0.12	1.17±0.14		
1.50	2.00			0.77±0.07	1.01±0.11	0.93±0.09	1.50±0.14		
	2.00			0.58±0.08	0.95±0.11	0.84±0.09	1.20±0.11		
2.50	3.00			0.32±0.07	0.68±0.07	0.69±0.08	1.19±0.11		
	3.00			0.39±0.08	0.87±0.10	0.82±0.11	1.10±0.11		
3.50	4.00			0.31±0.06	0.60±0.07	0.58±0.09	1.03±0.11		
	4.00			0.23±0.04	0.41±0.05	0.70±0.09	0.79±0.07		
5.00	6.50			0.16±0.03	0.26±0.03	0.56±0.06	0.67±0.05		
	6.50			±	0.14±0.02	±	0.45±0.04		
0.075	0.100			0.50	0.75	0.73±0.12	1.09±0.16	1.61±0.20	2.13±0.26
					0.75	0.80±0.10	1.54±0.16	1.13±0.11	1.56±0.15
		1.00	1.25	1.08±0.11	1.37±0.13	0.98±0.09	1.31±0.12		
			1.25	0.73±0.08	1.30±0.11	0.88±0.10	1.43±0.15		
		1.50	2.00	0.68±0.06	1.03±0.09	0.94±0.08	1.29±0.10		
			2.00	0.48±0.05	0.92±0.07	0.96±0.09	1.43±0.11		
		2.50	3.00	0.41±0.05	0.80±0.07	0.93±0.08	1.28±0.10		
			3.00	0.34±0.04	0.56±0.05	0.54±0.08	0.97±0.07		
		3.50	4.00	0.14±0.05	0.43±0.05	0.51±0.07	0.88±0.07		
			4.00	0.09±0.02	0.33±0.03	0.47±0.05	0.57±0.06		
		5.00	6.50	0.021±0.008	0.14±0.02	0.26±0.03	0.31±0.02		
			6.50	±	0.037±0.008	±	0.17±0.02		

Table 41: HARP results for the double-differential π^+ and π^- production cross-section in the laboratory system, $d^2\sigma^\pi/(dpd\Omega)$, for π^+ - Sn interactions at 8 GeV/c. Each row refers to a different ($p_{\min} \leq p < p_{\max}, \theta_{\min} \leq \theta < \theta_{\max}$) bin, where p and θ are the pion momentum and polar angle, respectively. A finer angular binning than in the previous set of tables is used. The central value as well as the square-root of the diagonal elements of the covariance matrix are given.

θ_{\min} (rad)	θ_{\max} (rad)	p_{\min} (GeV/c)	p_{\max} (GeV/c)	$d^2\sigma^{\pi^+}/(dpd\Omega)$ (barn/(GeV/c rad)) 8 GeV/c	$d^2\sigma^{\pi^-}/(dpd\Omega)$ (barn/(GeV/c rad)) 8 GeV/c		
0.025	0.050	0.50	0.75	0.78±0.18	0.58±0.14		
		0.75	1.00	0.63±0.10	0.57±0.11		
		1.00	1.25	0.34±0.07	0.68±0.14		
		1.25	1.50	0.27±0.08	0.34±0.11		
		1.50	2.00	0.63±0.13	0.82±0.16		
		2.00	2.50	0.55±0.13	0.59±0.11		
		2.50	3.00	0.59±0.13	0.67±0.11		
		3.00	3.50	0.52±0.09	0.48±0.08		
		3.50	4.00	0.54±0.07	0.45±0.07		
		4.00	5.00	0.61±0.06	0.52±0.07		
		5.00	6.50	0.98±0.06	0.39±0.06		
		0.050	0.075	0.50	0.75	0.85±0.19	0.88±0.19
				0.75	1.00	0.61±0.12	0.54±0.11
				1.00	1.25	0.60±0.11	0.66±0.13
				1.25	1.50	0.97±0.16	0.81±0.15
1.50	2.00			0.85±0.11	0.49±0.08		
2.00	2.50			0.67±0.11	0.61±0.10		
2.50	3.00			0.54±0.09	0.41±0.07		
3.00	3.50			0.44±0.09	0.42±0.07		
3.50	4.00			0.39±0.08	0.39±0.06		
4.00	5.00			0.77±0.08	0.28±0.04		
0.075	0.100	0.50	0.75	1.33±0.26	0.91±0.17		
		0.75	1.00	1.01±0.15	0.74±0.11		
		1.00	1.25	0.82±0.12	0.67±0.11		
		1.25	1.50	0.79±0.12	0.68±0.10		
		1.50	2.00	0.70±0.23	0.69±0.08		
		2.00	2.50	0.68±0.35	0.44±0.06		
		2.50	3.00	0.72±0.28	0.40±0.05		
		3.00	3.50	0.62±0.08	0.32±0.05		
		3.50	4.00	0.65±0.11	0.22±0.03		
		4.00	5.00	0.62±0.08	0.13±0.02		
		5.00	6.50	0.42±0.15	0.044±0.009		

Table 42: HARP results for the double-differential π^+ and π^- production cross-section in the laboratory system, $d^2\sigma^\pi/(dpd\Omega)$, for π^- -Ta interactions at 8 and 12 GeV/c. Each row refers to a different ($p_{\min} \leq p < p_{\max}, \theta_{\min} \leq \theta < \theta_{\max}$) bin, where p and θ are the pion momentum and polar angle, respectively. A finer angular binning than in the previous set of tables is used. The central value as well as the square-root of the diagonal elements of the covariance matrix are given.

θ_{\min} (rad)	θ_{\max} (rad)	p_{\min} (GeV/c)	p_{\max} (GeV/c)	$d^2\sigma^{\pi^+}/(dpd\Omega)$ (barn/(GeV/c rad))		$d^2\sigma^{\pi^-}/(dpd\Omega)$ (barn/(GeV/c rad))			
				8 GeV/c	12 GeV/c	8 GeV/c	12 GeV/c		
0.025	0.050	0.50	0.75	1.47±0.25	1.65±0.32	2.65±0.39	2.44±0.39		
			0.75	0.72±0.08	1.11±0.15	1.18±0.12	1.34±0.16		
		1.00	1.25	0.57±0.07	1.02±0.15	0.43±0.06	0.89±0.13		
			1.25	0.90±0.12	1.19±0.18	0.76±0.13	1.61±0.24		
		1.50	2.00	0.72±0.11	1.21±0.17	1.09±0.11	1.51±0.19		
			2.50	0.90±0.15	1.26±0.17	1.10±0.12	1.80±0.23		
		2.50	3.00	0.90±0.15	1.26±0.16	0.92±0.13	1.34±0.18		
			3.50	0.51±0.12	1.49±0.18	0.50±0.08	1.50±0.16		
		3.50	4.00	0.51±0.11	0.77±0.14	0.32±0.06	1.08±0.13		
			4.00	0.44±0.08	0.55±0.08	0.44±0.08	0.93±0.10		
		5.00	6.50	0.35±0.07	0.55±0.07	0.53±0.09	0.92±0.11		
			8.00	±	0.36±0.05	±	0.96±0.09		
		0.050	0.075	0.50	0.75	0.82±0.14	1.39±0.25	1.27±0.18	2.13±0.31
					0.75	0.75±0.11	1.38±0.18	1.12±0.12	1.35±0.18
1.00	1.25			1.12±0.14	1.27±0.17	0.89±0.11	1.62±0.20		
	1.25			1.41±0.16	1.87±0.25	1.08±0.15	1.92±0.22		
1.50	2.00			1.21±0.11	1.23±0.13	1.43±0.12	1.64±0.16		
	2.50			0.77±0.11	1.16±0.12	1.21±0.13	1.70±0.15		
2.50	3.00			0.32±0.09	1.02±0.11	1.11±0.11	1.43±0.14		
	3.50			0.40±0.10	0.95±0.11	0.89±0.13	1.41±0.13		
3.50	4.00			0.42±0.08	0.87±0.12	0.82±0.13	1.06±0.11		
	4.00			0.24±0.04	0.54±0.06	0.75±0.10	0.88±0.08		
5.00	6.50			0.21±0.04	0.31±0.04	0.73±0.09	0.73±0.06		
	8.00			±	0.19±0.03	±	0.53±0.05		
0.075	0.100			0.50	0.75	1.21±0.19	1.42±0.22	2.19±0.26	2.67±0.34
					0.75	1.31±0.14	2.10±0.22	1.17±0.12	2.23±0.21
		1.00	1.25	1.27±0.12	1.77±0.17	1.19±0.12	1.78±0.17		
			1.25	1.27±0.12	1.71±0.16	1.16±0.13	1.86±0.20		
		1.50	2.00	0.93±0.08	1.30±0.11	1.06±0.09	1.62±0.13		
			2.50	0.66±0.07	1.03±0.10	1.24±0.11	1.51±0.13		
		2.50	3.00	0.39±0.06	0.79±0.08	0.92±0.08	1.53±0.12		
			3.50	0.35±0.05	0.84±0.08	0.75±0.09	1.17±0.09		
		3.50	4.00	0.19±0.06	0.57±0.06	0.61±0.07	0.98±0.08		
			4.00	0.14±0.03	0.35±0.04	0.61±0.07	0.69±0.06		
		5.00	6.50	0.032±0.013	0.15±0.02	0.31±0.04	0.36±0.03		
			8.00	±	0.040±0.009	±	0.17±0.02		

Table 43: HARP results for the double-differential π^+ and π^- production cross-section in the laboratory system, $d^2\sigma^\pi/(dpd\Omega)$, for π^+ -Ta interactions at 8 GeV/c. Each row refers to a different ($p_{\min} \leq p < p_{\max}, \theta_{\min} \leq \theta < \theta_{\max}$) bin, where p and θ are the pion momentum and polar angle, respectively. A finer angular binning than in the previous set of tables is used. The central value as well as the square-root of the diagonal elements of the covariance matrix are given.

θ_{\min} (rad)	θ_{\max} (rad)	p_{\min} (GeV/c)	p_{\max} (GeV/c)	$d^2\sigma^{\pi^+}/(dpd\Omega)$ (barn/(GeV/c rad)) 8 GeV/c	$d^2\sigma^{\pi^-}/(dpd\Omega)$ (barn/(GeV/c rad)) 8 GeV/c		
0.025	0.050	0.50	0.75	1.66±0.37	0.92±0.25		
		0.75	1.00	1.02±0.16	0.60±0.13		
		1.00	1.25	0.50±0.10	0.96±0.21		
		1.25	1.50	0.39±0.12	0.33±0.13		
		1.50	2.00	0.66±0.16	0.87±0.19		
		2.00	2.50	0.62±0.17	0.63±0.14		
		2.50	3.00	0.72±0.18	0.54±0.11		
		3.00	3.50	0.58±0.12	0.82±0.15		
		3.50	4.00	0.59±0.11	0.63±0.11		
		4.00	5.00	0.56±0.08	0.56±0.09		
		5.00	6.50	1.12±0.08	0.48±0.07		
		0.050	0.075	0.50	0.75	1.15±0.27	0.79±0.22
				0.75	1.00	0.90±0.19	0.72±0.16
				1.00	1.25	0.95±0.19	1.02±0.22
				1.25	1.50	0.96±0.20	0.54±0.13
1.50	2.00			0.57±0.12	0.98±0.16		
2.00	2.50			0.70±0.15	0.60±0.11		
2.50	3.00			0.72±0.14	0.62±0.12		
3.00	3.50			0.46±0.12	0.36±0.07		
3.50	4.00			0.42±0.10	0.41±0.08		
4.00	5.00			0.95±0.11	0.31±0.05		
0.075	0.100	5.00	6.50	1.06±0.08	0.18±0.03		
		0.50	0.75	1.11±0.27	0.88±0.21		
		0.75	1.00	1.04±0.18	0.75±0.14		
		1.00	1.25	1.15±0.19	1.19±0.20		
		1.25	1.50	1.03±0.17	0.79±0.14		
		1.50	2.00	0.67±0.11	0.62±0.10		
		2.00	2.50	0.72±0.12	0.47±0.08		
		2.50	3.00	0.74±0.12	0.51±0.08		
		3.00	3.50	0.72±0.10	0.44±0.07		
		3.50	4.00	0.70±0.11	0.22±0.04		
		4.00	5.00	0.71±0.07	0.19±0.03		
		5.00	6.50	0.41±0.15	0.051±0.011		

Table 44: HARP results for the double-differential π^+ and π^- production cross-section in the laboratory system, $d^2\sigma^\pi/(dpd\Omega)$, for π^- -Pb interactions at 8 and 12 GeV/c. Each row refers to a different ($p_{\min} \leq p < p_{\max}, \theta_{\min} \leq \theta < \theta_{\max}$) bin, where p and θ are the pion momentum and polar angle, respectively. A finer angular binning than in the previous set of tables is used. The central value as well as the square-root of the diagonal elements of the covariance matrix are given.

θ_{\min} (rad)	θ_{\max} (rad)	p_{\min} (GeV/c)	p_{\max} (GeV/c)	$d^2\sigma^{\pi^+}/(dpd\Omega)$ (barn/(GeV/c rad))		$d^2\sigma^{\pi^-}/(dpd\Omega)$ (barn/(GeV/c rad))			
				8 GeV/c	12 GeV/c	8 GeV/c	12 GeV/c		
0.025	0.050	0.50	0.75	1.60±0.27	1.58±0.29	3.24±0.43	2.52±0.41		
			0.75	0.87±0.09	1.37±0.16	1.26±0.14	1.74±0.18		
		1.00	1.25	0.56±0.07	1.06±0.14	0.54±0.07	0.88±0.13		
			1.25	0.76±0.11	1.25±0.18	0.54±0.09	0.84±0.14		
		1.50	2.00	0.82±0.13	1.40±0.18	1.27±0.14	1.53±0.20		
			2.00	1.12±0.16	1.24±0.17	1.24±0.14	1.66±0.20		
		2.50	3.00	0.76±0.15	1.28±0.16	1.02±0.13	0.87±0.13		
			3.00	0.41±0.12	0.92±0.14	0.63±0.10	1.27±0.16		
		3.50	4.00	0.53±0.12	0.85±0.13	0.42±0.09	1.05±0.13		
			4.00	0.47±0.09	0.56±0.09	0.54±0.10	0.73±0.10		
		5.00	6.50	0.40±0.08	0.44±0.07	0.65±0.11	0.62±0.09		
			6.50	±	0.33±0.06	±	0.77±0.10		
		0.050	0.075	0.50	0.75	0.92±0.15	1.45±0.22	1.91±0.24	2.46±0.33
					0.75	0.75±0.11	1.33±0.17	1.39±0.15	1.34±0.18
1.00	1.25			1.00±0.13	1.82±0.20	1.12±0.14	1.56±0.19		
	1.25			1.72±0.20	1.70±0.20	1.15±0.16	1.49±0.18		
1.50	2.00			1.19±0.10	1.38±0.14	1.43±0.14	1.66±0.16		
	2.00			0.71±0.10	1.21±0.12	1.24±0.13	1.52±0.15		
2.50	3.00			0.36±0.10	1.00±0.10	0.95±0.11	1.29±0.13		
	3.00			0.41±0.11	1.04±0.11	0.90±0.14	1.16±0.12		
3.50	4.00			0.42±0.08	0.76±0.10	0.84±0.13	0.93±0.11		
	4.00			0.36±0.06	0.43±0.06	0.82±0.12	0.76±0.08		
5.00	6.50			0.20±0.04	0.29±0.04	0.67±0.08	0.65±0.06		
	6.50			±	0.13±0.02	±	0.51±0.05		
0.075	0.100			0.50	0.75	0.96±0.16	1.81±0.23	2.21±0.26	2.93±0.34
					0.75	1.25±0.15	1.83±0.18	1.28±0.13	1.92±0.19
		1.00	1.25	1.75±0.16	1.77±0.16	1.27±0.12	1.59±0.15		
			1.25	1.30±0.13	1.71±0.14	1.53±0.18	1.71±0.19		
		1.50	2.00	1.00±0.09	1.42±0.12	1.38±0.11	1.73±0.13		
			2.00	0.61±0.07	1.17±0.10	1.14±0.10	1.67±0.12		
		2.50	3.00	0.45±0.06	0.90±0.08	1.04±0.10	1.38±0.11		
			3.00	0.43±0.06	0.91±0.08	0.74±0.11	1.22±0.09		
		3.50	4.00	0.24±0.06	0.55±0.07	0.63±0.09	0.99±0.10		
			4.00	0.12±0.03	0.32±0.04	0.46±0.07	0.54±0.06		
		5.00	6.50	0.033±0.014	0.14±0.02	0.32±0.04	0.33±0.03		
			6.50	±	0.032±0.008	±	0.19±0.02		

Table 45: HARP results for the double-differential π^+ and π^- production cross-section in the laboratory system, $d^2\sigma^\pi/(dpd\Omega)$, for π^+ -Pb interactions at 8 GeV/c. Each row refers to a different ($p_{\min} \leq p < p_{\max}, \theta_{\min} \leq \theta < \theta_{\max}$) bin, where p and θ are the pion momentum and polar angle, respectively. A finer angular binning than in the previous set of tables is used. The central value as well as the square-root of the diagonal elements of the covariance matrix are given.

θ_{\min} (rad)	θ_{\max} (rad)	p_{\min} (GeV/c)	p_{\max} (GeV/c)	$d^2\sigma^{\pi^+}/(dpd\Omega)$ (barn/(GeV/c rad)) 8 GeV/c	$d^2\sigma^{\pi^-}/(dpd\Omega)$ (barn/(GeV/c rad)) 8 GeV/c		
0.025	0.050	0.50	0.75	1.72±0.38	0.75±0.21		
		0.75	1.00	1.04±0.16	0.85±0.17		
		1.00	1.25	0.42±0.09	0.73±0.17		
		1.25	1.50	0.58±0.15	0.79±0.25		
		1.50	2.00	0.73±0.17	0.66±0.17		
		2.00	2.50	0.63±0.20	0.72±0.16		
		2.50	3.00	0.49±0.15	0.60±0.13		
		3.00	3.50	0.65±0.13	0.51±0.10		
		3.50	4.00	0.59±0.10	0.67±0.12		
		4.00	5.00	0.63±0.08	0.58±0.09		
		5.00	6.50	1.18±0.08	0.49±0.08		
		0.050	0.075	0.50	0.75	0.66±0.18	0.75±0.20
				0.75	1.00	0.77±0.18	0.73±0.16
				1.00	1.25	0.43±0.12	0.69±0.17
1.25	1.50			0.75±0.18	1.00±0.20		
1.50	2.00			0.69±0.13	0.77±0.13		
2.00	2.50			0.74±0.15	0.69±0.13		
2.50	3.00			0.85±0.16	0.49±0.10		
3.00	3.50			0.55±0.13	0.51±0.10		
3.50	4.00			0.50±0.11	0.52±0.09		
4.00	5.00			1.09±0.12	0.40±0.06		
0.075	0.100	0.50	0.75	1.11±0.09	0.22±0.03		
		0.75	1.00	1.04±0.27	1.05±0.23		
		1.00	1.25	1.02±0.19	1.27±0.20		
		1.25	1.50	0.86±0.16	1.30±0.21		
		1.50	2.00	0.99±0.17	0.91±0.15		
		2.00	2.50	0.84±0.13	0.81±0.12		
		2.50	3.00	0.88±0.15	0.33±0.06		
		3.00	3.50	0.66±0.11	0.53±0.08		
		3.50	4.00	0.66±0.09	0.34±0.06		
		4.00	5.00	0.82±0.13	0.30±0.06		
		5.00	6.50	0.75±0.07	0.21±0.03		
				0.44±0.15	0.065±0.013		

Normalization factors, incident π^+

Generator	Be 3 GeV		Ta 3 GeV		Be 5 GeV		Ta 5 GeV		Be 8 GeV		Ta 8 GeV		Be 12 GeV	
	π^+	π^-	π^+	π^-	π^+	π^-	π^+	π^-	π^+	π^-	π^+	π^-	π^+	π^-
bert	1.1	1.1	0.9	0.6	1.3	1.3	1.1	1.1	1.7	1.4	1.5	1.4	2.0	1.4
lhep	1.3	0.6	2.8	1.0	1.5	0.8	2.5	1.1	1.3	0.8	1.0	0.5	1.0	0.8
qgsb	4.8	1.8	2.1	1.5	3.8	1.3	2.2	1.1	1.9	1.0	1.4	0.8	0.9	0.8
qgsc	-	-	-	-	-	-	-	-	1.6	1.0	1.2	0.7	0.8	0.7
qgsp	-	-	-	-	-	-	-	-	1.9	1.0	1.2	0.6	0.9	0.8
ftfp	-	-	-	-	-	-	-	-	-	-	0.8	0.7	1.1	1.0
mars	1.3	1.2	1.2	0.9	0.9	1.0	0.7	0.6	1.0	1.1	0.8	0.6	0.8	1.0
rpg	1.4	0.6	2.7	0.8	1.2	0.7	1.8	0.9	1.1	0.6	0.7	0.4	0.9	0.7

Normalization factors, incident π^+

Generator	Be 3 GeV		Ta 3 GeV		Be 5 GeV		Ta 5 GeV		Be 8 GeV		Ta 8 GeV		Be 12 GeV	
	π^+	π^-	π^+	π^-	π^+	π^-	π^+	π^-	π^+	π^-	π^+	π^-	π^+	π^-
bert	1.0	1.1	0.5	0.6	1.2	1.4	0.9	1.2	1.6	2.1	1.4	1.9	1.2	1.6
lhep	0.5	1.6	0.7	2.9	0.8	1.9	1.0	2.6	0.9	1.7	0.6	1.2	0.6	1.0
qgsb	1.7	4.8	1.1	1.7	1.2	4.0	0.9	2.3	1.2	2.2	0.8	1.7	0.6	0.8
qgsc	-	-	-	-	-	-	-	-	1.1	1.8	0.7	1.3	0.6	0.7
qgsp	-	-	-	-	-	-	-	-	1.2	2.2	0.7	1.4	0.6	0.8
ftfp	-	-	-	-	-	-	-	-	-	-	0.7	1.1	0.7	1.0
mars	1.1	1.2	0.7	1.0	0.9	0.9	0.6	0.6	1.2	1.2	0.7	0.9	0.8	0.7
rpg	0.6	1.7	0.7	2.8	0.7	1.7	0.8	1.9	0.8	1.5	0.5	0.9	0.5	0.9